UNIVERSIDADE BEIRA INTERIOR

PolyThymine cryogels as a novel approach to the purification of mRNA encoding anti-ADAM17 antibodies.

Bruno Daniel Lopes Rodrigues

Dissertação para obtenção do Grau de Mestre em
Bioquímica
(2º ciclo de estudos)

Orientadora: Prof.ª Doutora Cândida Ascensão Teixeira Tomaz
Co-orientadora: Prof.ª Doutora Fani Pereira de Sousa

Janeiro de 2023

Folha em branco

Declaração de Integridade

Eu, Bruno Daniel Lopes Rodrigues, que abaixo assino, estudante com o número de inscrição M10906 de Bioquímica da Faculdade de Ciências, declaro ter desenvolvido o presente trabalho e elaborado o presente texto em total consonância com o **Código de Integridades da Universidade da Beira Interior**.

Mais concretamente afirmo não ter incorrido em qualquer das variedades de Fraude Académica, e que aqui declaro conhecer, que em particular atendi à exigida referenciação de frases, extratos, imagens e outras formas de trabalho intelectual, e assumindo assim na íntegra as responsabilidades da autoria.

Universidade da Beira Interior, Covilhã 31 /01 /2023

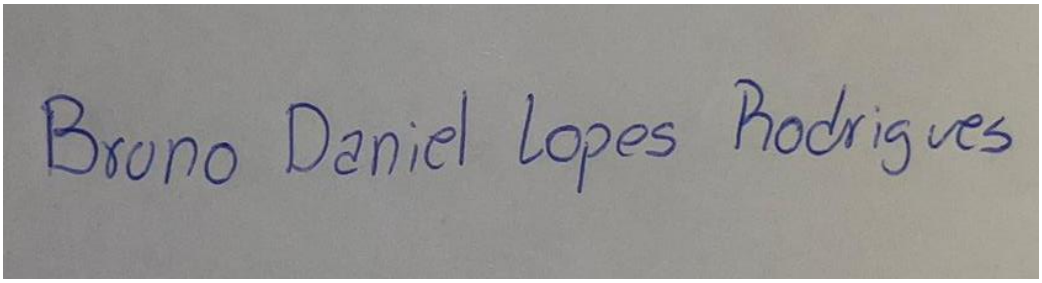

Folha em branco

“Success is not final, failure is not fatal.
It is the courage to continue that count.”

Winston Churchill

Folha em branco

Agradecimentos

A presente dissertação simboliza o final de uma etapa crucial na minha formação académica. Ao longo do meu percurso académico, todas as dificuldades e metas realizadas foram partilhadas com pessoas, sem as quais não seria possível a realização do presente trabalho e, por isso, aqui fica um especial e sentido agradecimento a todos vocês.

Agradeço à Professora Cândida Tomaz, por me ter aceitado como seu aluno, por todos os ensinamentos passados desde a orientação no Projeto final da Licenciatura em Biotecnologia. Obrigado por ter acreditado em mim e nas minhas capacidades, por me fazer crescer tanto a nível pessoal como a nível académico. Obrigado por sempre ter aquela palavra amiga que tanto me ajudou a superar alguns dos momentos menos bons ao longo do meu percurso, obrigado por tudo…

Agradeço, de igual modo, à Professora Fani Sousa, por me ter aceitado como seu aluno e por me ter integrado no seu grupo de investigação, sendo um dos pilares que sustentou o desenvolvimento da minha dissertação. Obrigado por todos os conselhos, por todo o tempo despendido e por todos os exemplos que me passou. Graças a si acabo o mestrado com uma mentalidade diferente à que entrei, obrigado por me ter ajudado a crescer tanto a nível pessoal como profissional Professora.

Agradeço também, ao Professor Renato Boto, sem o qual o presente trabalho não seria possível, obrigado por tudo aquilo que me ensinou, pelas horas passadas a ensinar-me e pelos conselhos que me deu. Agradeço também ao Professor Cláudio Maia, por toda ajuda que deu na construção e design da sequência do vetor pNZY-28 BruMEDI3622, sem o qual não teria sido possível concretizar o presente trabalho. À Eng.ª Ana Paula, agradeço o tempo e ajuda disponibilizada para a realização da análise das minhas amostras, sendo cruciais para a interpretação dos resultados do presente trabalho.

Da mesma forma, agradeço a toda a minha família, aos meus irmãos, aos meus tios, primos e avós que sempre me incentivaram, acreditaram e apoiaram em todos os momentos do meu percurso académico. Agradeço especialmente aos

meus pais por toda a confiança que depositaram em mim e por me terem ajudado a alcançar os meus objetivos.

Agradeço ainda a todos os meus colegas de laboratório, especialmente à Margarida Videira e ao Sérgio Nunes que me acompanharam desde a Licenciatura. Sem vocês este último ano teria sido mais difícil, obrigado por todos os conselhos que me deram e por todas as memórias que criámos ao longo deste ano. Por último, mas não menos importante, quero agradecer à Micaela Riscado e à Rita Carapito por me terem recebido e integrado tão bem no grupo de investigação da Professora Fani Sousa. Obrigado por todos os ensinamentos e experiência transmitidos à medida que ia realizando o trabalho prático, sem vocês teria sido mais árduo o desenvolvimento da parte prática da minha dissertação.

Agradeço ainda, à Margarida Mota, à Mariana Martins, à Joana Soares e à Renata Brito por todos os conselhos, incentivos e pela preocupação que demonstraram para comigo ao longo de todo o percurso académico, especialmente nesta última fase da elaboração da dissertação. Obrigado por me ouvirem e aconselharem ao fim de um dia exaustivo no laboratório.

Por fim, saio da Covilhã, com o coração cheio de memórias e experiências, cheio de pessoas incríveis e cheio de saudade. Não é uma despedida, mas sim um até já. Obrigado, Covilhã, por me teres recebido tão bem nesta fase tão importante da minha vida que é a vida académica.

Folha em branco

Folha em branco

Resumo Alargado

A metaloprotease "*A Desintegrin And Metalloproteinase 17*" (ADAM17) tem vindo a ganhar destaque devido à sua importante ação nas vias de sinalização onde participa, particularmente na interação com o recetor solúvel da interleucina - 6 (*soluble interleukin receptor – 6,* sIL-6R), o recetor *do* fator de crescimento epidérmico (*Epithermal Growth Factor Receptor*, EGF-R) e o recetor do fator de necrose tumoral (*Receptor of Tumour Necrosis Factor*, TNF-αR), estabelecendo a ADAM17 como um alvo atrativo na terapêutica contra o cancro e doenças infeciosas. Assim, devido à grande especificidade dos anticorpos para reconhecer um determinado epítopo, foi possível desenvolver um anticorpo anti-ADAM17, denominado de MEDI3622, que demonstrou ter a habilidade de bloquear especificamente a atividade da ADAM17. Além disso, o ácido ribonucleico mensageiro (mRNA) tem vindo a demonstrar grande potencial e aplicabilidade em diversas áreas, nomeadamente na imunização passiva, através da expressão *in vivo* de anticorpos. Deste modo, no presente trabalho foi preparado mRNA com a sequência codificante do MEDI3622 para expressão deste anticorpo anti-ADAM17.

Assim, dado o grande potencial terapêutico do mRNA, a elevada procura por parte da indústria biofarmacêutica e a necessidade de ser obtido na forma estável e pura, torna-se urgente otimizar os processos de produção e purificação desta biomolécula. Os criogeis surgiram como uma nova alternativa aos suportes cromatográficos particulados convencionais para a purificação de moléculas com elevado peso molecular, tendo já sido demonstrado o seu potencial na purificação da isoforma superenrolada do ácido desoxirribonucleico plasmídico (pDNA). Devido à sua estrutura supermacroporosa, os criogeis permitem difusão facilitada, altas taxas de fluxo e alta capacidade. Atualmente, a estratégia de eleição para a purificação do mRNA é a cromatografia de afinidade, através do uso de nucleótidos como ligandos, cuja especificidade do emparelhamento das bases adenina e timina promove interações altamente seletivas e específicas.

Deste modo, o objetivo deste trabalho foi sintetizar criogéis funcionalizados com timina, para purificar a sequência de mRNA produzida por transcrição *in vitro* que codifica o anticorpo anti-ADAM17, o MEDI3622. Para isso, o ligando 1-(2-propenil) Timina (ProT) foi sintetizado e caracterizado por ressonância magnética nuclear (RMN), sendo posteriormente preparados criogeis à base do monómero 2-hidroxietilmetacrilato (HEMA), por copolimerização dos monómeros HEMA e ProT, com diferentes proporções mássicas de ProT e submetidos a um tratamento criogénico. Os criogeis foram caracterizados por microscopia eletrónica de varrimento (*scanning electron*

microscopy, SEM), análise de energia dispersiva de raios-X (*energy dispersive X-ray analysis*, EDXA), e testes de capacidade de reidratação. Posteriormente, para avaliação do comportamento dos criogeis poli-Timina, foram realizados ensaios de purificação em diferentes condições, variando a força iónica, o tipo de sal (cloreto de sódio (NaCl) ou sulfato de amónio ($(NH_4)_2SO_4$)) e o pH na fase móvel, tirando partido da afinidade entre os ligandos ProT e as adeninas presentes em amostras de *low molecular weight RNA* (LMW RNA) como moléculas modelo, visando identificar as melhores condições em que ocorreria ligação e eluição. Numa segunda fase, após a otimização destas condições, testou-se a capacidade dos criogeis poli-Timina para purificar o mRNA, por variação da concentração de NaCl no eluente, de forma a promover a separação entre o mRNA e pDNA utilizado na sua produção.

Como principais resultados, destaca-se a síntese do ligando 1-(2-propenil) timina que foi bem-sucedida. Além disso, nesta tarefa foi ainda possível isolar a timina que não reagiu e um subproduto da reação no qual ocorreu a di-alquilação da timina (1,3-bis(2-propenil) timina). O isolamento destes dois compostos mostra que o presente trabalho se enquadra nos princípios da economia circular, reduzindo os custos da síntese do ligando, permitindo a reutilização da timina, ao mesmo tempo que são eliminados desperdícios de subprodutos através da possibilidade do uso da timina di-alquilada como agente de reticulação, ao invés da N, N'-metilenobisacrilamida. Contudo, encontraram-se vestígios de um segundo subproduto (3-(2-propenil) timina), não tendo sido possível isolar totalmente o ligando de interesse devido à sua semelhança estrutural com este subproduto, sendo necessário otimizar o passo de isolamento no futuro.

Relativamente à caracterização dos criogéis, observou-se que os suportes funcionalizados não apresentaram alterações significativas na capacidade de reidratação, em comparação com o não funcionalizado. Além disso, visualizaram-se diferenças ao nível da morfologia entre os criogéis poli-Timina e o controlo, podendo estar relacionadas com a presença do ligando na matriz polimérica dos criogéis. Estas diferenças podem, ainda, ter resultado das condições utilizadas no processo de síntese dos criogéis. Através de EDXA foi possível confirmar que houve funcionalização dos criogéis, contudo este método não é o mais indicado devido à sua limitada sensibilidade, sendo desejável a utilização de outros métodos, como análise elementar e RMN em estado-sólido, para confirmar os resultados ao nível da funcionalização.

Os resultados dos ensaios cromatográficos demonstraram que os criogéis funcionalizados com ProT conseguiram ligar e eluir o mRNA e o pDNA, apresentando maior afinidade para o mRNA, e portanto, potencial para separar estas biomoléculas. O criogel de controlo também demonstrou capacidade para ligar e eluir tanto o mRNA como o pDNA, contudo não apresentou seletividade para separar estas duas

biomoléculas. Assim, os criogeis funcionalizados com ProT parecem ser uma abordagem inovadora para superar alguns dos desafios na purificação do mRNA.

Palavras-Chave

ADAM17; MEDI3622; Timina; Criogéis; Cromatografia de Afinidade; mRNA

Folha em branco

Abstract

Currently, the metalloprotease "A disintegrin and metalloproteinase 17" (ADAM17) has been gaining prominence due to its important action in signalling pathways where the soluble interleukin receptor - 6 (sIL-6R), the epidermal growth factor receptor (EGF-R) and the tumour necrosis factor alfa receptor (TNF-αR) participate, establishing ADAM17 as an attractive target in cancer therapy and infectious diseases. Thus, due to the high specificity of antibodies to recognize a particular epitope, it was possible to develop an anti-ADAM17 antibody, named MEDI3622, which has been shown to have the ability to specifically block the activity of ADAM17. Furthermore, the messenger Ribonucleic Acid (mRNA) has been showing great potential and applicability in several areas, namely in passive immunization, by the *in vivo* expression of antibodies, making mRNA a highly attractive method. Thus, in the present work, an mRNA sequence was prepared with the coding sequence of MEDI3622 for expression of this anti-ADAM17 antibody.

Therefore, given the great therapeutic potential of mRNA, the high demand from the biopharmaceutical industry and the need to obtain it in a stable and pure form, it is important to optimize the production and purification processes of this biomolecule. The cryogels have emerged as a new alternative to conventional particulate chromatographic media for the purification of high molecular weight molecules, and their potential has already been demonstrated in the purification of the supercoiled isoform of plasmidic deoxyribonucleic acid (pDNA). Cryogels also have a supermacroporous structure that allows for facilitated diffusion, high flow rates, and high capacity. Currently, the strategy of choice for mRNA purification is affinity chromatography, using nucleotides as ligands, whose adenine and thymine base pairing specificity promotes highly selective and specific interactions.

Thus, the aim of this work was to synthesize thymine-functionalized cryogels to purify the mRNA sequence produced by *in vitro* transcription, that encodes the anti-ADAM17 antibody MEDI3622. To this end, the ligand 1-(2-propenyl) thymine (ProT) was synthesized and characterized by nuclear magnetic resonance (NMR), the cryogels were subsequently prepared based on the monomer 2-hydroxyethyl methacrylate (HEMA), by copolymerization of the monomers HEMA and ProT, with different mass ratios of ProT and subjected to cryogenic treatment. The cryogels were characterized by scanning electron microscopy (SEM), energy dispersive X-ray analysis (EDXA), and rehydration capacity tests. Subsequently, to evaluate the behaviour of poly-thymine cryogels,

purification tests were first performed under different conditions, varying the ionic strength, the type of salt (sodium chloride (NaCl) or ammonium sulphate ($(NH_4)_2SO_4$)) and the pH in the mobile phase, taking advantage of the affinity between ProT ligands and adenines present in low molecular weight RNA (LMW RNA) used as a model sample, aiming to identify the best conditions under which binding and elution occurred. In the second phase, having already optimized the binding and elution conditions, the ability of cryogels to purify the mRNA was tested. In this phase, the NaCl concentration in the elution buffers was varied in order to achieve the separation between mRNA and pDNA used for its production.

As the main results, the synthesis of the ligand 1-(2-propenyl) thymine was successfully achieved. Furthermore, in this task, it was also possible to isolate the unreacted thymine and a by-product of the reaction in which di-alkylation of thymine occurred (1,3-bis(2-propenyl) thymine). The fact that it was possible to isolate these two compounds makes the present work fit in with the principles of circular economy, reducing the costs of the synthesis of the ligand by reusing the isolated thymine, while eliminating the waste of by-products by the possibility of using di-alkylated thymine as a cross-linking agent instead of N, N'-Methylenebisacrylamide. However, traces of a second by-product (3-(2-propenyl) thymine) were found, and it was not possible to fully isolate the ligand of interest due to its structural similarity to this by-product, thus the isolation step needs to be optimized in the future.

Regarding the characterization of the cryogels, the functionalized ones did not show significant changes in rehydration capacity compared to the non-functionalized one. Differences in morphology were visualized, which may denote the presence of the ligand in the polymeric matrix of the cryogels. Also, they may have resulted from the conditions used in the synthesis process of cryogels. Furthermore, through the EDXA, it was possible to confirm that there was functionalization of the cryogels, however, this method is not the most indicated for this type of confirmation, other methods, such as elemental analysis and solid-state NMR, can be used in the future to corroborate the results at the functionalization level.

The results of the chromatographic assays demonstrate that the ProT functionalized cryogels were able to bind and elute mRNA and pDNA. Moreover, they showed potential to separate pDNA and mRNA, demonstrating a higher affinity for mRNA. The control cryogel (with no ProT ligand incorporated) also demonstrated the ability to bind and elute both mRNA and pDNA, however, it showed no aptitude to separate these two

biomolecules. Thus, ProT functionalized cryogels appear to be a novel approach to overcoming challenges in mRNA purification.

Keywords

ADAM17; MEDI3622; Thymine; Cryogels; Affinity chromatography; mRNA

Folha em branco

Table of Contents

Folha em branco

List of figures

Folha em branco

List of Tables

Folha em branco

List of Acronims

$((NH_4)_2SO_4)$ ..... Ammonium sulphate
(5´ UTR) .....5´ Untranslated Region
(A) ..... Adenine
(AC) ..... Affinity chromatography
(ADAM) ..... “A desintegrin and metalloproteinase”
(ADAMTS) ..... ADAM with thrombospondin type-1 motif
(AdeM) ..... Adenine methacrylate
(AEC) ..... Anion-exchange chromatography
(Am) .....2´- O-methyladenosine
(APA) .....Alternative polyadenylation
(APS) .....Ammonium persulphate
(ARE) ..... AU-rich element
(AUBPs) ..... AU-binding proteins
(C) ..... Cytosine
(cap - 0) .....m^7G(5´)pppN1pN2p
(cap - 1) .....m^7G(5´)pppN1mpN2p
(cap - 2) ..... m^7G(5´)pppN1mpN2mp
(CMV) ..... Cytomegalovirus
(DEPC) ..... Diethyl pyrocarbonate
(DMSO-d_6) .....hexadeuterated dimethyl sulfoxide
(DNA) ..... Deoxyribonucleic acid
(dsDNA) ..... Double-stranded DNA
(dsRNAs) ..... Double-stranded RNA
(EA) ..... Elemental Analysis
(EDXA) ..... Energy dispersive X-ray analysis
(EDXS) ..... Energy dispersive X-ray spectroscopy
(EGF-R) ..... Epidermal growth factor receptor
(eIF4E) ..... Eukaryotic initiation factor 4E
(eIF4F) ..... Eukaryotic initiation factor 4F
(eIF4G) ..... Eukaryotic initiation factor 4G
(EMA) ..... European Medicine Agency
(FDA) .....Food and Drug Administration
(G) ..... Guanine
(GMP) ..... Good Manufacturing Practices

(GRE) .....GU-rich element
(GTP) .....Guanosine triphosphate
(HEMA) .....2-hydroxyethyl methacrylate
(hGH) ..... Human growth hormone
(HIC) ..... Hydrophobic interaction chromatography
(HIV) .....Human immunodeficiency virus
(HPLC) .....,.....High performance liquid chromatography
(IE1) ..... Immediate early 1
(IEC) ..... Ionic exchange chromatography
(IPC) .....Ion-pair reverse-phase chromatography
(iPSCs) ..... Induced pluripotent stem cells
(IRES) ..... Internal ribosome entry site
(IVT) ..... *In vitro* Transcription
(LMW RNA) ..... Low molecular weight RNA
(LPS) ..... Lipopolysaccharide
(mAbs) .....Monoclonal antibodies
(MBAAm) .....N, N'-methylene-bis(acrylamide)
(miRNA) ..... MicroRNA
(MMPs) .....Matrix metalloproteinases
(mORF) .....Main Open Reading Frame
(N%) .....Nitrogen percentage
(NaCl) .....Sodium chloride
(ncRNA) .....Non-coding RNA
(NMR) .....Nuclear magnetic resonance
(ns-T0) .....New synthesis - T0
(ns-T25) .....New synthesis – T25
(ns-T37.5) .....New synthesis – T37.5
(ns-T50) .....New synthesis – T50
(PABP) .....Poly(A) binding protein
(PAGE) .....Polyacrylamide gel electrophoresis
(PAP) .....Poly (A) polymerase
(PAS) .....Polyadenylation sites
(PCR) .....Polymerase chain reaction
(pDNA) .....Plasmid DNA
(PIC) .....Pre-initiation complex
(pre-mRNA) .....Pre-messenger RNA
(ProT) .....1 - (2-propenyl) thymine

(RBP) .....RNA binding protein
(RNA) .....Ribonucleic Acid
(RNAP II) .....RNA polymerase II
(RNases) .....Ribonucleases
(rRNA) .....Ribosomal RNA
(SD) .....Shine-Dalgarno sequence
(SEC) .....Size exclusion chromatography
(SEM) .....Scanning electron microscopy
(sIL-6R) .....Soluble interleukin receptor 6
(siRNA) .....Small interfering RNA
(ssDNA) .....Single-stranded DNA
(ssRNA) .....Single-stranded RNA
(T) .....Thymine
(To) .....pHEMA-ProTo
(T25) pHEMA-ProT25
(T37.5).....pHEMA-ProT37.5
(T50) pHEMA-ProT50
(TACE) .....Tumour Necrosis Factor Alfa Converting Enzyme
(TEMED) .....N, N, N', N'-tetramethylene diamine
(TF) .....Transcription factors
(TFF) .....Tangential flow filtration
(TFII) .....Transcription factors for RNAP II
(TFIID) .....Transcription factor IID
(TISU) .....Translation initiator of short 5´UTR
(TLC) .....Thin layer chromatography
(TNF-α) .....Tumour necrosis factor alfa
(TNF-αR) .....Tumour necrosis factor alfa receptor
(TOP) .....Terminal oligopyrimidine
(Tris) .....Tris(hydroxymethyl)aminomethane
(tRNA) .....Transfer RNA
(U) .....Uracil
(UFLMP) .....Unfrozen liquid microphase
(uORF) .....Upstream open reading frame
(VCE) .....Vaccinia virus capping enzyme

Folha em branco

Chapter 1 - Introduction

1.1. Nucleic Acids

Ribonucleic Acid (RNA) is a biopolymer, very similar to deoxyribonucleic acid (DNA), composed of four different ribonucleotides monophosphates, with Adenine (A), Guanine (G), Cytosine (C) and Uracil (U) as nitrogenous bases (Figure 1), a pentose (ribose), and a phosphate group [1]. RNA differs from DNA in two aspects: RNA has the nitrogenous base U instead of Thymine (T), and the 2´- OH group in RNA ribose is not present. So, DNA has a deoxyribose sugar conferring higher stability compared to RNA [1, 2], due to a greater resistance to alkaline hydrolysis which is related to the nucleophilic cleavage of the 3´-phosphodiester bond in RNA [1, 2]. Additionally, the nucleotides can interact between them through hydrogen bonds (Adenine-Uracil/Thymine and Guanine-Cytosine), being responsible for the acquisition of different structures. In fact, DNA is commonly observed in a double-stranded structure, however, single-stranded DNA can also be found as an intermediate in biological processes, e.g., replication, recombination, DNA repair and transcription [2, 3]. On the other hand, RNA is commonly found in a single-stranded structure, although it also has the propensity to fold and acquire secondary/tertiary structures because of the intrinsic complementary regions in the RNA sequence, being the tertiary structure related to catalytic reactions [2, 4].

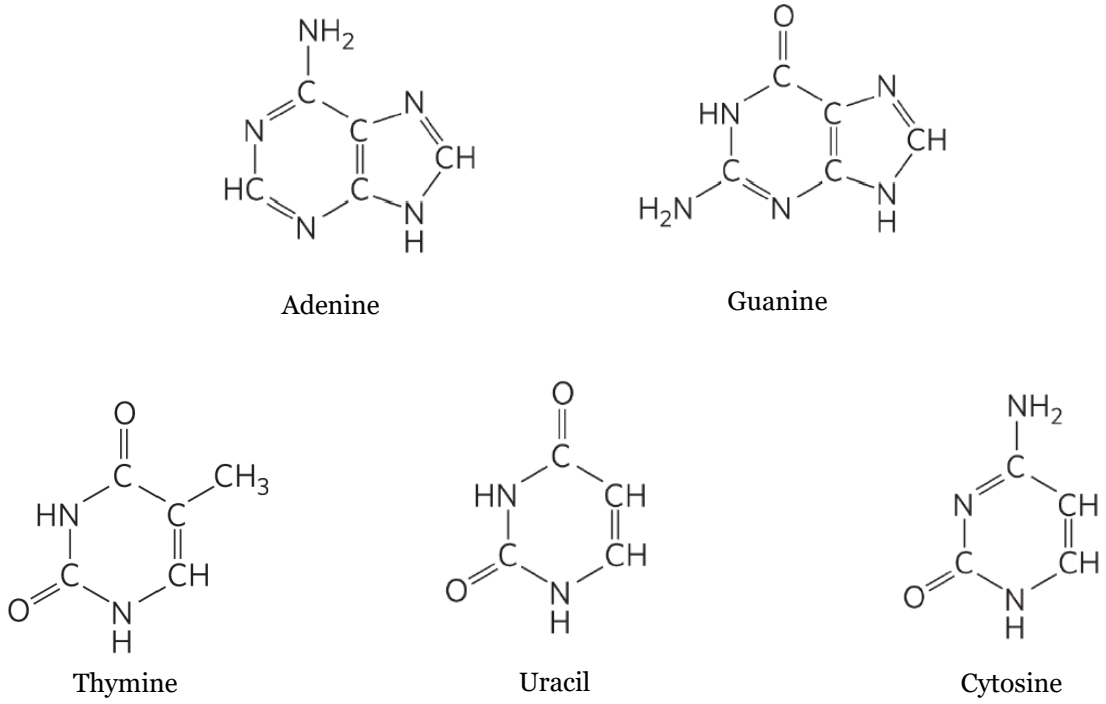

Figure 1. Nitrogenous bases of DNA and RNA.

The presence of secondary structures in RNA can be related to its function, since the variety of configurations that RNA can acquire makes this molecule a versatile biologic component that can participate in numerous cellular processes with specific functions [5, 6]. Some of those structures are described in the subsection 1.2.3.2.
RNA can be divided into two categories: coding RNA and non-coding RNA (ncRNA). The former includes messenger RNA (mRNA), while ncRNA is divided into housekeeping ncRNA, which includes transfer RNA (tRNA) and ribosomal RNA (rRNA), and regulatory ncRNA, in which microRNA (miRNA) is integrated (Figure 2). [7, 8].

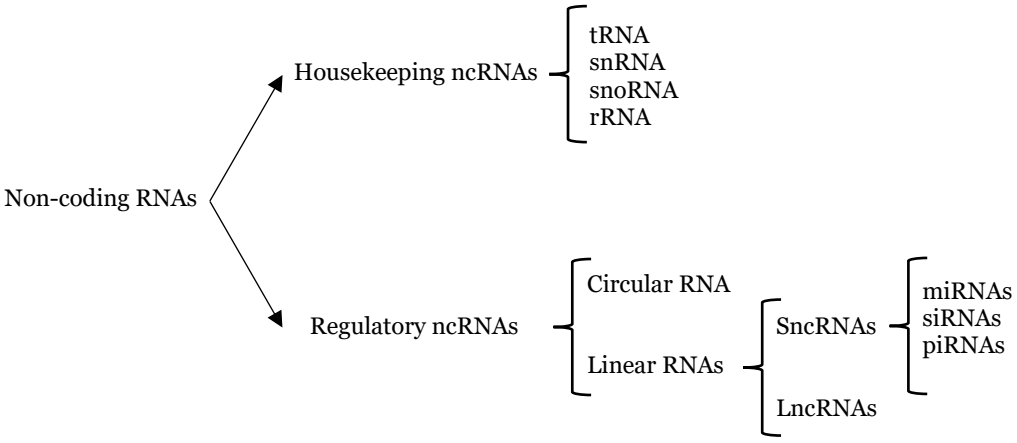

Figure 2. Schematic representation of ncRNAs classes.

Nowadays, it is well known that only 2% of the human genome is used to synthesize proteins, so it could be expected that only a small part of the genome is transcribed, but that is not the case. Approximately 76% of the human genome is transcribed into RNA, being the majority ncRNA products instead of mRNA [1, 7]. As reviewed by *Batista et al. 2021*, in recent years, particular interest in regulatory ncRNA has increased, mainly due to its important role in the regulation of several pathologies and because of that, these regulatory molecules began to be considered as potential therapeutic agents or biomarkers for some pathologies [8].

However, more recently, mRNA technology demonstrated remarkable success with the Covid-19 pandemic and the worldwide campaign of vaccination against the novel SARS-CoV-2 virus and its variants. Additionally, the mRNA technology has demonstrated enormous potential and has expanded beyond the area of vaccines in a variety of fields.

1.2. Messenger Ribonucleic Acid

1.2.1. Historical Perspective

mRNA was first discovered in the 1960s by Brenner, S., Jacob, F., and Meselson, M. who presented an integrated picture of many aspects of the intermediary role of mRNA in protein synthesis [9]. This transient nature of mRNA confers tremendous flexibility and broader therapeutic utility than nearly all other classes of known drugs [7]. As a result, the mRNA was no longer considered an intermediary between DNA and proteins due to its fundamental role as a regulator of gene expression in all biological organisms. Herein, mRNA was first delivered into cells in 1978 [10], and years later, mRNA as therapeutic was proposed by *Malone et al. 1989*, with the development of a broad and reproducible transfection technique based on lipofectin, a liposome containing cationic lipids [11]. In the following year, Jon A. Wolff and colleagues demonstrated, for the first time, that an intramuscular injection of pDNA and *in vitro* transcribed mRNA in mice led to the subsequent expression of proteins encoded by these molecules [12]. Unfortunately, mRNA was set aside, and the investigation then focused on DNA rather than mRNA, because of its instability, immunogenicity, and susceptibility to being destroyed by ubiquitous ribonucleases (RNases) when compared to DNA [13-15]. Nevertheless, mRNA technology research persisted, even though it moved slowly, until the late 1990s when David Boczkowski demonstrated that *in vitro* transcribed mRNA transferred to dendritic cells stimulated cytotoxic T lymphocyte responses *in vitro*. From this point, the interest in this molecule increased [16].

In the late 2000s, the first clinical trial performed in patients with metastatic melanoma, with direct injection of mRNA, was published [17]. In fact, since Jon A. Wolff´s article, only five original mRNA-based vaccines of naked non-self-replicative mRNA have been disclosed [18].

Additionally, understanding mRNA structure allowed the optimization of structures to enhance the molecule's stability, boost translational effectiveness, and minimize immunogenicity. In fact, a study conducted by Katalin Karikó and co-workers showed that by using modified nucleotides, the autoimmune response against mRNA was reduced or eliminated, resolving one of the major drawbacks of mRNA therapeutics, and giving new insights into mRNA production [19]. Nevertheless, for the successful therapeutic use of mRNA, several extracellular and intracellular barriers still need to be surrounded [20]. Its sensitivity to enzymatic cleavage, particularly by ubiquitous RNases found in the blood and tissues, is one of the limitations of using mRNA as a therapeutic agent. The systemic use of non-encapsulated mRNA is significantly hampered by the

presence of these nucleases and also by the existence of another barrier, such as the cell membrane, which still needs to be overcome [21-23]. Thus, mRNA encapsulation is a prerequisite for this molecule to get beyond those limitations. The improvement of mRNA distribution into target cells and tissues will enable the achievement of an increased and targeted transfection, e.g., by adding specific ligands that can recognize receptors on the cell membrane [7, 22, 24].

Nevertheless, these advances in RNA stability and targeted delivery of *in vitro* transcribed mRNA, made the scientific community start to look at mRNA as a delivery vector rather than DNA (Table 1.). This interest was also supported by the better mRNA pharmaceutical properties, such as the absence of risk of integration into genome and mutagenesis, and the transient expression of mRNA that allows a controlled exposure, and a higher protein expression when compared to DNA [25, 26].

Table 1. Advantages and disadvantages of DNA and mRNA as therapeutics (adapted from [25]).

Nucleic Acid	Advantages	Disadvantages
DNA	• Expression can last for a year. • Production is simple to scale-up. • Intramuscular injection. • Cell-free manufacture.	• Usually, low expression. • Hyaluronidase and an electroporation device are required for increased uptake. • Takes several days to get into the expression peak. • Risk of insertional mutagenesis. • Probability of repeated injections producing autoimmune antibodies against DNA.
mRNA	• Expression peak in hours. • Production is simple to scale-up. • Clinically safe and well-tolerated profile. • Various biodistribution possibilities. • Cell-free manufacture.	• Transient expression.

1.2.2. Biogenesis, Processing and Translation

1.2.2.1. Biogenesis

All RNAs are synthesized from DNA templates through the process of transcription. In eukaryotes, as in bacteria, transcription is divided into three steps: initiation, elongation, and termination. Eukaryotic cells have three different RNA polymerases that participate in the transcription of different classes of RNA, being RNA polymerase II (RNAP II) the responsible for the transcription of pre-messenger RNA (pre-mRNA), and so, is the one that will be referred to in this section. Also, there is a set of specific regulatory proteins that take part in the binding of RNAP II to the DNA template, known as the transcription factors for RNAP II (TFII) [1, 27].

Pre-mRNA synthesis occurs in the nucleus and is complementary and antiparallel to the DNA template strand, so transcription proceeds in a 5´→ 3´ direction and the ribonucleotides are added to the 3´-OH group of the growing RNA (Figure 3) [1]. The stretch of DNA that encodes for a pre-mRNA molecule and the sequences for its transcription is called a transcription unit. This sequence has three major regions: the promoter, which is responsible for the binding of the transcription apparatus and RNAP II; an RNA-coding region that possesses the nucleotide sequence of DNA that will originate the pre-mRNA molecule; and a terminator, which consists of a nucleotide sequence that signals where the transcription will end [1].

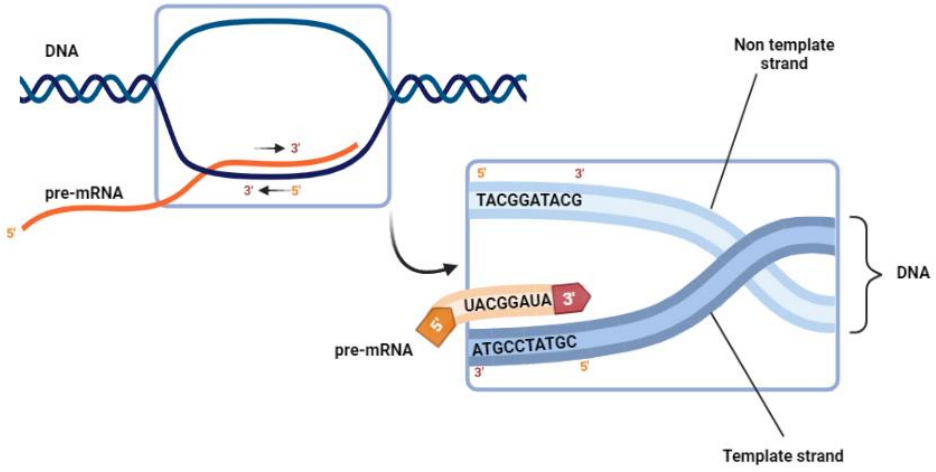

Figure 3. Representation of the transcription mechanism.

For transcription to start, a specific set of transcription factors (TF) work in two ways: first, by interacting directly with the transcription machinery, and second, by attracting proteins that modify the chromatin structure. Acetylation and methylation play a major role in modifying the chromatin structure, making it more open and accessible [1, 28]. RNAP II only binds to the promoter when the general transcription factor IID (TFIID) is attached to the TATA box sequence of DNA, which is typically roughly 25 bases upstream

from the initial ATG sequence of a protein-encoding gene [1, 29]. TFIIB recognition element, initiator element, and downstream element are additional core promoter sequences. These sequences act as binding sites for additional transcription machinery subunits, positioning those subunits asymmetrically at the promoter to control the unidirectional transcription of genes from a 5′ → 3′ direction [1, 30].

RNAP II and the general transcription factors are in an inactive state known as the Pre-initiation Complex (PIC) after binding to the promoter. The promoter is then positioned inside the active cleft of RNAP II to create the open complex, after a conformational change takes place in which 11–15 base pairs surrounding the ATG transcription start site of the gene are hydrolysed [1, 30]. The creation of the first phosphodiester bond in RNA signals the beginning of transcription.

Then, in the elongation process, the template strand of DNA enters through the RNAP II and the complementary ribonucleotides are added to the growing 3´ end of the pre-mRNA molecule [1]. Concerning the end of the transcription, RNAP II adds ribonucleotides to the 3′ end of the expanding pre-mRNA molecule until it transcribes the terminator. Transcription ends only after the terminator has been fully transcribed. At that point, the pre-mRNA molecule separates from the DNA, proceeds to the processing stage and the RNAP II separates from the DNA template [1].

1.2.2.2. Processing

During transcription, pre-mRNA passes through a series of processing stages in the nucleus before being transferred to the cytoplasm [31]. The 5' end-capping is the first RNA processing step, occurring after around 30 RNA nucleotides have been transcribed [31]. The guanylyltransferase and methyltransferase enzymes work together to change a 5´terminus G nucleotide into the cap structure commonly found in almost all eukaryotic mRNAs [32, 33]. Another structure that also participates in the pre-mRNA processing is the spliceosome. This complex molecular apparatus comprises five small nuclear ribonucleoproteins: U1, U2, U4, U5, and U6, and more than 100 distinct polypeptides that work together to precisely remove intronic regions and produce the mRNA [34]. This structure acts through two successive trans-esterifications, leveraging the exon/intron boundary (5´ and 3´ splice sites) to eliminate the intron. From a single pre-mRNA, multiple mRNA molecules are produced through alternative splicing processes, which use distinct combinations of donor and acceptor sites from different exons [6, 35]. Finally, 3′ end processing of eukaryotic pre-mRNA is made up of two stages: the endonucleolytic cleavage of the pre-mRNA and the addition of a poly (A) tail by poly (A) polymerase (PAP) at the 3´ end of the cleaved pre-mRNA [31, 36].

1.2.2.3. Translation

Translation can be subdivided into three stages: initiation, elongation, and termination. The majority of regulation occurs at the first stage, where the methionyl tRNA with initiation-specificity (Met-tRNAi) recognizes and decodes the AUG start codon. Additionally, bacteria and eukaryotes have different mechanisms for selecting the start codons, and as a result, their initiation-control strategies are also different. In bacteria, the 30S ribosomal subunit is directly recruited to the initiation region of the mRNA by base-pairing the Shine-Dalgarno (SD) sequence, just upstream of the start codon with the complementary anti-SD sequence in rRNA [37].

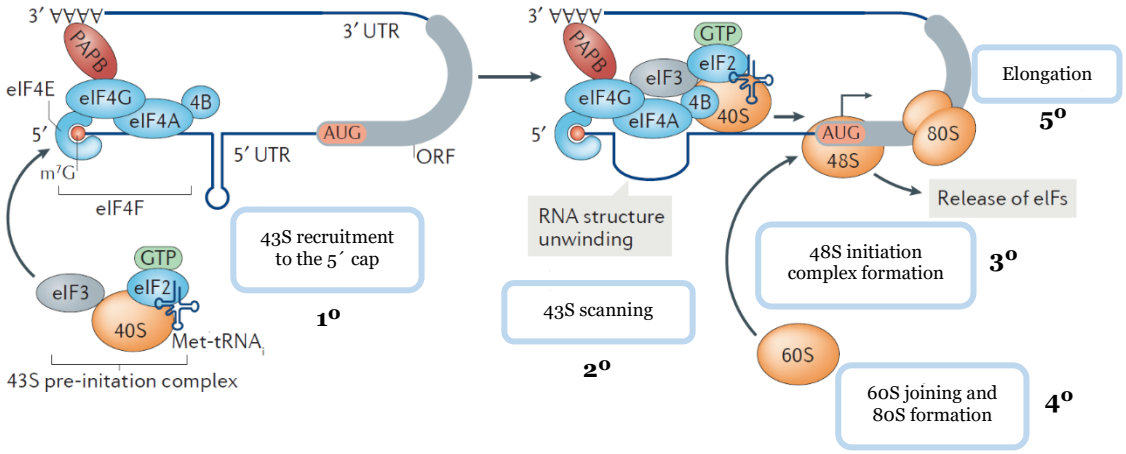

Figure 4. Schematic representation of the translation mechanism in eukaryotes (adapted from [38]).

In eukaryotes, the start codon only is efficiently identified when it is located in a suitable sequence, known as the Kozak consensus sequence, e.g., 5′ - GCCGCCRMCaugGCG-3′ (M = A or C / R = A or G) [31, 39, 40]. The poly(A) binding protein (PABP) can promote the circularization of the mRNA by interacting with eukaryotic initiation factor 4G (eIF4G) and joining the cap and poly(A) tail in a "closed loop" (Figure 4). This characteristic is believed to be responsible for PABP's capacity to enhance mRNA binding to the 43S pre-initiation complex, at least in part by improving eukaryotic initiation factor 4F (eIF4F) binding to the capped 5´ end of mRNA [37, 41]. Also, a scanning process takes place in which the small 43S pre-initiation complex, composed of 40S ribosomal subunit and the eukaryotic initiation factors eIF1, eIF1A and eIF3, binds to the mRNA at the 5' cap and scans the 5' UTR for the AUG (or in rare cases a near-cognate AUG) codon, base paring between AUG and the Met-tRNA anticodon in the ribosome [37, 42]. Next, the 60S ribosome subunit joins the 43S pre-initiation complex creating the functional 80S initiation complex for protein elongation. In this intermediary phase, the codon sequence of the mRNA instructs the 60S subunit's peptidyl transferase activity to link together amino acids until it founds a STOP codon (UAA, UAG, UGA), leading to

the dissociation between the ribosome and the mRNA, resulting in the termination of translation [37, 42]. The newly synthesized polypeptide is then allowed to fold to its native structure and proceed to the post-translation modifications.

1.2.3. Structure and Function

mRNA is composed of 5 distinct sequences, each of them specialized in a specific function, which are: 5´ Cap; 5´ Untranslated Region (5´ UTR); main Open Reading Frame (mORF); 3´ UTR; and a poly (A) tail (Figure 5). Generally, 5´ Cap and Poly (A), are associated with mRNA translation stability. On the other hand, the 5´ UTR and 3´ UTR are related to the mRNA translation half-life. The mORF sequence is subdivided into codons which are responsible for coding amino acids monomers that will originate the protein after translation.

Figure 5. Structure of the messenger RNA.

1.2.3.1. 5´Cap

The 5´cap structure is found in almost every eukaryotic mRNA molecule. This cap structure, also known as $m^7G(5´)pppN1pN2p$ (cap – 0) (Figure 6), refers to a guanosine nucleotide that suffers methylation at the N^7 position. This structure attaches to the first nucleotide through a 5´- 5´ bond via two pyrophosphoryl bonds. Additionally, the capping process is carried out by different enzymes, including guanylyltransferase and methyltransferase. The first two nucleotides of the mRNA can also undergo the methylation process in the 2´-hydroxyl group. In that case, if the first nucleotide is methylated, then it is referred to as $m^7G(5´)pppN1mpN2p$ structure (cap - 1), but if the first and second nucleotides are methylated, the cap structure is known as $m^7G(5´)pppN1mpN2mp$ (cap – 2) (Figure 6) [43, 44]. Herein, the molecular pattern responsible for distinguishing self-mRNA from nonself-mRNA is precisely the presence of the methylations in the cap structure e.g., cap-1 and cap-2 [43, 45]. Uncapped transcripts or mRNAs with cap-0 are recognized by the innate immune receptor RIG-1 and considered pathogenic [43, 46].

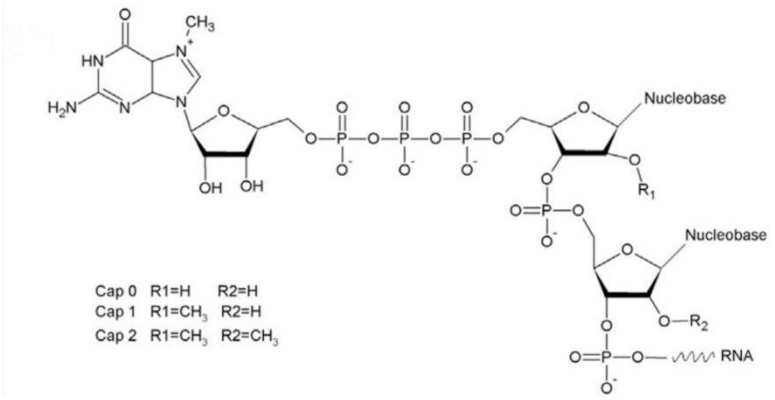

Figure 6. Molecular structure of the cap 0, cap 1 and cap 2.

If the first nucleotide where the cap structure attaches is a 2´-O-methyladenosine (A_m) [47], it can be further methylated at the N6 position of Adenine, forming a m^6A_m. This methylation process confers to mRNA enhanced stability by increasing the resistance to the mRNA-decapping enzyme DCP2 [44, 47]. Furthermore, the demethylation process of the m^6A_m to A_m can also occur, being mediated by the obesity-associated protein, suggesting that the modifications at the 5´- end cap are a dynamic process and could be related to some extent to the regulation of gene expression [43, 48].

The cap structure is one of the hallmarks of the regulation of protein synthesis in eukaryotes, as it is essential for splicing, polyadenylation, mRNA stability, and translation [43, 49]. The mRNA cap functions are linked to the interactions of proteins and complexes with this structure, where modifications to the 5´ end Cap can enhance or inhibit the affinity to its co-factors [49]. The previously described modifications are essential for the (1) recruitment of several translation initiation factors to mRNA, as is the case of the eukaryotic initiation factor eIF4E that binds to the mRNA via cap. This structure is also crucial to the (2) recognition of this molecule as an intrinsic biological cell component and enabling the cell to discriminate it from other viral RNAs [50]. Moreover, it is important to (3) cap-binding proteins that can act on gene expression with different outcomes and finally to (4) prevent the mRNA degradation by preventing exonucleases action [44, 49].

1.2.3.2. 5´ Untranslated Region

The 5´ UTR structure in eukaryotes varies from 53 nucleotides (yeast) to 218 nucleotides (humans). Still, 5´ UTR lengths change profoundly among individual genes, implying that may exist a greater regulation of mRNA expression [38]. For example, all mRNA species in mammalian mitochondria lack the 5´ UTR [51], in other cases, this structure can be extremely short (12 nucleotides) being known as the translation initiator of short 5´UTR (TISU) not following the initiation scanning mechanism [52], other 5´ UTR species can acquire a highly complex structure capable of blocking the entry of the

ribosome [53]. However, even though mRNAs with no/or very short 5´ UTR can undergo translation initiation, it is believed that the minimal length required is 20 nucleotides for efficient recognition of the start codon by the ribosome [43].

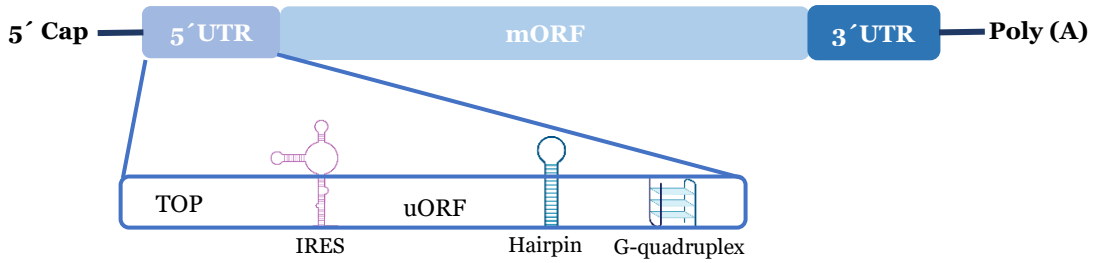

Figure 7. Cis-regulatory elements present in 5´UTR.

Moreover, in the 5´ UTR sequences there are a variety of cis-regulatory elements (Figure 7) responsible for the transport, stability, and translation efficiency of the mRNA molecules [43]. The terminal oligopyrimidine (TOP) is located immediately before the cap structure and possesses a conserved 5´cytidine residue followed by a sequence of 4 to 15 pyrimidine nucleotides. This motif is present in mRNAs from the TOP family that encodes practically all the ribosome proteins, some translation factors, and its target of the rapamycin complex 1 signaling pathway, directly affecting the gene expression [43, 54]. On average, the 5´ UTR on TOP mRNA contains 40 nucleotides long and is free from secondary structures [43]. The regulation of the translation in TOP mRNAs is entirely associated with this motif, and its function is completely dependent on the presence and location of the conserved 5´ cytidine residue insofar as, if the 5´cytidine residue is replaced by another nucleotide, or even just proceeded by an Adenosine residue the translation initiation does not occur [54, 55].

The internal ribosome entry site (IRES) is responsible for the direct recruitment of the 40S subunit of the ribosome without the need for the 5´ cap. IRES can be found in some eukaryotic mRNAs and in viral genomes. Also, this sequence allows the mRNA translation when the cap-associated initiation mechanism is suppressed, e.g., during stress conditions, mitosis, and apoptosis [56-58].

Concerning the upstream open reading frame (uORF), it is present in at least 50% of mammalian mRNAs [59]. In contrast to the mORF, this sequence can be translated into short peptides through a non-AUG as the start codon, being the most common CUG, GUG, UUG and ACG near-cognate codons, although with much lower efficiency than AUG [43, 60]. Also, the short-translated peptides from uORF are associated with the regulation of the mORF, generally acting as repressors of translation [61, 62]. Still, in certain conditions like stress, the uORFs are necessary to activate the mORF, allowing

the cell to adjust the abundance of a certain protein regarding a surrounding environmental stimulus [61, 62]. It has also been described that uORFs play an important role in mammalian development by regulating the protein levels during the cell differentiation in this early stage [62, 63], being one of the best-characterized examples, the regulation of the activating transcription factor 4 in mammals by its uORF [43, 62, 64].

As previously referred, the structure of the nucleic acids depends on their sequence. Their nucleotide composition causes the mRNA to have an inherent tendency to fold and form a higher-order structure, therefore exhibiting a second level of structural information beyond the linear sequence. The presence of secondary structures like hairpins and G-quadruplexes in the 5´UTR and others (reviewed in [38]) has been reported as influencing mRNA translation, preventing the ribosome loading and the scanning process, or enhancing the translation, functioning as activators and promoting the binding of eukaryotic initiation factors to the ribosome [38, 43, 65].

1.2.3.3. mORF

The mORF contains the codons necessary to determine the order by which the amino acids will be added during translation. The mORF starts with an AUG codon that codes for methionine and ends with a STOP codon (UGA, UAA, UAG), not encoding any amino acid [1, 43].

1.2.3.4. 3´ Untranslated Region

Similar to the 5′UTR, the 3′UTR has a large number of cis/trans-regulatory elements that significantly affect RNA stability, subcellular localization, and translation efficiency (Figure 8). The 3′UTR can be between a few and a thousand nucleotides long. It is generally accepted that a shorter 3′UTR increases the stability of the transcript, perhaps as a result of the lack of microRNA binding sites that prevent mRNA degradation. Additionally, multiple polyadenylation sites (PAS) enable alternative polyadenylation (APA) to produce a variety of 3′UTRs. Increasing data indicate that APA is responsive to signaling pathways and occurs in a cell type-specific manner [43, 66, 67].

Numerous cis-regulatory components found in the 3′ UTR influence the localization, turnover, and translation of mRNA. The adenylate uridylate (AU-rich) element (ARE), denoted by the pentamer "AUUUA," is the most prevalent cis-regulatory element. The recruitment of the degradation apparatus by some AU-binding proteins (AUBPs) results in a process known as ARE-mediated decay [68]. In addition to the ARE, there are numerous other cis-elements, GU-rich elements (GRE), CU-rich elements and CA-rich elements.

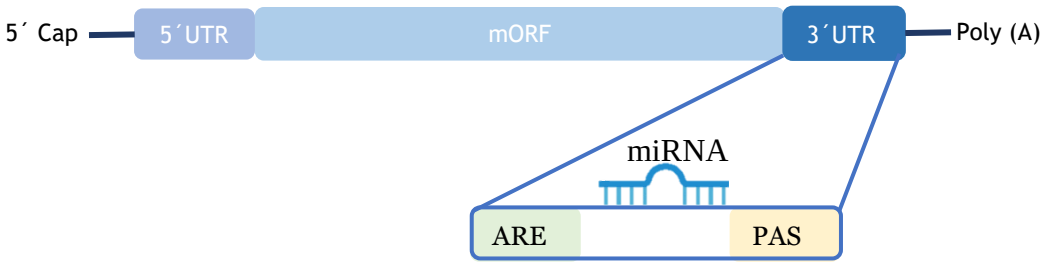

Figure 8. Cis-regulatory elements and Trans-regulatory elements present in 3´UTR.

Their functional impact varies based on the related trans-acting factors. miRNAs, which control the expression of more than 60% of human protein-coding genes by translational repression and/or mRNA degradation, are arguably the most well-known 3′UTR trans-acting factors, as they interact with complementary regions on 3′UTRs to cause target RNA degradation [43, 69].

Interestingly, even though the great majority of ARE-binding proteins suppress the translation of target mRNAs by inducing their decay or repression, ELAV/HuR proteins enhance the stability and/or translation of target mRNAs, at least in part by preventing the repression caused by other RNA binding proteins (RBPs) and miRNAs [70].

1.2.3.5. Poly (A) tail

Poly(A) tails are non-templated additions of adenosines at the 3' end of most eukaryotic mRNAs, being composed of 200–250 adenosines and are produced after endonucleolytic cleavage of the pre-mRNA. RBPs, such as the PABP, have a binding site for mRNA that is polyadenylated. The poly(A) tail and the proteins that are linked to it help to mediate mRNA degradation in the cytoplasm while defending mRNA against enzymatic cleavage in the nucleus. The poly(A) tail not only contributes to mRNA turnover but is also essential for mRNA translation. The finding of the relationship between the 5′ cap structure and 3′ poly (A) tail binding proteins led to the initial formulation of the "closed-loop" concept of translation initiation in eukaryotes. The "closed-loop" model enables the direct recycling of the 40S ribosome subunit after termination and helps us to explain the synergistic effect of the 5´cap structure and poly(A) tail in promoting translation initiation [41].

1.2.4. Engineering and Design

In the past decades, significant work has been done regarding the optimization of the five main sequences of the mRNA and its constituents, e.g., 5′ Cap, 5′UTR, mORF, 3′UTR and poly (A) tail, in order to systematically increase its intracellular stability, translational effectiveness and lower the immunogenicity (Figure 9). A well-optimized mRNA sequence can produce protein in considerable amounts for extended periods of

time, ranging from a few minutes to more than 29–31 weeks, according to the intended time of the mRNA application. [43, 71].

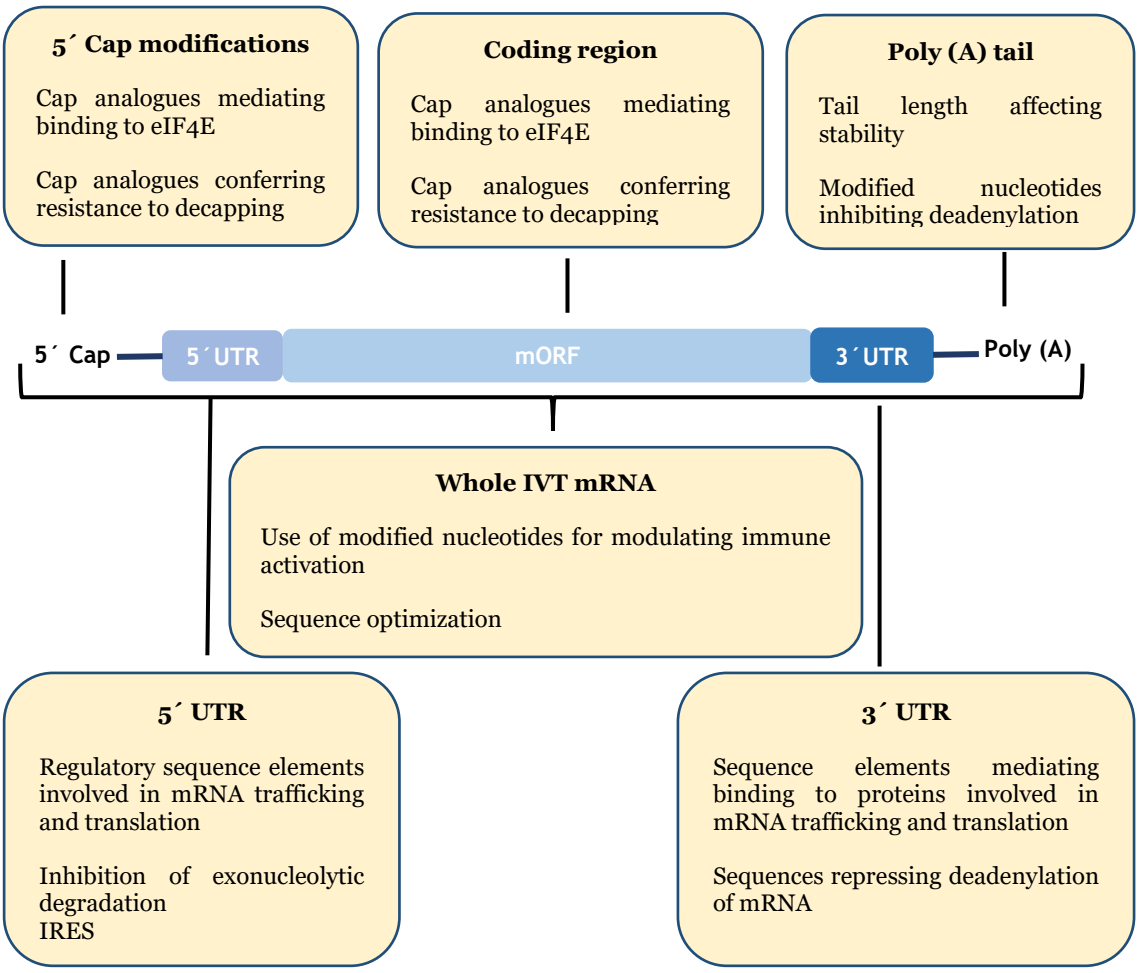

Figure 9 Structural modifications and optimization for tuning mRNA pharmacokinetics.

1.2.4.1. Cap

Concerning the 5´Cap, several strategies for modifying and augmenting the translation efficacy have been published [71]. The most popular method combines capping and *In Vitro* Transcription (IVT) in a single step by adding a synthetic cap analog to the IVT reaction. Numerous cap analogs have been studied until today (Table 2). mRNA capping can be performed after the mRNA IVT synthesis, with a subsequent reaction using capping enzymes generated from recombinant vaccinia viruses, and the resulting cap structure is the same that occurs naturally in eukaryotes [72]. Additionally, a co-transcriptional capping technique can be used to create a naturally occurring Cap-1 structure, such as m^7GpppAmG, with a high efficacy known as the clean cap [73].

Table 2. Features of the different cap analogs.

Cap Analogue	Features	Ref.
m^7GpppG	▪ Low yields of capped mRNA; ▪ Possibility of being reverse incorporated; ▪ No resistance to decapping enzymes; ▪ Lower half-lives.	[74]
m^7Gpppm^7G	▪ Incorporated at the correct orientation.	[43, 71]
$m^7Gppppm^7G$	▪ Incorporated at the correct orientation; ▪ Better results at the translation level.	
$m_2^{7,2-O}GpppG$ $m_2^{7,3-O}GpppG$ Anti Reverse Cap Analogue (ARCA)	▪ No risk of reverse incorporation; ▪ Superior translation efficacy; ▪ Prolonged protein production.	[75]
$m_2^{7,3-O}GppspG$ $m_2^{7,3-O}GppspspG$ (phosphate-modified ARCA)	▪ No risk of reverse incorporation; ▪ Greater affinity to translation factors; ▪ Resistance to decapping enzymes; ▪ Bigger half-life.	[76]
m7GpppAmG (Clean cap)	▪ Naturally occurring cap structure; ▪ High efficacy.	[73]

1.2.4.2. 5´ and 3´ Untranslated Regions

Most therapeutic mRNA applications require 5´ and 3´ UTRs that result in the maximum level of translation; however, depending on the mRNA applications it may be required an extremely fast translation or brief protein translation times. Accordingly, these two regions can be optimized in order to promote a longer or shorter translation time, depending on the therapeutic objective [43, 71]. A shorter 5′UTR with at least 20 nt is advised to reduce the scanning process. Additionally, potential upstream start codons (particularly AUG) should be avoided to prevent the occurrence of uORF, which frequently inhibits translation. Highly stable secondary structures should also be avoided, especially those close to the 5′ end, as they can interfere with ribosome loading, scanning, and start codon selection [43, 77]. Since the 3′-UTRs contain the majority of the destabilizing cis-acting regions, mRNAs with shorter 3′-UTRs usually lack regulatory motifs and exhibit higher levels of stability. For instance, the two instability sequences that are most frequently present in the 3′-UTR are AREs and GREs. In synthetic mRNA, avoiding those motifs can slow down rapid turnover [43, 71].

Finally, the most well-known and characterized UTRs sequences used in mRNA engineering were 5´ UTR and 3´ UTR based on β-globin mRNAs, which have been used

from basic applied research to clinical trials [78, 79]. Although, recent studies have started to integrate other sequences, which offer also good translation efficiency and stability, e.g., 5' UTR consisting of a partial sequence of the cytomegalovirus immediate early 1 (IE1) gene and 3' UTR consisting of a partial sequence of the human growth hormone (hGH) gene with proved functionality *in vivo* [80].

1.2.4.3. mORF

Due to the degeneracy of the genetic code, apart from methionine and tryptophan, each amino acid is frequently represented by numerous synonymous codons. tRNAs can decode synonymous codons that code for the same amino acid, with varying degrees of efficiency and at varied frequencies. Based on tRNA abundance, codons can be divided into optimal and nonoptimal. This idea is supported by the fact that highly expressed genes typically have optimal codons, while non-optimal codons are thought to slow down the translation elongation [43, 71]. Therefore, in order to increase translational efficiency, optimal codon utilization makes sense. Codon optimization is often accomplished by selecting the best optimal codon for a certain amino acid, based on the frequency of occurrence in various species [43, 71]. However, as revised by Sergio Linares-Fernández and colleagues, high mRNA translation rates do not always have a positive effect, since some proteins need a slower translation rate to maintain appropriate folding and stability. Therefore, codon optimization should be done taking into account the complexity of the protein to be translated by the mRNA [81].

Additionally, it is also been demonstrated that compared to adenine and thymine rich counterparts, mRNAs with high guanine and cytosine content are more stable and have higher translation efficiency [82, 83]. Because of this, it is a common practice in the designing of therapeutic mRNA to optimize the guanine and cytosine content in the whole mRNA sequence together with the codon optimization in the mORF [84].

1.2.4.4. Poly (A) tail

The ability of poly(A) tail to bind to PABP depends on its length. For effective translation and closed-loop formation, exogenously delivered mRNAs with at least 16 nt of the poly(A) tail are required. The idea "the longer the better" is not necessarily accurate, despite the fact that the length of the poly(A) tail has been shown to positively correlate with mRNA translation, shorter poly(A) sequences have been shown to encourage the production of mRNA with closed loops for effective translation [41, 85]. It has been also demonstrated that a mixed poly(A) tail with sporadic non-A residues, especially guanine, blocks the mRNA decay pathway and stabilizes mRNA [86].

1.2.4.5. Modified Nucleotides

Therapeutic mRNAs frequently use modified nucleosides to avoid being recognized as a pathogenic agent by reducing immune response mediated by several immune receptors (reviewed in [87]). The nucleosides 5-methylcytidine, pseudouridine, N(1)-methylpseudouridine and others are frequently utilized [88-90]. It is noteworthy that many of these modified nucleosides have relatively decreased T7 RNA polymerase incorporation efficiency during IVT. Additionally, decoding efficiency and fidelity may be impacted when a specific codon contains these alterations [43, 91].

1.3. mRNA Production Strategies

1.3.1. Chemical Synthesis

Concerning chemical synthesis, the standard model used is phosphoramidite chemistry which has been used and optimized to produce oligonucleotides. The synthesis success depends on the yields of the sequential deprotection-coupling-oxidation reactions. Since this method could not produce high-quality RNA, it needs to be further purified by HPLC in order to acquire the desired purity to be market available [8, 92]. Nevertheless, some interesting advantages make this method more attractive when it comes to developing a more stable RNA molecule with enhanced pharmacokinetics properties, e.g., the incorporation of phosphorothionate can improve the nucleolytic resistance and increase the oligonucleotide binding affinity for plasma proteins, which is crucial for the *in vivo* clearance of synthetic molecules. Also, this particular type of modification is relatively simple and inexpensive and is commonly found in antisense therapeutics like small interfering RNA (siRNA), miRNA and RNA aptamers [8, 92, 93].

Notwithstanding, chemical synthesis provides a wide range of modifications capable of enhancing the properties of the oligonucleotides, and despite that nucleotides are naturally modified intracellularly, the fact that those alterations could be placed in a different location during chemical synthesis can stimulate the immune system by recognizing this synthetic RNA molecules as a pathogenic element. Additionally, these modifications can alter the RNA structure, leading to a compromised function of the therapeutic agent [8, 92].

Finally, when the intent is to synthesize RNAs longer than 100 nucleotides, this method is not adequate because as the molecular length and content of modifications increase, the costs associated with the synthesis also increase, and the yields decrease. Furthermore, the quantities obtained are extremely modest (micromolar scale), limiting animal and clinical investigations [8, 92, 94]. Herein, one alternative to chemical

synthesis that can surpass some of these limitations is the enzymatic synthesis which will be described next.

1.3.2. Enzymatic Synthesis

Presently, enzymatic synthesis by IVT is the standard method for mRNA production. The template can be a linearized pDNA or a polymerase chain reaction (PCR) model. With the PCR template method, two primers must be used. One, with the promoter sequence for IVT reaction, binds at the 5´ end of a single-stranded DNA (ssDNA) template, and the other hybridizes at the 3´ end with a poly(A) tail, resulting in a dsDNA template ready for IVT. The major advantage of this approach is related to the non-variability of the length of poly(A) tail that can occur using the linearized pDNA. In addition, it is fast and does not put plasmid vectors with poly[(A/T)] stretches at risk of replication instability [95]. Additionally, a PCR template may be preferred if a longer poly(A) is required and/or if the plasmid does not contain the T7 promoter region needed for IVT [96].

Concerning the linearized pDNA approach, pDNA is commonly digested with an IIS-type restriction enzyme, mainly because it prevents the incorporation of unwanted nucleotides (non-A nucleotides) at the 3´ end, which can mask the poly(A) tail and compromise its function by altering its structure [7, 97]. However, the pDNA digestion can also be performed by enzymes that leave 3´ over-hangs. In that case, the formation of aberrant by-products may occur, e.g., large amounts of long template-sized RNA transcripts can hybridize with the pDNA [98].

Additionally, mRNA contains structural sequences, all of them except 5´ - Cap can be transcribed from the original pDNA template, being the incorporation of poly[(A/T)] tail optional [99]. The initial mixture for an IVT reaction contains all the necessary nucleotides, chemically modified or not [19], a bacteriophage RNA polymerase (T7, T3 or SP6) that recognizes the promoter located upstream of the sequence to be transcribed and a previously linearized pDNA template. The IVT reaction initiates when the RNA polymerase recognizes its promoter and only terminates when it reaches the cleavage site of the enzyme used to digest the pDNA [7, 44, 100].

Regarding the addition of a cap to the 5´ end, a synthetic cap analog (Table 2) can be added during the IVT reaction. If the cap analog is in excess to the detriment of guanosine triphosphate (GTP), the transcription begins with the cap analog rather than GTP, producing capped mRNA [7, 100, 101]. In addition, mRNA capping can also be performed after IVT reaction through a vaccinia virus capping enzyme (VCE), which

possesses guanylyltransferase and methyltransferase activity, thus adding a 2´-*O*-methyl group to the penultimate nucleotide. The resulting cap 1 structure mimics the naturally occurring cap structure found in eukaryotic cells. Although this post-transcriptional capping through VCE seems advantageous, it requires further purification steps, so it is not indicated for large-scale mRNA production [7, 43].

Similarly, the poly(A) tail can as well be added next to the IVT reaction, using the PAP, enabling the incorporation of various nucleosides into de poly(A) tail, however, this method is not consistent and reproducible, giving origin to poly(A) tails of different lengths [7, 43, 44].

1.4. mRNA Downstream Processing

1.4.1. Precipitation

Most purification strategies for the selective isolation of RNA from complex mixtures have a preliminary refinement of the sample before proceeding to more advanced separation methods [2]. Therefore, methods like precipitation and solvent extraction benefit from the different biomolecule's solubilities in various solvents and ionic environments [2]. Precipitation is typically carried out after *in vitro* enzymatic reactions to separate the target RNA from the protein and DNA contaminants or simply for buffer exchange, whereas solvent extraction followed by precipitation is the preferred method to isolate large volumes of total RNA from natural sources [2]. RNA is very soluble in water due to its negative charge and polar backbone. When many cations are employed with ice-cold ethanol as a co-solvent, the backbone charges can be successfully neutralized, and the solubility can be decreased to the point where the RNA selectively precipitates out of the solution. Depending on the size and concentration of the RNA to be precipitated, a variety of cations and their salts, including lithium chloride and ammonium acetate, can be utilized [2, 102].

1.4.2. Solvent Extraction

The development of acid guanidinium thiocyanate-phenol-chloroform extraction as a method for isolating RNA was initially made as an alternative to the time-consuming ultracentrifugation method for total RNA isolation from mammalian tissues. In this procedure, the sample is incubated with an equimolar mixture of phenol and chloroform, allowing proteins to be denatured by the guanidinium thiocyanate and then separated in the organic phase, while RNA is dissolved in the aqueous phase. Following centrifugation to separate the two phases, ethanol or lithium chloride precipitation can be used to recover the RNA. The polar phase is maintained under acidic conditions (pH 4-6) in acid

guanidinium thiocyanate-phenol-chloroform, allowing the RNA to stay soluble while the DNA undergoes repartition at the interface [2, 103].

1.4.3. Preparative denaturing PAGE

Polyacrylamide gel electrophoresis (PAGE) has been the standard for decades since it can be used to purify high amounts of RNA (micrograms to milligrams scale) with single-nucleotide resolution and only needs a small setup of affordable reagents. Like all electrophoretic methods, PAGE separates molecules by size, as charged macromolecules move through an electric field. The process is quite time-consuming because, after denaturing PAGE, the RNA must be eluted from a gel matrix, concentrated, equilibrated in the correct buffer, and finally refolded. Additionally, this method can introduce acrylamide impurities, which can interfere with the RNA analysis and are difficult to remove from RNA products [2, 104].

1.4.4. Tangential Flow Filtration

Tangential flow filtration (TFF) is used in large-scale production of mRNA by IVT, because unlike dead-end filtration, which passes the feed through a membrane and releases the filtrate at the other end, TFF involves a feed containing a biomolecule solution flowing tangentially across the surface of the filter. The main benefit of TFF is that, unlike dead-end filtration, it can be a continuous operation. The TFF filtration process washes away the filter cake, lengthening the period the filter unit is in operation. Also, solid materials can quickly block the filter surface in dead-end filtration, hence TFF is primarily employed for feeds containing small-size particles. The feed flow is forced through the filter by the supplied pressure, and the retentate is sent back to the feed reservoir for recirculation [105].

Although RNA precipitation methods have been employed on a laboratory scale in the past, they are time-consuming and require the use of organic solvents, such as alcohols, which makes them unsuitable for large-scale good manufacturing practices (GMP). The TFF approach is more commonly employed, instead of mRNA precipitation techniques, including for the production of SARS-CoV-2 mRNA vaccines and others [106-109].

1.4.5. Liquid Chromatography

Nowadays, chromatography is the gold-standard method in the biotechnological industry to purify different types of biomolecules. This technique possesses attributes like selectivity, versatility, scalability, and cost-effectiveness, making it a powerful method to meet the directives of regulatory agencies such as Food and Drug Administration (FDA) and European Medicine Agency (EMA) [110]. Generally,

chromatography is defined as a method where a complex mixture of different molecules interacts between two phases, the stationary phase and the mobile phase. Preferentially the molecules of interest are retained in the stationary phase, and the remaining ones that do not interact are eluted together with the mobile phase, commonly called contaminants [110].

When it comes to mRNA purification, unless it suffers an initial treatment, the initial mixture contains all the IVT reagents, including template DNA, nucleotides, enzymes and sub-products of IVT [105, 111]. Until now, mRNA could be purified by DNase digestion followed by precipitation using a lithium chloride solution [18]. Also, silica membrane columns are frequently employed. These techniques can successfully remove free ribonucleotides and other minor impurities but cannot eliminate fragmented DNA, aberrant mRNA sequences, or multimeric RNA species. As a result, Katalin Karikó and her team employed a reversed-phase HPLC to remove impurities from synthetic mRNA and showed that modified mRNA purified in this way produced higher amounts of proteins [19]. Furthermore, reversed-phase HPLC purification not only reduced the immunological stimulation of unmodified mRNA, but also eliminated it totally for modified mRNAs. However, reversed-phase HPLC has the drawback of using organic solvents and is also less effective for longer mRNA sequences [112]. As a result, size exclusion chromatography (SEC), TFF, and anion-exchange chromatography (AEC) are equally effective approaches for purifying mRNA [112]. In fact, there has been shown that synthesized mRNA can be effectively purified by SEC [113]. Additionally, small IVT RNA molecules (less than 500 ribonucleotides) have primarily been purified using AEC [114, 115]. The purity of the synthetic mRNA can also be improved by combining several purification methods. For instance, cellulose and hydroxyapatite chromatography can be combined to purify synthesized mRNA and to separate a mixture of single-stranded RNAs (ssRNAs), double-stranded RNAs (dsRNAs), dsDNAs, and ssDNAs [116].

Thereby, eliminating the sub-products of the IVT is essential since their presence is linked to a lower translation efficiency and can modify the immunostimulatory profile of the mRNA [19, 105]. Given the high demand for pure and stable mRNA in the biopharmaceutical industry and the well-known benefits that liquid chromatography has shown in this field, a more detailed description of the chromatographic techniques is presented below.

1.5. Chromatographic Techniques in mRNA Purification

1.5.1. Size Exclusion chromatography

SEC fractionates and purifies our target molecule according to size differences and can be used as a single step or in sequence with other chromatographic methods [2]. SEC is the most basic type of chromatography for the purification of oligonucleotides. Short oligoribonucleotides purified by HPLC can benefit from SEC polishing usage for eliminating salts. With this additional desalting step, harmful effects from limited amounts of solvents or by-products of synthesis that might remain after purification are avoided [117]. This method has also been investigated as a substitute for preparative denaturing PAGE in the purification of homogeneous-length RNA produced by IVT [118, 119]. However, several time-consuming preparatory steps still need to be completed before using SEC-based methods, such as protein removal via phenol/chloroform extractions, followed by desalting and sample concentration [114]. These methods enabled a preparative scale purifying procedure that produced excellent yields and purity, although it has drawbacks because it cannot get rid of contaminants of comparable sizes, including dsDNA and is not effectively scalable to an industrial level [2, 105, 120].

1.5.2. Ion Pair Reverse Phase Chromatography

Ion-pair reverse-phase chromatography (IPC) has been proven to be a very effective technique in mRNA purification [121]. Quaternary ammonium compounds, which ion-pair with the negatively charged sugar-phosphate backbone of the oligonucleotide, are commonly used in IPC. These ion-paired complexes then become lipophilic and interact with the stationary phase of a reversed-phase chromatography column [105, 122]. The elution process is carried out using a gradient of an appropriate solvent, such as acetonitrile. Despite this method successfully eliminates dsRNA contaminants while preserving the high yield of the procedure, it uses denaturing conditions, and the utilization of toxic chemicals like acetonitrile should not be considered because scaling it up is difficult and expensive [105, 122]. Although, a novel cellulose-based chromatographic technique using an organic solvent for the separation of ssRNA and dsRNA has been published [116]. Also, another study used the same strategy where the capacity of dsRNA to bind to cellulose in the presence of ethanol has demonstrated remarkable success with yields superior to 65 % and a dsRNA removal greater than 90 %. However, other impurities were not eliminated, requiring the introduction of pre-purification steps [120].

1.5.3. Ionic Exchange Chromatography

Ionic exchange chromatography (IEC) explores how the target mRNA species, and the other contaminants differ in charge. For instance, mRNA and IVT contaminants have been successfully separated using weak AEC. In AEC, the anionic oligonucleotide can interact with the cationic groups that are present in the stationary phase. After that, a salt (NaCl) gradient is used to elute and separate the mRNA from other impurities [114]. However, certain AEC techniques still require denaturing conditions to achieve complete oligoribonucleotide resolution, either using severe alkaline conditions or with heated mobile phase and salt concentrations [2, 105, 123]. Denaturation frequently results in a misfolded, aggregated, or even degraded product becoming unusable and economically disadvantageous [2, 105, 123].

1.5.4. Hydrophobic Interaction Chromatography

Another popular chromatography technology for mRNA purification is hydrophobic interaction chromatography (HIC). It is similar to reversed phase and takes advantage of the differential in hydrophobicity between mRNA and its contaminants. Since no hazardous chemicals are required, it has the potential to replace the conventional reversed-phase approach. In addition, native purification is possible, and the resins are scalable. HIC columns separate single-stranded RNA from proteins and short abortive transcripts, however, they are more suitable for polishing than for capture due to the chromatographic media's propensity for fouling, caused by extremely high protein and aggregates binding, triggered by the high salt concentrations present in the mobile phase [124, 125].

1.5.5. Affinity Chromatography

Affinity chromatography (AC) has emerged as a significant platform in the manufacture of therapeutic bioproducts due to its unique ability to mimic and take advantage of real biological interactions, like molecular recognition to selectively purify the target molecule [2, 126, 127]. Due to the specific biorecognition of the target biomolecule by the ligand, affinity chromatography has the unique ability to establish a variety of interactions, including electrostatic and/or hydrophobic interactions, Van der Waals forces and hydrogen bonds, giving AC an incredibly high selectivity and high resolution. As a result, the target biomolecule can be extracted from a crude sample in a single step with enhanced purity and good recovery [2, 126, 127]. Depending on the employed matrix and the chemical properties of the biomolecules, elution stages can be carried out either specifically, employing a competitive ligand, or non-specifically, by modifying the pH, ionic strength, or polarity of the mobile phase [2, 128].

Due to the adaptability of the stationary phases, various RNA purification techniques have been developed with different ligands, e.g., antibodies, oligonucleotides, dyes, boronate groups, or chelated metal ions, some of which have been reviewed [2, 127]. Although considering the purification of mRNA, the most promising and already used strategies are those based on nucleotide-based affinity chromatography [124, 129-131]. For instance, in laboratory applications, the deoxythymidine (dT) single-stranded sequence known as Oligo d(T) is frequently utilized to trap mRNA. The poly-A tail of the single-stranded mRNA produced during IVT attaches to the stationary phase while contaminants are washed off, which allows the effective removal of dsRNA, the DNA template, and unconsumed chemicals from IVT [2, 132]. Although AC can produce highly pure products, usually, it is a very expensive procedure [105].

1.6. Cryogels

Agar, dextrose, or silica have all been used as particle matrices in the aforementioned chromatographic procedures. Despite their high efficiency, these supports have numerous limitations, including limited flow rates, losses at high pressures, and risk of environmental impact. Additionally, they have a poor binding capacity and significant mass transfer resistance when it comes to the purification of large biomacromolecules like some proteins and nucleic acids [133-136]. A number of supermacroporous supports have been developed to circumvent these limitations, enabling the creation of convective channels with lower mass transfer resistance [133, 134]. However, in these systems, diffusion transport is still seen. Therefore, in recent years, the creation and use of continuous beds, such as monoliths and cryogel-based systems, have been developed as alternatives to address some of the shortcomings of traditional chromatographic matrices [133, 134, 136].

The method of mass transfer is one key distinction between cryogels and conventional chromatographic supports. Cryogels ensure unrestricted convectional transport, while conventional supports only carry out mass transport by diffusion [133-135]. These supports enable an effective chromatographic separation of nanoparticles, cell organelles, and even whole cells thanks to this convective mass transfer [133, 134, 136]. These chromatographic supports can be used in the form of monoliths as well as membranes, combining the advantages of membrane chromatography in terms of high flow rates and high reproducibility [133, 136, 137]. Short diffusion distances allow the utilization of the immobilized ligand on the pore walls of cryogels [133, 134, 136].

Cryogels are gel systems formed under cryogenic conditions (freezing - polymerization in the frozen state - thawing) of solutions or colloidal dispersions of specific precursors

[133, 134, 136]. Gels, unlike cryogels, although they are immobilized polymer systems in which macromolecules form a three-dimensional matrix like cryogels, do not exhibit a cryotopic formation process, having a essentially different morphology when compared to cryogels produced by cryotopic gelation process [134, 138]. Cryogels possess distinctive and adaptable features, which may be controlled during the production process (e.g., polymer selection, temperature, solute concentration, and cooling rate), making them advantageous in a variety of applications [133, 134]. However, cryogels showed certain drawbacks, compared to other polymeric structures like microbeads and nanoparticles, cryogels have a smaller surface area. This can lead to low ligand density and thus reduced adsorption capacity of cryogels. To overcome this issue, composite cryogels could be produced. To improve the specific surface area of cryogels to be employed in the capture of target molecules, particle embedding and the manufacture of cryogels utilizing nanoparticles can be carried out [133, 134, 138].

1.6.1. Cryogels Synthesis

A number of monomers, including pre-made vinylic monomers, 2-hydroxyethyl methacrylate (HEMA) [135] or acrylamide [139], can be used to make cryogels. Hyaluronic Acid [140], alginate [141], agarose [141], gelatin [142], or chitosan [143] are examples of natural or synthetic polymers that can be functionalized with vinylic groups and then cross-linked via free radical cryo-polymerization. The most popular initiator systems in cryogels synthesis are ammonium persulphate (APS) and N, N, N', N'-tetramethylene diamine (TEMED) [134].

The process of making cryogels is known as cryogelation, and it takes place between -5 and -20 ºC, depending on the solvent's crystallization point [134]. Figure 10 illustrates the three steps of cryogels synthesis. The initial solution should contain the monomers that will form the structural network of the cryogel, plus a cross-linking agent such as N, N'-methylene-bis(acrylamide) (MBAAm), initiators of the polymerization reaction such as TEMED, APS and the solvent that will serve as the pore-forming agent [134]. The preparation of the initial solution is a crucial step because changes in the amount of water (the most used solvent), changes in solute concentration, precursor composition and other monomer polymerization conditions will affect the cryogel characteristics, such as pore size, pore wall thickness and other properties [134, 144]. There are two key components in the polymerization in the frozen state: the frozen solvent, which forms ice crystals, and the unfrozen liquid microphase (UFLMP), which houses the highly concentrated polymer precursors promoting the gel formation. The ice crystals then join to each other as the crystallization develops, creating a network of connections [134, 144].

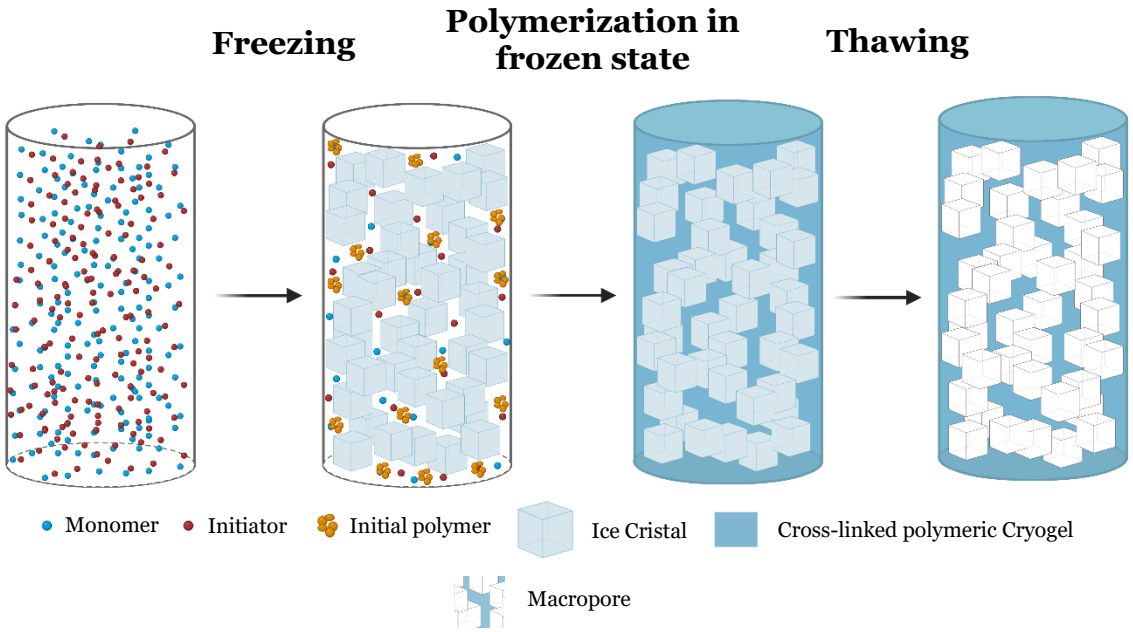

Figure 10. Schematic representation of the preparation of a macroporous cryogel.

The cryo-freezing temperature that the cryogel is subjected to in solution is an important feature, being responsible for defining both the size and the amount of pores in the cryogel [134, 144]. When prepared by the cryo-freezing process at lower temperatures, for example between -10 to -20°C, the solvent crystallizes more rapidly resulting in the nucleation of a greater number of crystals. This leads to the formation of larger amounts of porous particles by the ice crystals, possessing a smaller size [134, 144]. The greater the amount of frozen solvent, the smaller the volume of the UFLMP, thus increasing the concentration of the soluble substances and leading to the formation of a thinner and denser pore wall [134, 144]. At the final stage, after a period of thawing, the cryogel is removed and brought to room temperature. As the solvent crystals melt and the polymeric network is hydrated, an interconnected and macroporous cryogel is finally formed [133, 134]. The frozen solvent crystals will act as a pore-shaping agent, and as these melt, they leave a continuous system of gaps forming an interconnected network of pores providing channels for the mobile phase get through [133, 134]. An approximate determination of the pore size can be achieved by scanning electron microscopy (SEM) after it has been dried, but this is not a very accurate determination. Cryogels can be dried and re-hydrated very quickly when placed in an aqueous solution, without causing damage to the pore structure due to the elasticity of the pore wall [135] and allowing the degree of porosity to be approximately calculated. It can also be stored for long periods without causing changes in its performance [145].

1.6.2. Cryogel Functionalization Methods

There are several methods for functionalizing cryogels. Functionalization often involves either physical entrapment (embedding) or covalent coupling (ligand is chemically joined to a prepared cryogel) [145]. However, a number of restrictions can be applied to embedding, because only a few functional monomers are acceptable for cryogelation and not all of the functional groups are accessible to the mobile phase [134, 146]. Furthermore, the creation of brittle, nonelastic cryogels is possible when functional monomer concentrations are large [147]. Copolymerization techniques have numerous advantages, such as in controlling the degree of functional groups in the product by controlling its structure and introducing necessary and desired properties into the polymer system [134]. The introduction of a ligand will create a specific interaction between the support and the target molecule, thus ensuring its specific retention and purification. Cryogels can be prepared with biopolymer, biodegradable and ionic polymers depending on the properties required for their application [134]. Copolymerization of one monomer with another is done by one having a functional group, capable of reacting with the functional group of the ligand, such as a vinyl group, which is often used in the synthesis of functionalized cryogels. For instance, as reviewed by *Bakhspour et al. 2019* and *Memic et al. 2019* there is a myriad of ligands and matrices exhibiting properties similar to those of IEC and AC techniques described previously [133, 134].

In this context, for the purification of mRNA no published work using cryogels has been disclosed. Although, Akshay Srivastava and co-workers confirmed the ability of poly(hydroxyethylmethacrylate-co-vinylphenylboronic acid) [poly(HEMA-co-VPBA)] to effectively separate RNA from a crude sample of *E. coli* lysate in one step. However, the analysis of impurities in the purified RNA samples was not carried out [148]. Additionally, two works published by Kazim Köse and colleagues, described a RNA purification strategy with two novel cryogel supports [129, 130]. The substitution reaction between adenine and methacryloyl chloride produced adenine methacrylate (AdeM), a polymerizable derivative of adenine. After the AdeM synthesis, HEMA-based cryogels were created by copolymerizing the AdeM and HEMA monomers in a partially frozen solution, the results showed a successful purification of RNA molecules from a rotavirus homogenates [129]. Additionally, with the aim of obtaining highly purified RNA, based on the natural interaction between guanine and cytosine, the same research team also developed a novel cryogel composed of a pHEMA matrix incorporating a guanine derivative (GuaM) to also purify RNA molecules from rotavirus homogenates [130]. Here, experiments were conducted with three distinct supports: the p(HEMA-

GuaM) cryogel, a conventional pHEMA cryogel and a commercial kit. Results revealed that the novel p(HEMA-GuaM) cryogel had a significantly higher adsorption capacity, when compared to the standard pHEMA cryogel and the commercial kit [130]. Due to the organic connection, the target molecule was quickly and selectively adsorbed to the ligand without the disadvantages of diffusion. Moreover, the RNA adsorbed onto this novel cryogel was successfully recovered without any denaturation in a quick, low-cost and single-step RNA purification. However, the ability to remove contaminants from crude samples was not studied [130].

1.7. Applications of the mRNA technology

Currently, there are three major fields where mRNA technology is showing promising results: protein replacement therapy, cell reprogramming and immunotherapy [7].

Table 3. Major fields of the mRNA application technology (taken from [7]).

Therapeutic Approach	Objective/Function
Protein Replacement	Restore function, increase expression, or replace protein in rare monogenic diseases.
Cell Reprogramming	Modulate cellular behaviour by expressing transcription and/or growth factors.
Immunotherapies	Elicit specific immune responses against target cells, for example through therapeutic antibodies.

1.7.1. Protein Replacement Therapy

In protein replacement therapies, the objective is to promote the expression of a certain protein that present low levels or that has an aberrant structure and, therefore, its function compromised. [7, 149]. Haemophilia B is a perfect example of a disease for protein replacement therapy mediated by mRNA as it is caused by a single defective protein and very small amounts of hFIX protein are needed to accomplish the therapeutic effect [150, 151].

1.7.2. Cell Reprogramming

Concerning cell reprogramming, mRNA-based approaches are becoming increasingly more common to achieve “footprint-free” reprogramming in the field of developmental, cell-based, and cell-free regenerative biology [152]. mRNA-based procedures are either utilized to reprogram somatic cells into induced pluripotent stem cells (iPSCs), which can be further differentiated into any desired cell type. Also, mRNA can be transferred

into stem cells or somatic cells, facilitating guided differentiation to acquire cells suitable for cell replacement therapy [152]. For cell-free strategies, mRNA technology enables the delivery of signalling molecules into the tissue of interest [152]. For instance, mRNAs encoding growth or transcription factors have been successfully applied *in vivo* to promote tissue regeneration. Ajit Magadum and co-workers showed an increase in cardiac function by inducing cardiomyocytes proliferation through N180Q hFSTL1 modified mRNA delivery to the myocardium of rats [152-154].

1.7.3. Immunotherapy

Regarding immunotherapy, mRNA can be used as an agent of active immunization, stimulating the immune system through the translation of an antigenic mRNA, allowing the recognition of a specific type of infectious agent or even by recognizing cancer cells [7, 155]. In addition mRNA can also be used for passive immunization, delivering the antibody sequence to target cells allowing the *in situ* production of the antibody [7, 25].

1.7.3.1. mRNA in Active Immunization

mRNA-based vaccines provide a wide range of advantages over conventional-based vaccines. For example, through mRNA is possible to simultaneously delivery several antigens covering various pathogens, which enhances drastically the chance of survival for cancer patients by eliciting both humoral and cell-mediated immune responses, overcoming another problem associated with conventional vaccines, e.g., vaccine resistance [155]. Additionally, unlike peptide-based vaccines, mRNA can encode the full-length antigen, allowing the immune system to recognize a vaster range of epitopes and thus increasing the likelihood of activating the T cell response [156]. Also, mRNA vaccines are thought to be well tolerated for both preventive and therapeutic uses because they are not contagious like live-attenuated vaccines and don't include any protein- or virus-derived contamination during manufacture [157].

1.7.3.2. mRNA in Passive Immunization

The antibody industry started in 1975 with Kohler and Milstein through the development of the hybridoma technology, making possible the production of a high amount of single antibody type, the so-called monoclonal antibodies (mAbs). In recent years, the development of novel biotechnology methods has largely increased the range of uses for mAbs [158]. Additionally, a wide range of mAbs has so far been authorized for the treatment of numerous disorders. Because of their capacity to either directly or indirectly modify tumour biology, a sizable portion of mAbs that have been approved is indicated for the treatment of cancer, and also for infectious diseases [159].

Although mAbs have emerged as key players in a variety of fields, the entire manufacture and purification process can be costly, complicated, and difficult. Additionally, problems

like protein aggregation can occur with pure antibodies. Such aggregates can impair the functionality of the monomeric protein and trigger immunological reactions that can neutralize the immune response [160, 161]. An exquisite alternative to surpass some of the complex problems associated with the production and purification processes is delivering the genetic sequence of the antibody itself, using mRNA, thus allowing the *in situ* production of antibodies in a cost- and labour-effective manner [25, 157]. In fact, this approach has demonstrated that when administered intravenously, several lipid-complexed antibody-encoding mRNAs can shield against influenza, rabies, chikungunya, HIV, and other viruses, toxins and tumours [25, 162-165]. Additionally, from a biotechnological perspective, as a direct consequence of the structural difference between mRNA and proteins, the production and purification of this molecule, do not need to be constantly studied and optimized for each and every single mRNA encoding antibody [25, 166].

1.8. ADAM-17

The family of "A desintegrin and metalloproteinase" (ADAMs) are a family of membrane-bounded proteins that are responsible for a wide range of functions in pathological and physiological mechanisms, including cell adhesion, proliferation, development, differentiation, immunity, inflammation, and others [167].

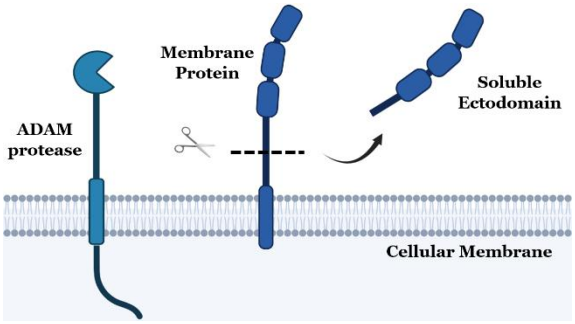

Figure 11. ADAM-17 shedding activity.

Since its discovery, over the past two decades, ADAM17 or Tumour Necrosis Factor Alfa Converting Enzyme (TACE) has gained great importance in the understanding of several pathologies. As it was investigated, it was seen to be increasingly interlinked with various biological processes, due to the shedding of the ectodomain of many substrates [167]. In immune and inflammatory responses, ADAM17 exert its function mainly by releasing tumour necrosis factor alfa (TNF-α) and the soluble interleukin receptor 6 (sIL-6R) which are crucial for the regulation of the immune system and the maintenance of inflammatory conditions [168]. Also, during development, ADAM17 activates membrane-associated ligands of the epidermal growth factor receptor (EGF-R) being its function crucial to this initial stage [169]. In fact, massive interleukin receptor – 6 (IL-

6R) and tumour necrosis factor alfa receptor (TNF-αR) shedding by ADAM17 was also seen during endotoxemia after intravenous lipopolysaccharide (LPS) injection, demonstrating that ADAM17 cellular activity is properly activated in infectious and inflammatory situations [170]. As reviewed by *Schumacher et al. 2022*, recent research highlighted the significance of the ADAM17 metalloprotease in sIL-6R and EGF-R signalling and established ADAM17 as an appealing target for anti-cancer therapy [167].

Giving the association of ADAM17 to the development of several pathologies, ADAM17 inhibitors have been the subject of intense research. Numerous small molecule ADAM17 antagonists have been reported [171]. The majority bind the ADAM17 catalytic site, which is impressively conserved among matrix metalloproteinases (MMPs), desintegrin and metalloproteases, and ADAM with thrombospondin type-1 motif (ADAMTS). The creation of particular ADAM17 inhibitor has been extremely challenging due to the structural conservation of the catalytic active site [171]. ADAM17 antagonist also showed cross-reaction with other metalloproteases that can disrupt the physiological processes in which these enzymes are involved, resulting in adverse effects that are not intended. To circumvent these restrictions, a variety of techniques have been used to develop compounds that can distinguish between ADAM17 and its relatives and block ADAM17 in a particular tissue or cell type [171].

Herein, because antibodies have a variety of epitopes and detect minor structural variations, they can overcome the problem of specificity. So, by exploring the special properties of the ADAM17 ectodomain Jonathan Rios-Doria and co-workers developed a highly specific anti-ADAM17 antibody (MEDI3622) [172], which blocked ADAM17 activity, and consequently, the liberation of TNF in LPS-stimulated mice and tumour progression in a head and neck patient-derived xenograft model [173].

In vivo investigations have shown that mRNA-encoded antibodies have several advantages over other strategies. In contrast to recombinant proteins, which deliver a single protein bolus after delivery, mRNA expression can be maintained for several days, depending on the mRNA half-life, after which regular antibody kinetics assume control. When repeated dosing is necessary, this might enable fewer frequent treatments. Additionally, because mRNA sequences contain the same nucleotides, they all have comparable physiochemical properties. This makes mRNA sequences more similar to one another than the proteins they encode for. Therefore mRNA synthesis is a more standard technique that allows for a quick antibodies production, which makes this technology incredibly beneficial [25].

Chapter 2 - Objectives

In modern medicine, the therapeutic class with the highest rate of progress are monoclonal antibodies. These biologic drugs have demonstrated a remarkable success and potential for treating a variety of conditions, such as cancer, allergies, autoimmune disorders, and infectious diseases. However, problems associated with the manufacturing and purification processes lead to the intensification of the costs and prolonged delivery times, making the wide accessibility to monoclonal antibody therapies more restricted. Also, researchers are working to develop faster and less expensive platforms for producing and delivering antibodies. Herein, with the remarkable advance in mRNA research over the past years, it has become clear that it offers a highly appealing method for encoding and generating any desired protein *in vivo*. Additionally, a promising monoclonal antibody (MEDI3622) has recently shown its potential in preventing TNF-α release and the progression of head and neck tumours by targeting ADAM17, a suitable and appealing target for the treatment of cancer and immunological disorders.

The significant need for pure and stable mRNA in the biopharmaceutical sector, the well-established advantages of liquid chromatography in this area and the potential of the supermacroporous matrices, like cryogels, in the purification of large molecules are the requisites that thrive the present work. Therefore, this study aimed to synthesize functionalized cryogels with thymine to purify *in vitro* transcribed mRNA encoding for anti-ADAM17 MEDI3622 antibody. In order to accomplish this aim, the following tasks were planned:

1) Synthesis and characterization of the ligand 1-(2-propenyl) thymine;
2) Synthesis, functionalization and characterization of cryogels;
3) Construction of an mRNA sequence capable of encoding the MEDI3622 antibody;
4) Production of the designed mRNA sequence by IVT;
5) Screening of the binding/elution behaviour of the different functionalized Poly-Thymine cryogels with low molecular weight RNA (LMW RNA) as a model;
6) Evaluation of the capacity of the functionalized Poly-Thymine cryogels to bind and elute mRNA.

Chapter 3 - Materials and Methods

3.1 Materials

For the synthesis of 1-(2-propenyl) thymine (ProT), it was used Allyl Bromide provided by Acros Oorganics (Geel, Belgium) and thymine supplied by Acros Oorganics (Geel, Belgium). Microwave assisted reactions were carried out in a Milestone MultiSYNTH (Single and Multi-Mode Microwave Synthesis System). The evolution of the reactions was followed by thin layer chromatography (TLC) using plates pre-coated with 0.2 mm Macherey-Nagel Alugram® SIL G/UV254 silica gel. The eluent consisted of a mixture of 10 % methanol in dichloromethane. After elution and drying, the plates were visualized under ultraviolet light at 254 nm.

The ^{1}H NMR and ^{13}C NMR spectra were performed on a Bruker Avance 400 MHz spectrometer (^{1}H NMR at 400 MHz and ^{13}C NMR at 101 MHz) and processed with TOPSPIN 3.1 software (Fitchburg, Wisconsin, USA) using hexadeuterated dimethyl sulfoxide (DMSO-d_6), as a solvent and internal standard. In the ^{1}H NMR data, the chemical shift (δ in ppm), the number of protons to which the signal corresponds, the multiplicity of the signal [singlet (s), broad singlet (sl) duplet (d), double doublet (dd), triplet (t), multiplet (m)], the value of the coupling constant (J in Hz), and the assignment of the signal to the corresponding protons are indicated. In the ^{13}C NMR data, the chemical shift (δ in ppm) and the assignment of the carbon in the molecule are given.

Posteriorly, for the cryogels synthesis N, N-Methylene-bis(acrylamide) (MBAAm), and 2-hydroxyethyl methacrylate (HEMA) were purchased from Acros Oorganics (Fair Lawin, New Jersey, USA). Cryogels were obtained by cryogelation process in an acetone bath at -20 °C in a refrigerator.

For *E. coli* DH5 and *E. coli* NZYStar growth, "Luria-Bertani" (LB) agar medium from Pronalab (Mérida, Mexico), yeast extract and tryptone from Biokar (Beauvais, France), glycerol from Himedia (Einhausen, Germany), potassium hydrogen phosphate (K_2HPO_4) from Panreac (Barcelona, Spain), potassium dihydrogen phosphate (KH_2PO_4) from Sigma-Aldrich (St. Louis, Missouri, USA), the antibiotics kanamycin and ampicillin from Thermo Fisher Scientific Inc. (Waltham, EUA) have been used.

For LMW RNA extraction, the reagents used were guanidine thiocyanate, N-Lauroylsarcosine sodium salt, sodium citrate and isoamyl alcohol from Sigma-Aldrich (St. Louis, Missouri, USA), isopropanol from Thermo Fisher Scientific Inc. (Waltham, USA), β-mercaptoethanol from Merck (Whitehouse Station, USA). All mentioned solutions were prepared with 0.01% diethyl pyrocarbonate treated water (DEPC) from Fluka, Sigma-Aldrich (St. Louis, Missouri, USA).

Posteriorly, the pNZY-28-BruMEDI3622 extraction from *E. coli* NZYStar culture was performed using NZYMiniprep kit (NZYTech Genes and Enzymes, Lisbon, Portugal). For the pNZY-28-BruMEDI3622 linearization, the endonuclease EcoR I (Vivantis) was used. Its purification was carried out with NucleoSpin Gel and PCR Clean-up Kit (Machery-Nagel, Düren, Germany).

IVT was performed with MEGAscript T7 Kit (Thermo Fisher Scientific Inc., Waltham, EUA). To confirm the integrity and purity of the RNA samples, 1% agarose gel electrophoresis was used with GRS Agarose LE and Green-Safe (Grisp, Porto, Portugal).

In the chromatographic assays, sodium chloride (NaCl) and ammonium sulphate ($(NH_4)_2SO_4$) both commercialized by Panreac (Barcelona, Spain) and tris(hydroxymethyl)aminomethane (Tris) and Sodium-Acetate from Merck (Darmstadt, Germany) were used. All solutions were prepared with Milli-Q water treated with 0.01% of DEPC.

3.2. Methods

3.2.1. 1-(2-propenyl) thymine synthesis and optimization

A suspension of thymine (500 mg, 3.96 mmol) in 3 mL of a solution of NaOH 2M was made and subjected to microwave irradiation for 4 min, at 60 ºC (200 watts). Then allyl bromide (517.6 µL, 5.95 mmol) was added to the reaction and the mixture was irradiated again for 30 min, at 60 ºC (Figure 12). Following this, four more cycles of 30 min at 60 ºC were done. Next, the reaction solution was recovered and treated with ethyl ether, and the aqueous phase recovered. Then, acetonitrile was added at a proportion of 1:3 (aqueous phase: acetonitrile, respectively), and the mixture was vigorously agitated and put at 4 ºC overnight to the unreacted thymine precipitate. After that, the total volume of the suspension was filtrated at room temperature and dried under sodium sulphate anhydrous. Finally, the remaining acetonitrile was evaporated under reduced pressure to obtain a crystallized white solid, which by cooling to room temperature becomes a translucid oil. 1-(2-propenyl) thymine (ProT) was obtained with a 57 % yield: ^{1}H-NMR (400 MHz, DMSO-d_6): δ = 11.25 (s, 1H, 3-NH); 7.44 (q, 1H, 6-H, J 1.1 Hz); 5.82 – 5.92 (m, 1H, 2´-H); 5.18 (dd, 1H, 3´-H, J 1.3 and 10.3 Hz); 5.13 (dd, 1H, 3´-H, J 1.4 and 17.1 Hz); 4.25 (dt, 2H, 1´-H, J 1.4 and 5.5 Hz); 1.76 (s, 3H, 5-CH_3) ppm. ^{13}C-NMR (101 MHz, DMSO-d_6): δ = 164 (C-4); 151 (C-2); 141 (C-6); 133 (C-2´); 117 (C-3´); 109 (C-5); 49 (C-1´); 12 (5-CH_3) ppm. Figure 13 shows a general representation of the entire synthesis process, from the ligand to the functionalization of the cryogels.

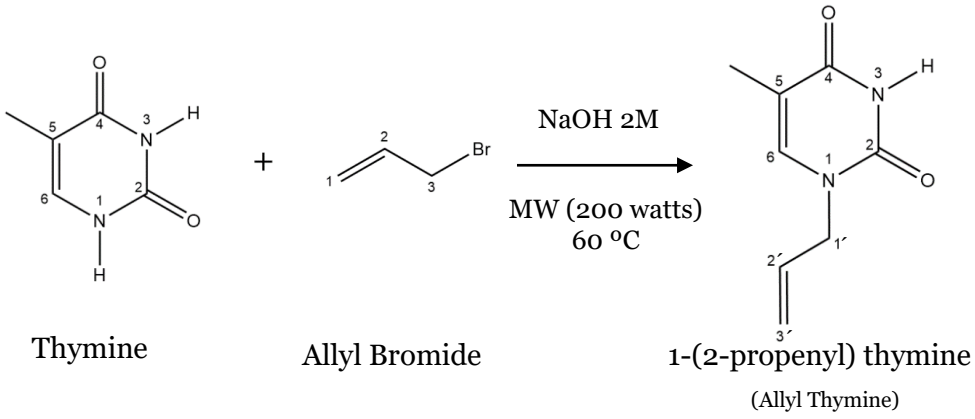

Figure 12. General reaction mechanism of the synthesis of 1-(2-propenyl) thymine.

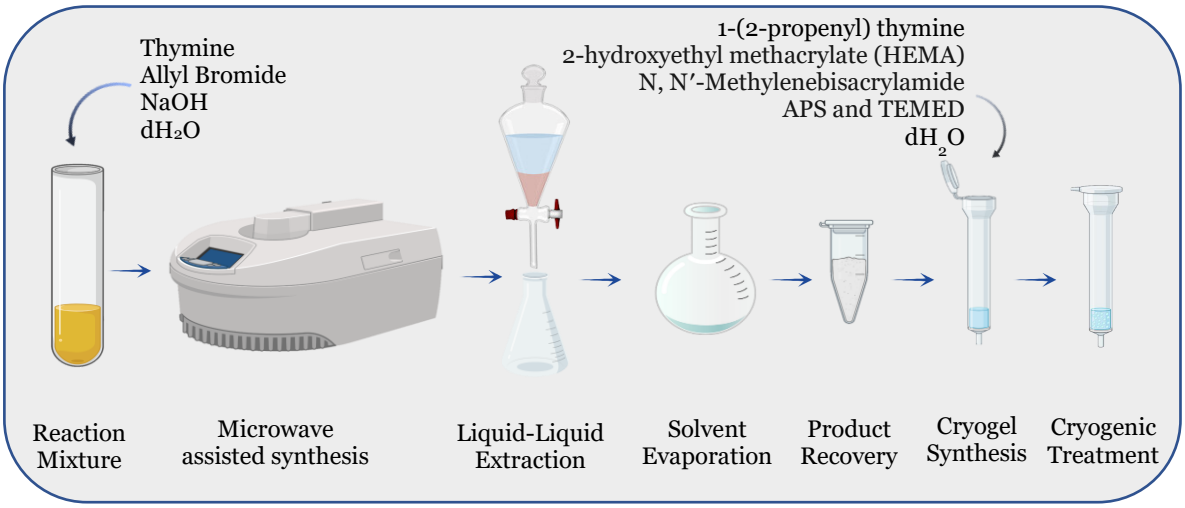

Figure 13. Methods for synthesizing 1-(2-propenil) thymine and the Poly-Thymine cryogels.

3.2.2. Synthesis and functionalization of p(HEMA) cryogels

Cryogels were synthesized in an Econo-Pac column (1.5 by 12 cm; Bio-Rad). HEMA and ProT monomer were copolymerized in free radical co-polymerization using APS and TEMED as initiators. Water and N´, N-Methylene-bis(acrylamide) (MBAAm) were included in the polymerization process as the porogenic agent and crosslinker, respectively. HEMA (0.225 mL) and 1-(2-propenyl) thymine (0, 25, 37.5 and 50 mg) (Figure 14) monomers were dissolved in 0.833 mL of deionized water and added to a second solution prepared with MBAAm (0.0433 g) dissolved in 1.66 mL deionized water. Then, the cryogel was produced by free radical polymerization initiated by the addition of TEMED (0.004 mL) and APS (0.033 g). After adding APS and TEMED the solution was stirred for 1 min. Finally, the polymerization mixture was frozen at −20 °C, for 24 h, in an acetone bath and then thawed at room temperature, with 300 mL of deionized water. The synthesised cryogels were then stored at 4 °C until use.

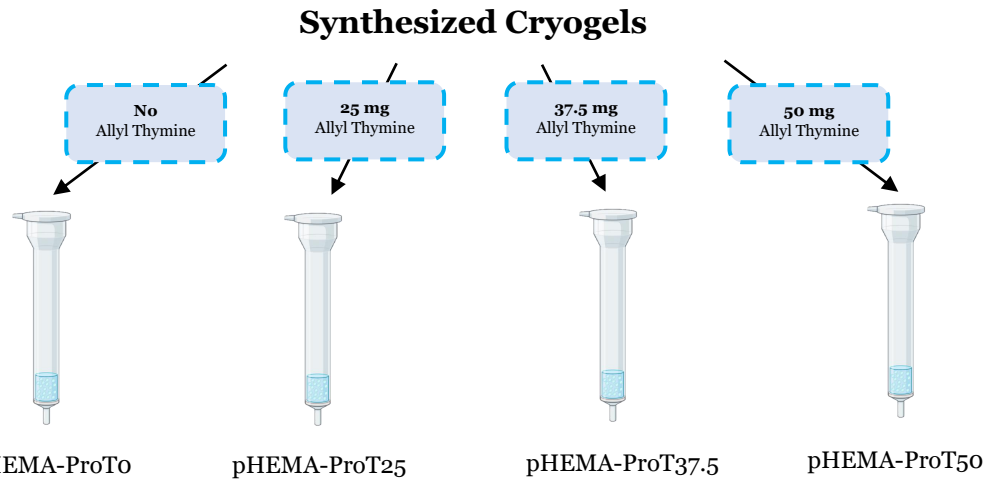

Figure 14. Cryogels synthesized in the present work.

3.2.3 Cryogels Characterization

The synthesized cryogels were analysed in terms of their swelling properties (Figure 15), estimated as the amount of water in swollen cryogel per gram of dried polymer. The water-holding capacity of the cryogels was determined by the following equation:

$$Swelling\ Degree = \left[\frac{Weight_{Swollen} - Weight_{Dry}}{Weight_{Dry}}\right] \quad (1)$$

SEM was used to evaluate the microstructural surface morphology of the cryogels (Figure 15). For that, cryogel samples were dried until constant weight by a freeze-drying process at the beginning. After that, the samples were assembled onto aluminium stubs using Araldite glue and sputter-coated with gold using a Quorum Q150R ES sputter coater (Quorum Technologies Ltd., Laughton, East Sussex, UK). The SEM images were obtained using the Hitachi S-3400 N Scanning Electron Microscope (Hitachi, Tokyo, Japan) at an accelerating voltage of 20 kV with different magnifications. Energy dispersive X-ray analysis (EDXA) was done by using energy dispersive X-Ray spectroscopy (EDXS) (Figure 15).

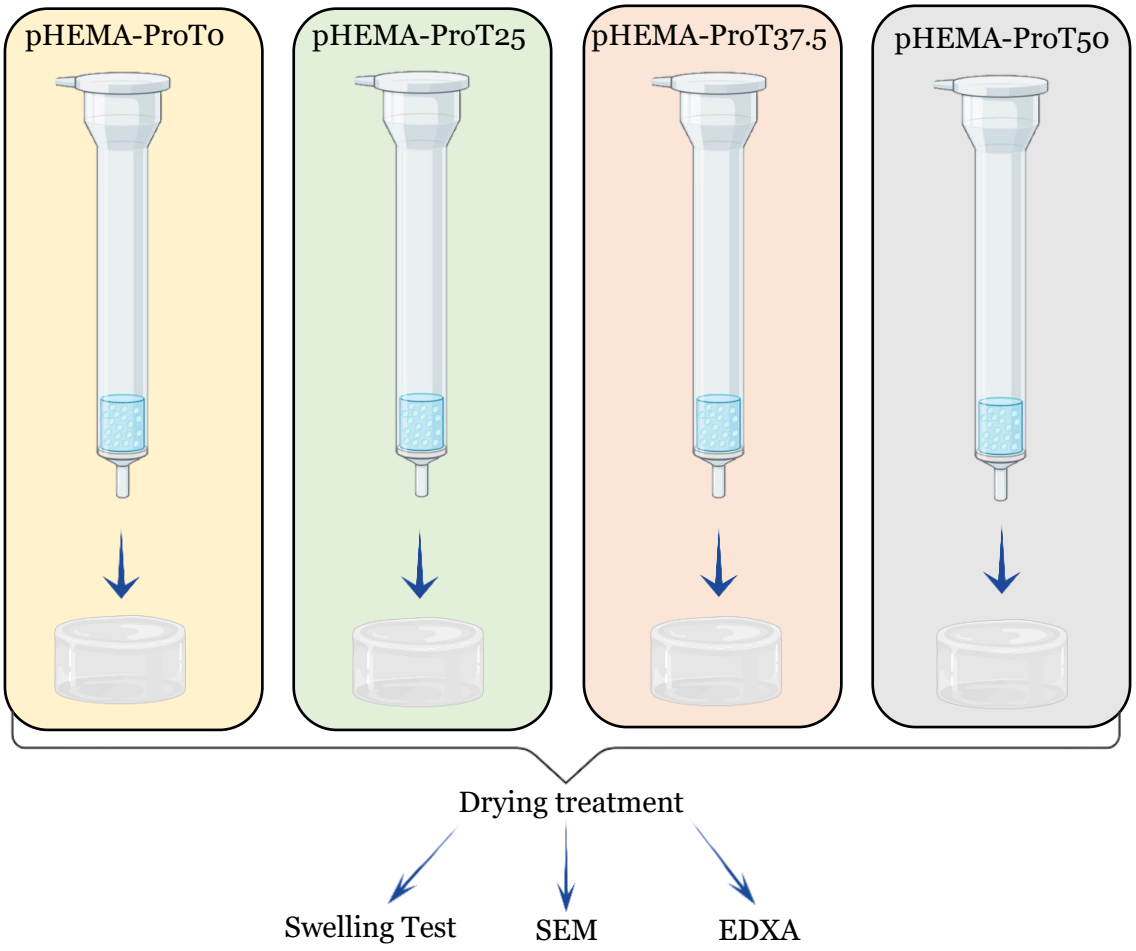

Figure 15. Cryogels characterization studies.

3.2.4. Design and construction of BruMEDI3622 - mRNA sequence

Structurally, an mRNA molecule consists of a 5´cap, 5′ and 3′ UTRs, an mORF and a poly (A) tail. First, the sequences for the mORF, which is composed of the variable heavy (VH) domain and variable light (VL) domains of the MEDI3622 antibody, were taken from World Intellectual Property Organization (WIPO) PATENTSCOPE database (WO2016089888 – Antibodies to ADAM17 and uses thereof), where VH corresponds to the SEQ ID NO: 19 and VL corresponds to the SEQ IN NO: 26. WIPO bears no responsibility for the integrity or accuracy of the data contained herein, in particular due, but not limited, to any deletion, manipulation, or reformatting of data that may have occurred beyond its control.

It was also used a 5′ UTR consisting of a partial sequence of the cytomegalovirus immediate early 1 (IE1) gene and a 3′ UTR based on the partial sequence of the human growth hormone (hGH) gene. These two regions have been shown to induce efficient protein expression in different tissues *in vivo* and were utilized in a previous work [80], where the nucleotide sequences corresponding to the 3´UTR and 5´UTR were taken. Concerning the 3′ poly (A) tail, it was obtained from another published work [174] along with the linker (GGAGGAGGCGGCTCTGGAGGTGGCGGCAGTGGTGGAGGCGGGTCTGGCGGTGGCG GATCTGGAGGTGGTGGGAGC) for the binding of the VH domain to the VL domain of the MEDI3622 antibody sequence. The poly (A) tail is composed of a 30 Adenines sequence, followed by a small sequence of 10 nucleotides (GCATATGACT), and another sequence of 70 Adenines. This specific poly (A) tail sequence was previously studied [175] and has shown to improve the stability of the final mRNA transcript. A resume of the different mRNA utilized sequences is present in table 4. The final BruMEDI3622 mRNA sequence is presented in Appendices (Appendix 1).

Table 4. mRNA nucleotide sequences.

mRNA Structure	Sequence
5´UTR - (IE1)	GGACAGATCGCCTGGAGACGCCATCCACGCTGTTTTGACCTCCAT AGAAGACACCGGGACCGATCCAGCCTCCGCGGCCGGGAACGGTG CATTGGAACGCGGATTCCCCGTGCCAAGAGTGACTCACCGTCCTT GACACGATG
MEDI 3622 VL Domain	GACATCCAGATGACCCAGTCTCCATCCTCCCTGTCTGCATCTGTAG GAGACAGAGTCACCATCACTTGCCGATCCAGTCAGAGCATTCCCA GCTATTTAAATTGGTATCAGCAGAAACCAGGGAAAGCCCCTAAGC TCCTGATCTATGCTGCATCCCGTTTACAATCCGGGGTCCCATCAAG GTTCAGTGGCAGTGGATCTGGGACAGATTTCACTCTCACCATCAG CAGTCTGCAACCTGAAGATTTTGCAACTTACTACTGTCAACAGAG TTACAGTACCCCCCTCACTTTCGGCGGAGGGACCAAGGTGGAGAT CAAA
Linker	GGAGGAGGCGGCTCTGGAGGTGGCGGCAGTGGTGGAGGCGGGT CTGGCGGTGGCGGATCTGGAGGTGGTGGGAGC
MEDI3622 VH Domain	GAAGTTCAATTGTTAGAGTCTGGTGGCGGTCTTGTTCAGCCTGGT GGTTCTTTACGTCTTTCTTGCGCTGCTTCCGGATTCACTTTCTCTT CCTACCCTATGAATTGGGTTCGCCAAGCTCCTGGTAAAGGTTTGG AGTGGGTTTCTTATATCTCTCCCTTCGGTGGCATGACTGATTATGC TACCTCCGTTAAAGGTCGCTTCACTATCTCTAGAGACAACTCTAAG AATACTCTCTACTTGCAGATGAACAGCTTAAGGGCTGAGGACACG GCCGTGTATTACTGTGCGAGAGACGCTATGAGGGGGGCAGAGGT GGACTACTGGGGCCAGGGCACCCTGGTCACCGTCTCAAGC
3´UTR – (hGH)	TGACGGGTGGCATCCCTGTGACCCCTCCCCAGTGCCTCTCCTGGC CCTGGAAGTTGCCACTCCAGTGCCCACCAGCCTTGTCCTAATAAA ATTAAGTTGCATCAAGCT
Poly (A) tail	AAAAAAAAAAAAAAAAAAAAAAAAAAAAAAGCATATGACTAAAAA AAAAAAAAAAAAAAAAAAAAAAAAAAAAAAAAAAAAAAAAAA AAAAAAAAAAAAAAAAAAA

3.2.5. Plasmid Selection and Synthesis

The BruMEDI3622 mRNA sequence and the plasmid pNZY-28 (Figure 16), which contain a T7 RNA polymerase promoter sequence from the nucleotides 24 to 44 (Table 5), were sent to NZYtech (NZYTech Genes and Enzymes, Lisbon, Portugal). It was instructed to clone the BruMEDI3622 mRNA sequence with a 5´flank region: Hind III and a 3´flank region: EcoR I in the provided pNZY-28. No further optimizations were requested or done. The synthesized pNZY-28-BruMEDI3622, which serves as the template for IVT, was supplied by NZYTech. The final pNZY-28-BruMEDI3622 construct sequence is represented in Appendices (Appendix 2).

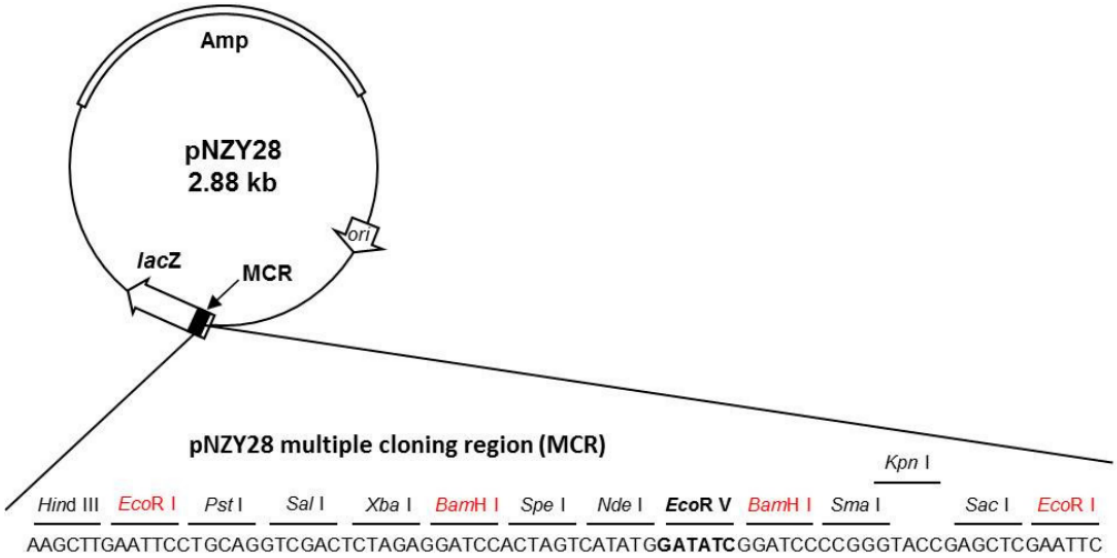

Figure 16. Map of pNZY-28.

Table 5. pNZY-28 vector sequence reference points.

Base pairs	2886
LacZ start codon	1
T7 RNA polymerase promoter	24-44
T7 promoter sequencing primer binding site	24-39
Multiple cloning region	45-126
M13/pUC U19-mer sequencing primer binding site	144-161
Phage f1 region	283-737
pUC/M13 Reverse Sequencing Primer binding site	2855-2878

3.2.6. Nucleic acids synthesis

To produce small RNAs (used as model molecules), *E. coli* DH5α cells transformed with the plasmid pBHSR1-RM, encoding for the human pre-miRNA29b, were used. Additionally, the plasmid pNZY-28-BruMEDI3622, which contains the sequence of the BruMEDI3622 mRNA, was used to transform competent *E. coli* NZYStar (NZYTech Genes and Enzymes, Lisbon, Portugal) by a heat-shock procedure in order to produce pDNA to be further used in IVT.

The first step consists of cultivating the *E. coli* on a plate using solid "Luria-Broth Agar" (LB-Agar) medium with 50 µg/mL kanamycin (*E. coli* DH5α) or 50 µg/mL ampicillin (*E. coli* NZYStar). This growth took place overnight at 37 ºC. Following growth on the solid medium, pre-fermentation was carried out by transferring a small number of colonies to an Erlenmeyer containing 125 mL of "Terrific Broth" medium (TB) (12 g/L Tryptone, 24

g/L yeast extract, 4 mL/L glycerol, 0.017 M KH_2PO_4, 0.072 M K_2HPO_4), supplemented with 50 μg/mL of kanamycin and using a medium/oxygen ratio of 1:4. Bacterial growth was carried out at 37 ºC and 250 rpm on an Aralab Agitorb 200 orbital shaker (Albarraque, Portugal), and was interrupted at the end of the log phase when it reached an optical density (OD) of almost 2.6 at 600 nm. In order to start the fermentation with an OD of 0.2, a precise volume of this growth medium was then transferred to 4 Erlenmeyers with TB media. From the equation (2), the volume to be transferred was calculated.

$$V_{pre-fermentation} = \frac{OD_{fermentation} \times V_{fermentation}}{OD_{pre-fermentation} - OD_{fermentation}}$$

A spectrophotometer Pharmacia Biotech Ultraspec 3000 UV/Visible (Cambridge, England) was used to measure the OD. The *E. coli* DH5α growth was stopped after 8 h and the *E. coli* NZYStar growth was stopped after 16 h. The entire fermentation volume was harvested and divided into 50 mL tubes and centrifuged at 3900 g for 10 min. The collected cells were then stored at -20 ºC until needed. A general scheme of the nucleic acid synthesis is present in Figure 17.

3.2.7. Low molecular weight RNA extraction

The procedure of acid guanidinium thiocyanate-phenol-chloroform was used to extract the RNA (Figure 17). *E. coli* DH5α pellets were first thawed and then resuspended in 0.8% NaCl. Next, a centrifugation at 6000 g, for 10 min, at 4 ºC was made, the supernatant was discarded, and the resultant pellets were resuspended in 5 mL of D Solution (4 M guanidinium thiocyanate, 0.025 M sodium citrate pH = 7, 0.5% sodium N-lauroylsarcosinate, and 0.1 M -mercaptoethanol), which was then incubated on ice for 10 min. After that, the suspensions were gently homogenized after each addition of 0.5 mL of 2 M sodium acetate pH = 4 and 5 mL of phenol. Next, 1 mL of a 49:1 chloroform/isoamyl alcohol mixture was added, and the mixture was vigorously shaken and allowed to sit on ice for 15 min. The suspensions underwent 20 min, 10 000 g centrifugation at 4 °C. Two aqueous phases form, where the bottom phase is DNA enriched and the top phase highly concentrated in RNA. As a result, the top phase must be transferred to new lysis tubes with extreme caution to prevent DNA contamination. The RNA was precipitated in these new tubes by adding 5 mL of isopropanol, and the tubes were then centrifuged at 10000 g for 20 min at 4 °C. The supernatant was discarded, the RNA pellets were dissolved in 1.5 mL of D Solution, 1.5 mL of isopropanol, and then centrifuged at 10000 g for 10 min at 4 °C. After discarding the supernatant, the pellets were resuspended in 2.5 mL of 75% ethanol in DEPC water, incubated for 10–15

min at room temperature, and then centrifuged again at 10000 g for 5 min at 4 °C. The pellet was then dried at room temperature for 5–10 min. After that, RNA pellets were then dissolved in 1 mL of DEPC-treated water and incubated for 10 to 15 min at room temperature. RNA concentration was determined using a Nano Photometer (IMPLEN, United Kingdom). After being prepared with 10 µL of sample and 2 µL of loading buffer (glycerol, bromophenol blue, milli-Q water), the samples were run in a horizontal electrophoresis in a 1% agarose gel (Hoefer, Holliston, MA, EUA) using Greensafe (0.012 µL/mL) as an intercalating agent to make the bands visible, to confirm the samples' integrity, at 130 volts, for 30 min, in TAE buffer (pH=8.0, 40 mM Tris-Base, 20 mM acetic acid, and 1 mM EDTA), and then visualized in an ultraviolet chamber (UVitec Cambridge) (Cambridge, UK). The samples were stored at -80 °C until use.

3.2.8. pNZY-28-BruMEDI3622 extraction and purification

The NZYMiniprep kit was used for the bacterial cells lysis in order to extract and purify the pDNA (Figure 17), with some alterations to the manufacturer's instructions. Briefly, 25 mL of 0.8% NaCl were used to resuspend the bacterial pellet, and then 2 mL fractions were prepared for centrifugation for 1 min at room temperature at 12300 g. The pellet was then resuspended in 250 µL of Buffer A1 and vortexed after the supernatant was removed. With the addition of 250 µL of buffer A2 and gently homogenized, the lysis process was started. 4 min later, 300 µL of buffer A3 were added for the neutralization stage, and the mixture was again gently homogenized. The mix was centrifuged for 10 min, at 12300 g, at room temperature. The supernatant was transferred to the NZYTech column and centrifuged at 11000 g for 1 min at room temperature. This procedure aids the DNA binding to the column, which was later washed by adding 700 µL of buffer A4. The column was once more centrifuged for 1 min at 11000 g, at room temperature. pDNA was obtained by adding 50 µL of buffer AE, incubated 1 min at room temperature and centrifuged at 12300 g, for 1 min, at room temperature. The final pDNA concentration was determined using a NanoPhotometer. Then, using Greensafe (0.012 µL/mL), a horizontal electrophoresis of 1% agarose gel was performed to assess the consistency and purity of the pDNA. After being prepared with 3 µL of sample and 0.5 µL of loading buffer, the samples were run at 130 volts, for 30 min, in TAE buffer, and then visualized in an ultraviolet chamber. The samples were stored at -20 °C.

3.2.9. pNZY-28-BruMEDI3622 Linearization

In order to advance to the *in vitro* transcription, the previously extracted and purified pNZY-28-BruMEDI3622 was linearized with EcoR I (Vivantis, Ref.1280) (Figure 17). The reaction mixture with a final volume of 50 µL, contained: 5 µL of 10X Buffer, 0.25 µL of EcoR I, 1 µg of purified pNZY-28-BruMEDI3622 and the remaining volume was

completed with nuclease-free water. The reaction mixture was then incubated for 1 h at 37 °C.

3.2.10. Purification of the products of the linearization reaction

The "NucleoSpin® Gel and PCR Clean-up" (Machery-Nagel, Düren, Germany) kit was used to purify the linearization reaction products, in accordance with the manufacturer's instructions. Prior to adding 100 µL of NTI buffer for every 50 µL of linearized products, all the reactions were transferred to 1.5 mL tubes and homogenized. The mixture was thereafter moved to the purification column. The material was then centrifuged at 11000 g, for 30 sec at room temperature. Then, 700 µL of N3 buffer was added, and the mixture was centrifuged again for 1 min at the same speed to remove any leftover buffer. 30 µL of NE buffer was added to the column for the purpose of retrieving the linearized DNA, which was incubated for 1 min at room temperature and then the mixture was centrifuged at 11 000 g for 1 min. The integrity and purity of the DNA were assessed using a horizontal electrophoresis of 1% agarose gel. After being prepared with 3 µL of sample and 0.5 µL of loading buffer, the samples were run at 130 volts, for 30 min, in TAE buffer, and then visualized in an ultraviolet chamber, and the amount of the linearized pDNA was measured using a NanoPhotometer. The samples were stored at -20 °C.

3.2.11. *In vitro* transcription

Using the MEGAscript T7 Kit, IVT was carried out to obtain BruMEDI3622 mRNA (Figure 17). The reaction mix with a final volume of 20 µL was composed of: 2 µL of 10X T7 Reaction Buffer, 2 µL of each ribonucleotides triphosphates (rNTP), 1 µg of purified and linearized pNZY-28-BruMEDI3622, 2 µL of T7 Enzyme Mix, and the remaining volume was filled with nuclease-free water. The reaction mixture was then incubated for 4 h, at 37 °C. The RNA was quantified using a NanoPhotometer, and its integrity and purity were verified using a horizontal 1% agarose gel electrophoresis. After being prepared with 3 µL of sample and 0.5 µL of loading buffer, the samples were run at 130 volts, for 30 min, in TAE buffer, and then visualized in an ultraviolet chamber. The samples were stored at -80°C until use.

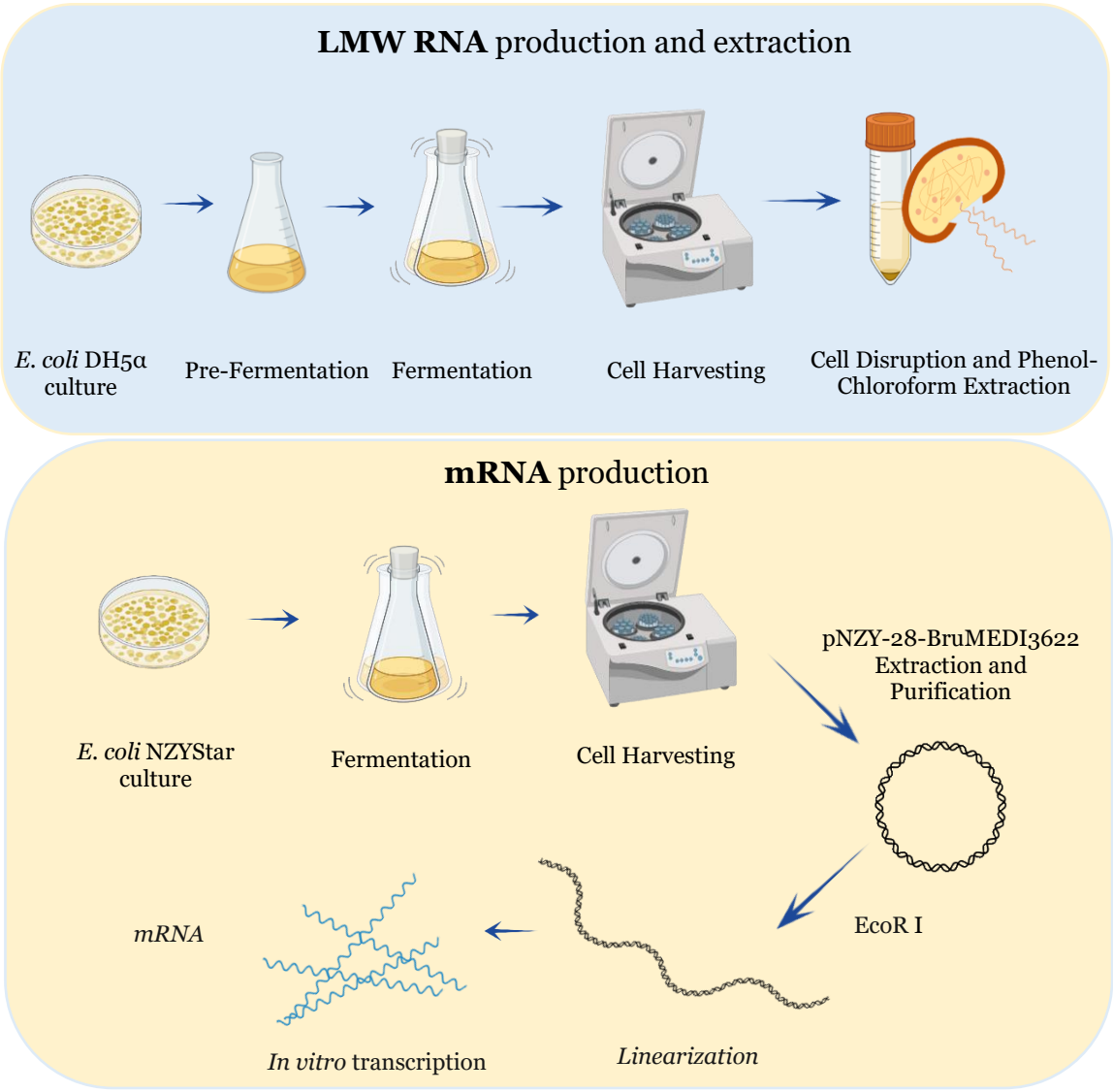

Figure 17. General process to obtain LMW RNA and *in vitro* transcribed mRNA.

3.2.12. Chromatographic Assays

3.2.12.1 Screening binding/elution of LMW RNA

Each of the synthesized cryogels (pHEMA-ProT0, pHEMA-ProT25, pHEMA-ProT37.5, pHEMA-ProT50) was evaluated in terms of their ability for binding and elution LMW RNA samples. First, a filter was carefully placed at the top of the synthesised cryogels. Then, a sample prepared in the appropriate buffer with 80 μg of LMW RNA was applied for each assay. Next, a series of buffers were studied (Table 6) to determine which would be the best for binding and eluting LMW RNA. For each single assay, a step of equilibration was made with 3 column volumes (CV) of binding buffer, followed by the application of the LMW RNA sample. Then, 3 CV of binding buffer were applied to wash the unbounded material, and 3 CV of elution buffer were finally loaded for the removal of the bound material, followed by washing with DEPC treated water and regeneration

with 2 mM NaOH. 1mL fractions were collected during binding, elution and washing steps of the assays and the absorbance at 260 nm and concentration were measured using a Nano Photometer (IMPLEN, United Kingdom).

Table 6. Buffers used for the binding and elution of LMW RNA.

Binding Buffers
Tris-HCl 10 mM pH = 8.0
250 mM NaCl in Tris-HCl 10 mM pH= 8.0
Sodium-Acetate 200 mM pH = 5.5
250 mM NaCl in Sodium-Acetate 200 mM pH = 5.5
Sodium-Acetate 10 mM pH = 5.0
1.5 M Ammonium Sulphate in Sodium-Acetate 10 mM pH = 5.0
1 M Ammonium Sulphate in Tris-HCl 10 mM pH = 8.0
1.5 M Ammonium Sulphate in Tris-HCl 10 mM pH = 8.0
2 M Ammonium Sulphate in Tris-HCl 10 mM pH = 8.0
2,5 M Ammonium Sulphate in Tris-HCl 10 mM pH = 8.0
Elution Buffers
Tris-HCl 10 mM pH = 8.0
250 mM NaCl in Sodium-Acetate 10 mM pH = 5.0
1.5 M NaCl in Sodium-Acetate 10 mM pH = 5.0

3.2.12.2 Screening binding/elution of mRNA

For the screening of the binding and elution profile of the mRNA, a sample prepared in Sodium-Acetate 10 mM, pH = 5.0 buffer, with 80 μg of mRNA was applied for each assay. The equilibrium stage was carried out by following the application of 3 CV of Sodium-Acetate 10 mM, pH = 5.0 to the cryogels and allowing it to elute by gravity flow. After applying the mRNA sample, 3 CV of binding buffer were loaded to remove the unbound material. Then, to study the elution behaviour of the mRNA on the different cryogels, 3 CV of 5 different elution buffers were used (table 7), followed by 3 CV of DEPC treated water to wash the column. Finally, a solution of 2 mM NaOH was used to regenerate the column. Additionally, 1 mL fractions were collected during binding, elution and washing steps of the assays and the absorbance at 260 nm was measured using a Nano Photometer (IMPLEN, United Kingdom). The fractions with the highest values of absorbance from each step (binding, elution, washing) were collected, desalted with Vivaspin 10 000 Da concentrators (Sartorius) and after reaching 200 μL, a 1% agarose

gel electrophoresis was done to evaluate the integrity and the elution profile of the BruMEDI3622 - mRNA.

Table 7. Elution buffers used in the mRNA elution Screening.

Elution Buffers
77 mM NaCl in Sodium-Acetate 10 mM pH = 5.0
100 mM NaCl in Sodium-Acetate 10 mM pH = 5.0
150 mM NaCl in Sodium-Acetate 10 mM pH = 5.0
250 mM NaCl in Sodium-Acetate 10 mM pH = 5.0
1.5 M NaCl in Sodium-Acetate 10 mM pH = 5.0

Chapter 4 - Results and Discussion

4.1 Synthesis of 1-(2-propenyl) thymine

To initiate our study, a polymerizable thymine derivative was synthesised through the alkylation reaction of thymine using allyl bromide with NaOH 2 M as a base, conducted under microwave irradiation, following the procedure of *Rocha et al. 2021* [176]. The authors described a yield of about 20 %, so we initially replicated the same conditions. The great advantages of using the prop-2-enyl chain linked to thymine are that it gives the ligand a spacer chain and simultaneously the ability to copolymerize through the vinylic group. The resulting reaction showed by thin layer chromatography (TLC) traces of 1-(2-propenyl) thymine (ProT) corroborating the yield stated in literature [176]. In order to increase the yield, optimizations of the amount of thymine and allyl bromide, as well as the reaction temperature and time under microwave irradiation were made. The optimized conditions (3.96 mmol of thymine and 5.96 mmol of allyl bromide in a temperature of 60 ºC, under 5 cycles of 30 minutes of microwave irradiation) resulted in a yield of 57% with a mixture of 1-(2-propenyl) thymine (**1A**) and 3-(2-propenyl) thymine (**1B**) which was calculated based on the mass of limiting reagent (thymine) and the mass of the product mixture (**1A** and **1B**) found in the round bottom flask at the end of the isolation procedure.

As a direct consequence of the reaction conditions optimization, the presence of subproducts of the reaction was observed, namely the (**1B**) and 1,3-bis(2-propenyl) thymine (**1C**) (Figure 18). This was due the presence of a labile N3 proton, which can react with allyl bromide giving origin to those by-products as a result of forcing the alkylation reaction to obtain a greater amount of the product **1A** [177, 178].

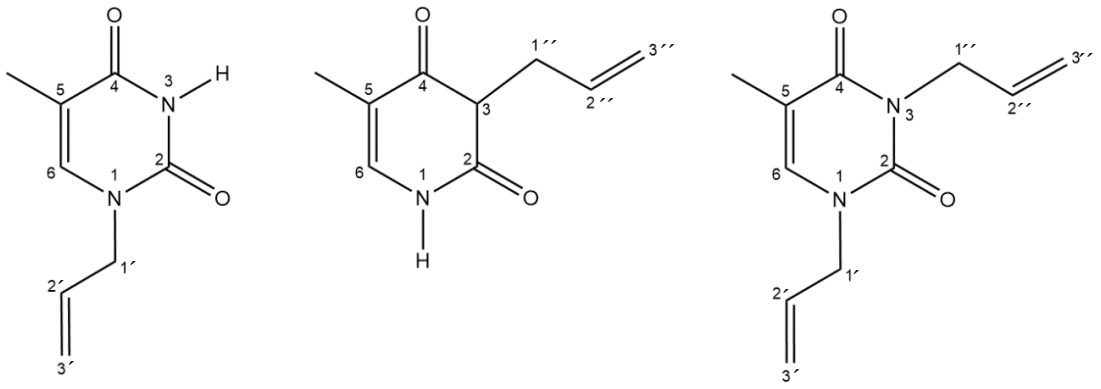

1A 1-(2-propenyl) thymine

1B 3-(2-propenyl) thymine

1C 1,3-bis(2-propenyl) thymine

Figure 18. Subproducts of the 1-(2-propenyl) thymine synthesis.

In order to extract and isolate the compound **1A**, a liquid-liquid extraction was made, taking advantage of the hydrophobicity and solubility of the different products present in the reaction mixture. Herein, product **1C** was the most hydrophobic due to the presence of two vinylic groups, so an extraction with ethyl ether successfully separate this sub-product from **1A**, **1B** and unreacted thymine, this method was previously utilized by *Vlád et al. 2002* to extract products with high hydrophobicity, like 2-Bromo-2-fluoropyrimidine and 2-iodopyrimidine [179]. **1C** structure was confirmed by ^{1}H NMR. Additionally, products **1A** and **1B** were separated from the unreacted thymine, by treating the mixture with acetonitrile under 4 ºC. This procedure was based on a study conducted by *Cong et al.* 2020, where it was documented, that thymine possesses lower solubility in acetonitrile under low temperatures, so we were able to precipitate de unreacted thymine, leveraging **1A** and **1B** in suspension to be isolated [180]. Additionally, given the similarity of the structure and molecular composition between **1A** and **1B**, a successful method capable of separating these two products lacks in the present work, so the presence of **1B** traces can be identified on the ^{1}H NMR and ^{13}C NMR spectrums (Figure 19 and 20). Purification attempts through column chromatography and recrystallization were made, although the separation between **1A** and **1B** was not achieved. A more profound study in the purification of **1A** should be done in the future.

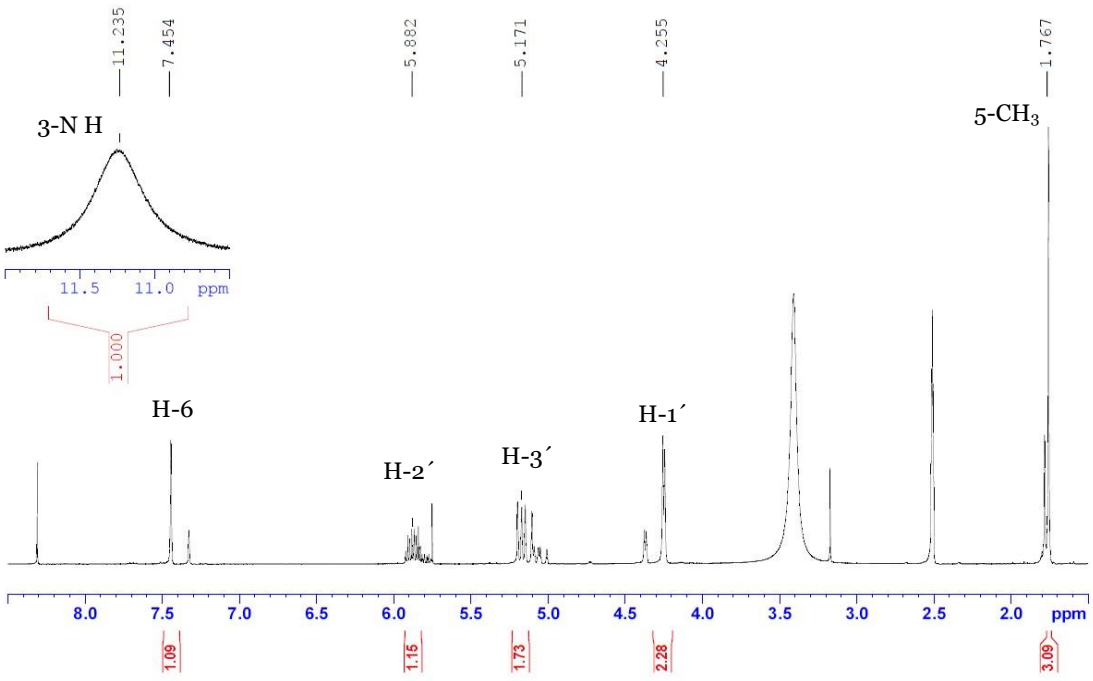

Figure 19. Confirmation of 1-(2-propenyl) thymine synthesis by NMR. ^{1}H NMR spectrum of 1-(2-propenyl) thymine in DMSO-d_6, 400 MHz.

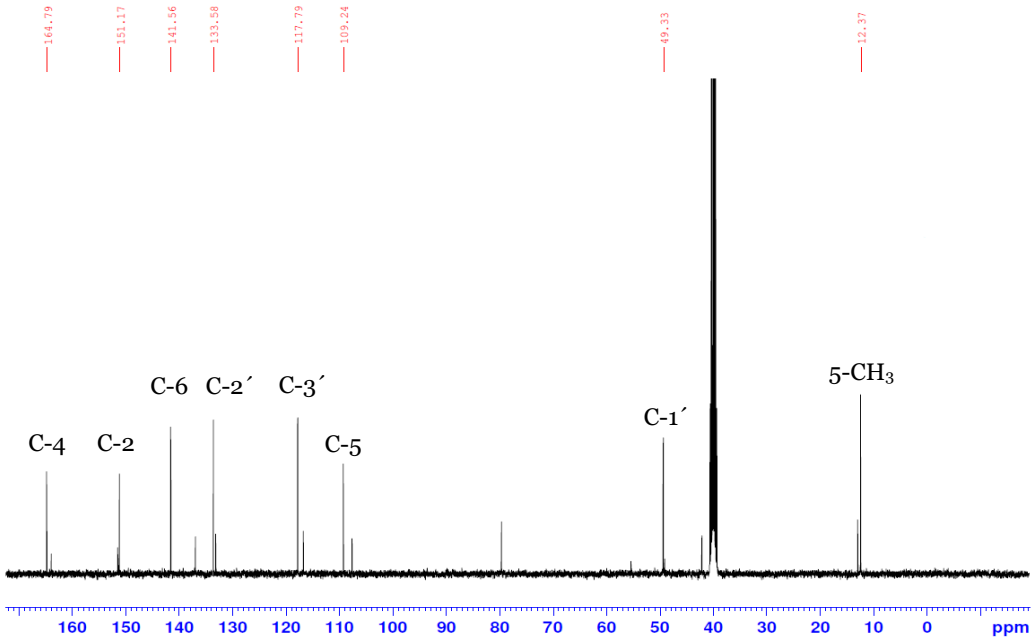

Figure 20. Confirmation of 1-(2-propenyl) thymine synthesis by NMR. ^{13}C NMR spectrum of 1-(2-propenyl) thymine in DMSO-d_6, 101 MHz.

Additionally, *Thibon et al. 1997* use a common strategy to eliminate the formation of these sub-products by masking the N3 proton of thymine with trimethylsilyl ether (Me_3Si), augmenting the purity of the desired product, which could be used in the future to eliminate the subproducts formation [178]. Although we were able to separate the **1C** product and the unreacted thymine, the current study fits the principles of the circular economy. Since the product **1C** can be used as a crosslinking agent in the cryogel synthesis due to the presence of two vinylic groups, which could be interesting to test, at the same time that the unreacted thymine can be used later to synthesize the ligand **1A** again, indirectly increasing the yield of the reaction and reducing the ligand synthesis costs and eliminating wastes.

4.2 Cryogels Characterization

4.2.1 SEM

This study allowed the characterization of the morphology as well as the approximate pore size of the different cryogels. For this purpose, scanning electron microscopy (SEM) images of cryogels with different quantities of ProT and the respective control were taken. The morphology of pHEMA-ProT0 (T0) (Figure 21) was significantly different, from pHEMA-ProT25 (T25), pHEMA-ProT37.5 (T37.5) and pHEMA-ProT50 (T50) (Figure 22).

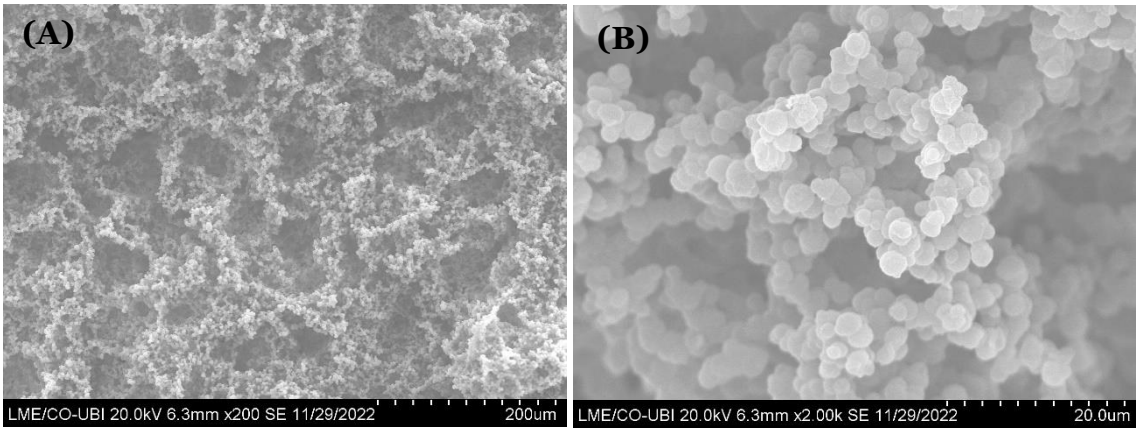

Figure 21. SEM images of pHEMA-ProT0 with amplifications of 200x (A) and 2000x (B).

In a study conducted by *Savina et. al. 2016*, pHEMA cryogels were synthesized using the conventional method and the pre-freezing method [144]. In the conventional method, the gel walls were smooth, and no aggregation of the polymer was observed, this could be explained by the fact that the freezing step occurs rapidly, which makes the unfrozen liquid microphase (UFLMP) highly concentrated with small volume and limited diffusion of the polymer. As a result, a polymer with smooth walls is formed which is the morphology of cryogels T37.5 and T50.
On the other hand, in the pre-freezing method, the polymer mixture is cooled until –2ºC, the ice crystals are allowed to start forming and only then the initiators are added to an already pre-concentrated solution which leads to a rapid polymerization under semi-frozen conditions. Then, a subsequent phase separation of the polymer formed in the liquid phase occurs, leading to the formation of a more complex structure of polymer aggregates (bead-like structure) with the combination of macro and micropores in polymer walls and larger porosity, giving a structure similar to T0 (Figure 21) [144].

Despite all cryogels, in the present work, were prepared following the same protocol, once that the cooling bath was put in a refrigerator without having its temperature precisely followed. It is possible that was not at – 20ºC when the T0 cryogel was placed in this exact bath, resulting in a slower cooling process, giving conditions for the phase separation described by *Savina et al. 2016* to occur during the synthesis of T0 cryogel. The cryogels T37.5 and T50 were prepared sequentially after T0, so the temperature of the acetone bath could be already in a temperature that promotes a rapid freezing of the solvent, resulting in cryogels with thinner polymer walls.

Therefore, this differences in the freezing temperatures, possibly encourage the formation of the same type of 3D structure observed in the cryogels synthesized by the pre-freezing method for the T0 cryogel. This hypothesis is correlated with the transient

morphology of T25, which was synthesized after T0. T25 has traces of the bead-like morphology of T0 and traces of the smooth wall observed in T37.5 and T50 which were the last cryogels to be synthesized. Additionally, the occurrence of a microstructure (small craters) was observed prevailing mostly in the T50.

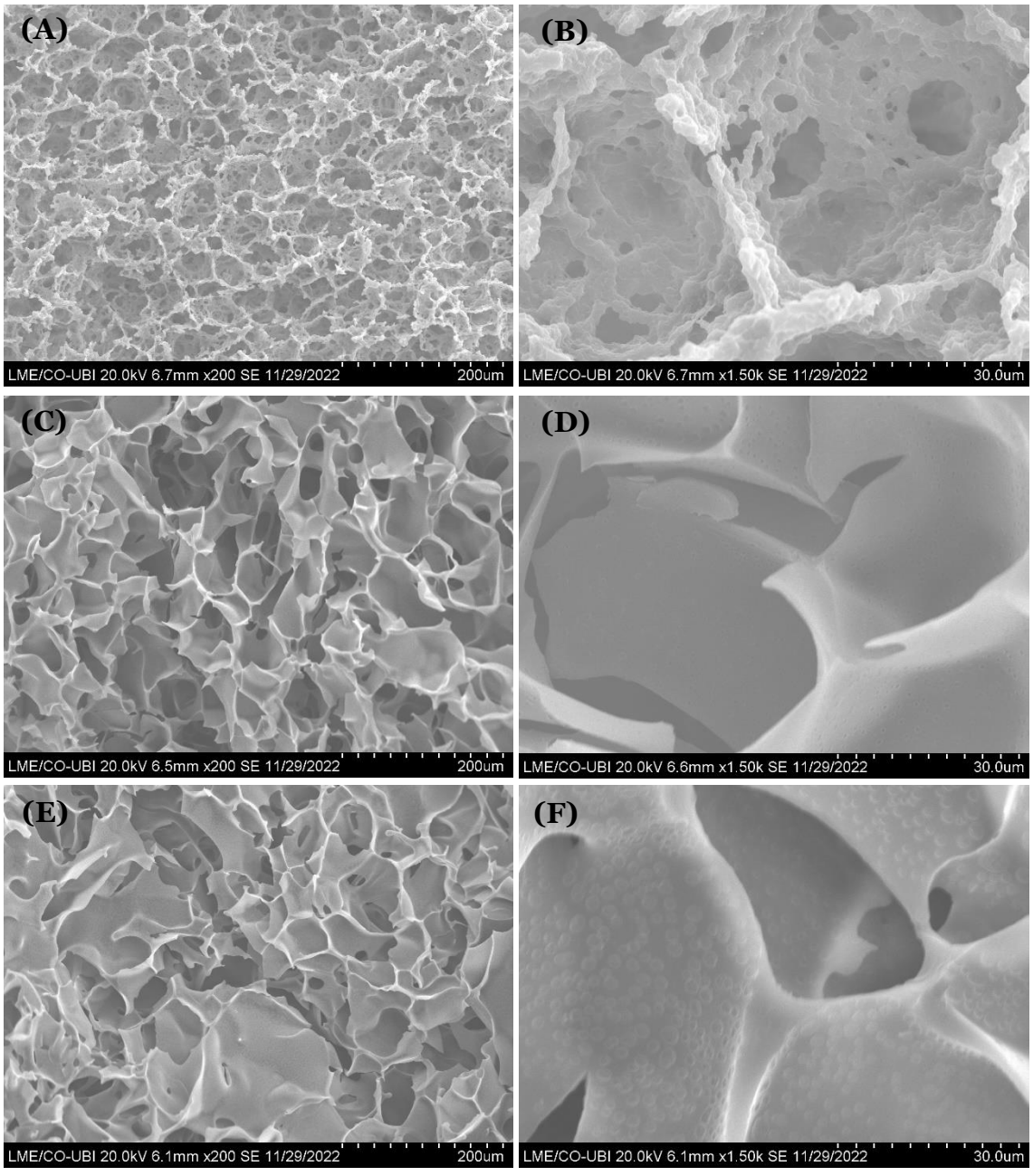

Figure 22. SEM images of pHEMA-ProT25 (A-B), pHEMA-ProT37.5 (C-D) and pHEMA-ProT50 (E-F) with amplifications of 200x (A, C, E) and 1500x (B, D, F).

Kose et al. 2016 described that the presence of this bead-like structure is a consequence of the use of sodium lauryl sulphate as a means to facilitate the solubilization of the more hydrophobic monomers, lowering the surface tension of water, a method used by Dogan *et al. 2015*, which obtained the same bead-like structure [129, 181]. Even though, this explanation is not consensual since the SEM images for p(HEMAdeM)-50 from Kazim

Köse do not show this structure, in fact, it doesn't seem to have any pores, and there is no direct comparison of the morphology of the functionalized cryogels with the unfunctionalized cryogel [129]. Moreover, *Kose et al. 2016*, have also cooled the polymer mixture before adding the initiators, this could have been the reason for the formation of the bead-like structure in the p(HEMAdeM)-100 cryogel [129]. Additionally, the results of *Kose et al. 2016* are in contradiction to those of *Savina et al. 2016* and those presented in this work once no surfactant agents were used [129].

Furthermore, the differences observed between T0 and the T25, T37.5 and T50 may also be due to the presence of the ligand, as T25 has a mixed morphology, while T37.5 and T50 cryogels have smooth polymer walls. This hypothesis was previously tested, being observed the same morphological differences between the control cryogel and the functionalized ones [182]. In that study, it was concluded that after the synthesis of functionalized cryogels with a crescent concentration of ligand (6, 7, 8 and 9 mg/mL, respectively) the morphology evolved from the bead-like structure to smooth walls [182]. These results can give a possible explanation for the morphological differences observed in the synthesized cryogels. However, the previous functionalization method [183] was different from the one used in the present work, because instead of a co-polymerization technique, where the ligand was mixed together with the other monomers, in the previous procedure, the ligand was only immobilized after the cryogels synthesis through a post-modification protocol. So, the morphology differences observed in T0, T25, T37.5 and T50, could not be totally explained by this assumption [182].
Finally, a similar study with a crescent gradient of the amount of ligand and a cryogel synthesis comparing the pre-freezing method with the conventional method should be done in order to confirm the aforementioned hypothesis. Also, the overall results reveal a large continuous interconnected pore structure with a pore size estimated between 10 and 100 μm. This structure allowed the flow-through of the mobile phase with negligible mass transfer resistance.

4.2.2 Swelling Test – Rehydration capacity

The rehydration capacity of the different cryogels was calculated using equation (1), and the values were recorded in Table 8. The swelling behaviour of cryogels is a crucial characteristic since it improves the surface area/volume ratio and pore size, which makes it easier for mRNA molecules to pass through the pores. The water accumulated in the pores of the cryogel was released during a dry treatment. When the cryogel was submerged in water, the opposite response was also seen: the cryogel quickly recovered its original size and shape.

Table 8. Rehydration capacity of the synthesized cryogels.

	Water Uptake (g H_2O/g Cryogel)
pHEMA-Pro**To**	7.73
pHEMA-ProT**25**	8.40
pHEMA-ProT**37.5**	8.99
pHEMA-ProT**50**	8.68

According to recent reports, for the To (control) cryogel, the support's equilibrium swelling degree was between 6.00 and 9.00 g of H_2O/g of dry cryogel [135, 183, 184]. Concerning the functionalized cryogels, the rehydration capacity slightly increased when compared with the control, which may indicate the presence of the ligand in the polymeric matrix. In contrast with other methods described in the literature, when an adenine derivative was incorporated in a pHEMA cryogel the rehydration capacity was 4.96 H_2O/g of dry cryogel [129], significantly lower when compared to the Poly-Thymine cryogels described in the present work, where the swelling behaviour of the cryogels was not negatively affected. The synthesized cryogel was opaque and had a structure resembling a highly elastic sponge. The dried cryogels soaked up water and expanded to their original size after 1-2 seconds of being submerged in water (Figure 23).

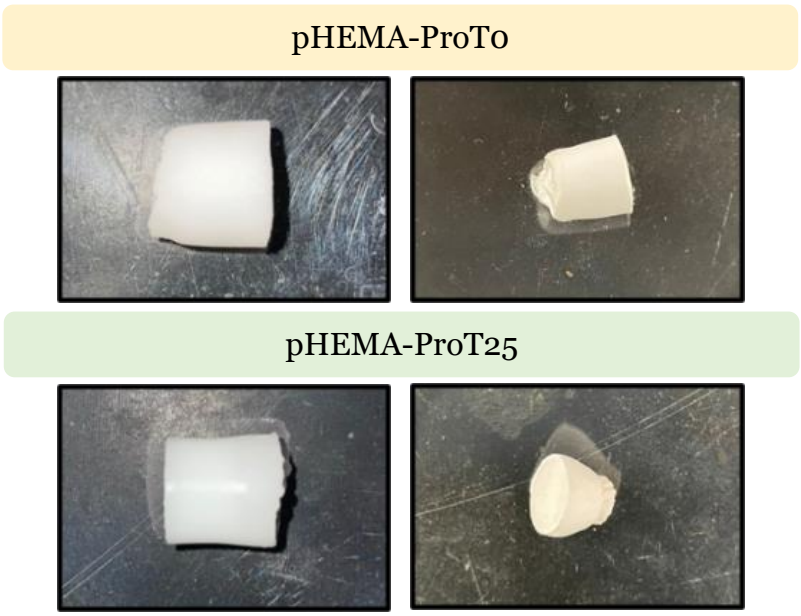

Figure 23. Swollen (left images) and dried (right images) structure of the synthesized cryogels.

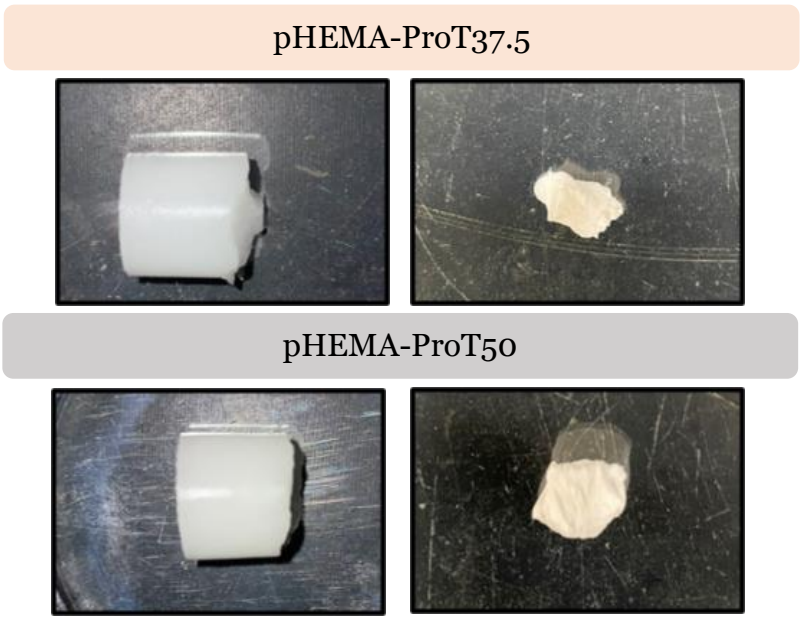

Figure 23. (Continuation) Swollen (left images) and dried (right images) structure of the synthesized cryogels.

4.2.3 Energy Dispersive X-ray Analysis

In order to evaluate the incorporation of the ProT ligand in the synthesized cryogels, the energy dispersive X-ray analysis (EDXA) was performed, where the nitrogen percentage (N%) of the cryogels dried by two different modes (sample 1: freeze-dried; sample 2: ethanol dried) was quantified. The results were evaluated by comparing the percentages between the control cryogel (T0) and the functionalized ones (T25, T37.5 and T50) (Table 9). It was found that in both samples, the N% was higher in T25 comparing to T0, suggesting the incorporation of the ligand in the T25 cryogel. However, for T37.5 in the freeze-dried sample, a decrease in the N% was observed, indicating that possibly the functionalization did not occur. Moreover, for the T50 freeze-dried sample, the %N increased in comparison to the control, though, by a smaller amount regarding T25. This can indicate that functionalization occurred, but in a lower extent, what was also unexpected given that T50 was synthesized using a higher amount of ligand (50 mg).

Table 9. Nitrogen percentage of the four synthesized cryogels.

	T0 (N%)	**T25 (N%)**	**T37.5 (N%)**	**T50 (N%)**
Sample 1 (Freeze-Dried)	5.35	6.52	3.97	6.05
Sample 2 (Ethanol dried)	7.14	7.39	7.14	7.14

Furthermore, in the given N%, two nitrogen atoms are included from the crosslinking agent N, N'-methylene-bis(acrylamide) which is why it is possible to measure it in the control cryogel. Moreover, there was a great variability in the results obtained between the two samples, making this analysis more difficult. One of the reasons that can justify the variability between the results for the same cryogels, may be the lack of homogeneity of the sample. One solution to this issue could be to grind the cryogels in a crucible to homogenize the sample before the measures. In addition, this method showed to have a high associated error with the measurements, in the order of two percentage points, being more specific for determining the presence of heavier chemical elements such as nickel, silver or gold [184, 185]. Actually, the error associated to the measurement is clearly visible by analysing the N% between sample 1 and 2.

Herein, other methods of confirming the presence of the ligand should be used in the future to corroborate the EDXA results, such as elemental analysis (EA) or solid-state nuclear magnetic resonance (NMR) [182, 186]. Thus, the present method served only to give an idea if, in fact, some changes in the N% of cryogels T25, T37.5 and T50 occurred in relation to the control, indirectly indicating the presence or not of the ProT ligand in their composition.

4.3 Screening Binding/Elution conditions for LMW RNA

To verify the best-suited purification conditions for the binding/elution of the IVT mRNA samples, a LMW RNA sample with 80 µg was first used as a model. The chromatographic assays were always accompanied by the respective control (poly(HEMA-ProT0)) without the ligand (ProT). For that, experiments were performed to determine how these novel cryogels supports interact with LMW RNA by using experimental settings (Table 10) to favour different interactions (Figure 24). The LMW RNA binding and elution behaviour was analysed, by measuring absorbance at 260 nm and calculating the mass of LMW RNA that bound (Table 11) and eluted (Table 13) in each stage of the chromatographic experiment.

Table 10. Binding buffers used in the screening binding/elution conditions for LMW RNA.

Assay	Binding Buffers
1	Tris-HCl 10 mM pH = 8.0
2	250 mM NaCl in Tris-HCl 10 mM pH = 8.0
3	Sodium-Acetate 200 mM, pH = 5.5
4	250 mM NaCl in Sodium-Acetate 200 mM pH = 5.5
5	Sodium-Acetate 10 mM, pH = 5.0
6	1 M Ammonium Sulphate in Tris-HCl 10 mM pH = 8.0
7	1.5 M Ammonium Sulphate in Tris-HCl 10 mM pH = 8.0
8	2 M Ammonium Sulphate in Tris-HCl 10 mM pH = 8.0
9	2.5 M Ammonium Sulphate in Tris-HCl 10 mM pH = 8.0
10	1.5 M Ammonium Sulphate in Sodium-Acetate 10 mM pH = 5.0

Table 11. Mass of LMW RNA that bound to the cryogels supports after the binding step.

Assay	pHEMA-ProT0	pHEMA-ProT25	pHEMA-ProT37.5	pHEMA-ProT50
1	22 µg	2 µg	23 µg	8 µg
2	30 µg	14 µg	25 µg	22 µg
3	34 µg	24 µg	27 µg	28 µg
4	30 µg	34 µg	37 µg	24 µg
5	67 µg	76 µg	60 µg	22 µg
6	38 µg	50 µg	40 µg	34 µg
7	23 µg	29 µg	40 µg	44 µg
8	58 µg	53 µg	58 µg	34 µg
9	42 µg	62 µg	43 µg	28 µg
10	17 µg	41 µg	22 µg	34 µg

To initiate our study, a binding step with Tris-HCl 10 mM, pH = 8.0 was made (Table 10 - Assay 1) to verify if the support could interact with the LMW RNA samples at pH = 8.0. The results showed that the majority of the LMW RNA eluted after the binding step (Table 11 – Assay 1), demonstrating that this condition was not suitable for the retention of LMW RNA. So, a binding step with 250 mM NaCl in Tris-HCl 10 mM pH = 8.0 was done (Table 10 - Assay 2) to "neutralize" the negatively charged groups present in the LMW RNA molecules and at the same time favouring the formation of hydrogen bonds between the RNA sample and the T0, T25, T37.5 and T50 cryogels. The results showed a slight increase in the amount of LMW RNA that was bound (Table 11 -Assay 2) in all supports, although no significant differences were observed between the Poly-Thymine cryogels and the control. The strategy of implementing some ionic strength at the binding buffer was previously described in literature for the purification of a pre-microRNA, at the same time that the majority of the impurities were washed off from an affinity chromatographic support with arginine as ligand, allowing the establishment of hydrogen bonds with the pre-miRNA [187].

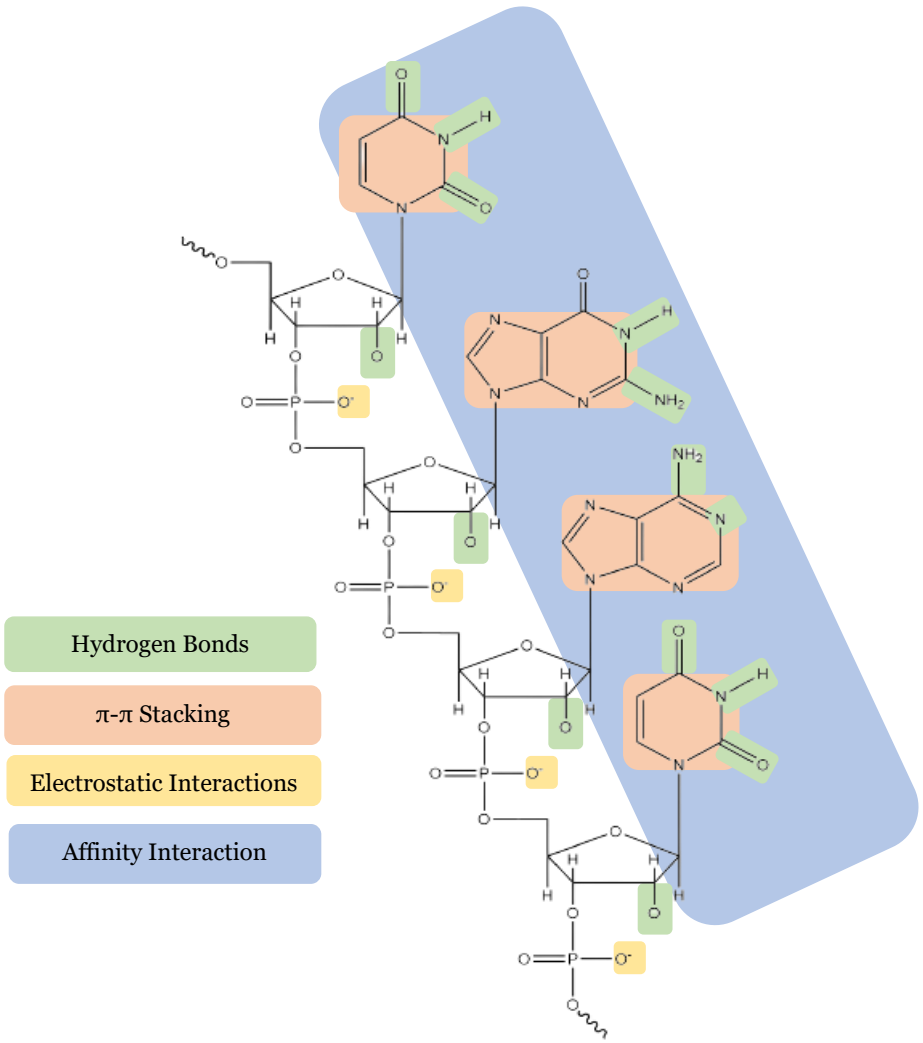

Figure 24. Schematic representation of the principal interactions that RNA can establish.

In assays 3, 4 and 5 (Table 10), the effect of the pH reduction was studied. Concerning assay 3 no significant changes in the binding of the LMW RNA sample were observed between the different cryogels (Table 11 – Assay 3). So, following the principle of assay 2, 250 mM NaCl was used in the binding step (Table 10 - Assay 4), and a slight increase on RNA binding was observed in T25 and T37.5 cryogels, although no significant changes were observed in T0 and T50 (Table 11 – Assay 4). This could be due to the fact that the buffers of assays 3 and 4 had a higher concentration of Sodium-Acetate (200 mM), and so, a higher mass of salt ions in the buffer solution, which could disturb the interactions between the RNA sample and the supports. When a lower concentration of binding buffer (Sodium-Acetate 10 mM) was established along with a reduction of the pH to 5.0 (Table 10, Assay 5), the results showed a significant increase in the retention of LMW RNA which is in accordance with the results of *Santos et al. 2018* in which the totality of nucleic acids bound to the cryogel matrix also using the same condition [135].

Additionally, it is worth noticing that the T25 cryogel demonstrates a higher LMW RNA retention compared to the T0, which could indicate the presence of the ligand in the support. In contrast for the T37.5 and T50, the amount of LMW RNA bound to the cryogels decreased compared to the T0. This could be a result from the higher ligand mass employed in the T37.5 and T50 cryogels synthesis. To confirm these results, a more detailed study with different quantities of the ligand should be done in order to determine if the amount used to synthesize the T37.5 and ProT50 exceeded the limit of the ligand that can co-polymerize when synthesizing the cryogels. If so, it could also be understood whether the excess of ligand in the solution is affecting the amount of ligand that is reacting during the co-polymerization reaction.

In addition, from assay 6 to 11 (Table 10) the capacity of the synthesized cryogels for establishing hydrophobic interactions was studied. The results showed some degree of retention of LMW RNA (Table 11), what could be due to the presence of an aliphatic chain formed during the polymerization process between the HEMA monomers. Also, the ligand possesses a spacer arm of 3 carbons which can also contribute to some degree with hydrophobicity allowing the retention of the sample, possibly explaining the differences of bound LMW RNA in the binding step, namely between the T0 and the T25 cryogels from assay 6 to 11 (Table 11).

Although no total binding was observed in the different studied hydrophobic conditions, implying that in the binding of LMW RNA to the cryogel, other types of interactions besides the hydrophobic ones can participate, but are not favoured in these conditions. It is noteworthy that affinity interactions involve different types of interactions, and besides hydrophobic interactions also participate electrostatic interactions, hydrogen bonds, π-π interactions and van der Waals forces. In this specific case and taking into

account the chemical structure of the HEMA monomer and allyl thymine, the prevalent bonds between the supports and the LMW RNA will be mostly by hydrogen bonds and hydrophobic interactions.

As expected, the control cryogel demonstrated the ability to bind LMW RNA, demonstrating that the major player in the retention of the LMW RNA is the HEMA monomer instead of the allyl thymine, even though the T25 cryogel showed in some assays an increased binding to the target molecule. The capacity of HEMA to bind RNA molecules was described by *Santos et al. 2018* who successfully separate pVAX1-*LacZ* isoforms from RNA after all nucleic acids were captured from a clarified lysate sample [135].

Table 12. Elution buffers used in the screening binding/elution conditions for LMW RNA.

Assay	Elution Buffers
1	1.5 M NaCl in Tris-HCl 10 mM pH = 8.0
2	Tris-HCl 10 mM, pH = 8.0
3	Tris-HCl 10 mM, pH = 8.0
4	Tris-HCl 10 mM, pH = 8.0
5	250 mM NaCl in Sodium Acetate 10 mMpH = 5.0/ 1.5 mM NaCl in Sodium Acetate 10 mM pH = 5.0
6	Tris-HCl 10 mM, pH = 8.0
7	Tris-HCl 10 mM, pH = 8.0
8	Tris-HCl 10 mM, pH = 8.0
9	Tris-HCl 10 mM, pH = 8.0
10	Tris-HCl 10 mM, pH = 8.0

Table 13. Mass of LMW RNA that eluted from the cryogels supports after the elution step.

Assay	pHEMA-ProT0	pHEMA-ProT25	pHEMA-ProT37.5	pHEMA-ProT50
1	6 µg	1 µg	3 µg	0 µg
2	23 µg	8 µg	3 µg	6 µg
3	19 µg	8 µg	16 µg	2 µg
4	10 µg	7 µg	11 µg	2 µg
5	39 µg	54 µg	30 µg	12 µg
6	6 µg	6 µg	7 µg	4 µg
7	14 µg	11 µg	27 µg	13 µg
8	25 µg	30 µg	22 µg	13 µg
9	27 µg	32 µg	26 µg	18 µg
10	9 µg	10 µg	9 µg	3 µg

Because the binding of LMW RNA to the majority of cryogels was relatively low, the elution results presented in Table 13 were also difficult to analyse and understand. In fact, it is not possible to conclude whether the low recovery is due to the experimental conditions and selected buffers or associated to the low RNA binding. Nevertheless, in the assays where hydrophobic interactions were favoured, namely in assays 8 and 9, the use of Tris-HCl 10 mM, pH = 8.0 as elution buffer, allowed the partial elution and recovery of the bound sample. This could have been due to the extreme conditions that were used to favour the binding of the LMW RNA, causing it to bind strongly to the cryogel matrix. The elution step with 10 mM Tris-HCl buffer at pH = 8.0, although it was able to elute some of bound RNA, failed to elute all the LMW RNA. Additionally, strategies such as step elution with a decreasing concentration of ammonium sulphate and elution at a higher pH, such as 9.0, were performed (data not shown), but no changes in the LMW RNA elution occurred. Moreover, compared to ammonium sulphate , NaCl is easier to remove from purified samples and poses less threats to the environment than the salts employed in hydrophobic interaction (ammonium sulphate). For this reason, NaCl is generally preferred to purify biomolecules.

Herein, assay 5 showed the best results in the elution screening. The fact that a very acidic pH was used in binding may have contributed to the strong binding of LMW RNA to the cryogels, namely in the T0, T25 and T37.5, resulting in the incomplete elution of the bound LMW RNA, even after using a buffer with a higher concentration of NaCl (1.5 M). The elution occurs because the interactions are weakened when ionic strength in the eluent increases. This change in the buffer may induce a neutralization of the RNA charge due to the interaction with sodium cations promoting its elution [135, 188]. It is worth noticing that T25 cryogel showed a higher elution of LMW RNA (54 μg) compared to T0, which had 39 μg, which in turn was higher than the amount of sample eluted from T37.5 (30 μg) and T50 (12 μg). Also, the differences in the amount of RNA that bound and eluted in Assay 5 (Table 11 and 13) further reinforce the need to perform a systematic study with different quantities of the ligand to understand the influence of the ligand density on the capacity of cryogels to bind and elute RNA.
In conclusion, the best-suited condition by which the cryogels supports interact with LMW RNA are the conditions of assay 5.

4.4 Reproducibility of the cryogels

A reproducibility study, utilizing the cryogel supports T0, T25 and T37.5 was made (Figure 25) in order to verify the consistency of the results obtained previously in the Assay 5 and move forward to the preliminary studies of binding and elution of mRNA. The cryogel T50 was removed from this study as it presented a poor binding ability for LMW RNA.

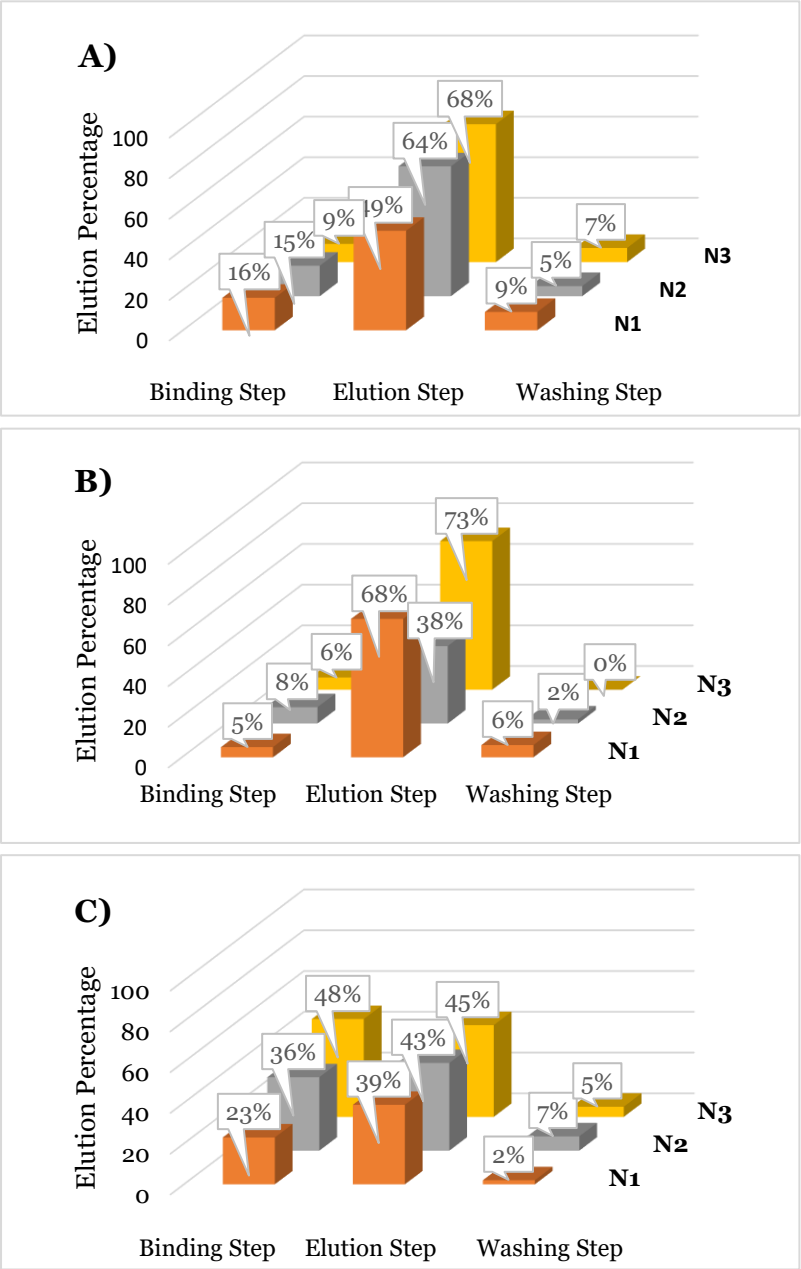

Figure 25. Reproducibility of the binding and elution behaviour in the conditions established for the assay 5. A) pHEMA-ProT0, B) pHEMA-ProT25 and C) pHEMA-ProT37.5.

From the analysis of the reproducibility assays, the cryogel T0 and T25 (Figure 25, A and B) had similar values in the binding step even though the ones from T0 were higher than

those observed in the T25 cryogel, being in accordance with the results presented in table 11. This indicated a higher retention for the T25 support. The elution percentage behaviour from T0, T25 and T37.5 was reproducible, in spite of the existence of an outlier assay, N1 in the case of T0 (Figure 25, A) and N2 for T25 (Figure 25, B).

Prior to starting the studies of mRNA binding and elution, a new synthesis of cryogels was carried out, to not compromise the retention behaviour as a result of the high use of cryogels. This is important as it has already been extensively demonstrated that the binding capacity of cryogels decreases as the number of experiments increases [129].

Figure 26 depicts the outcomes of the newly synthesized (ns) cryogels (ns-T0, ns-T25, ns-T37.5, and ns-T50) that were subjected to the identical binding/elution conditions used in assay 5. The results show some variability, what is already pointed as a limitation of cryogels, the difficulty of obtaining identical and reproducible cryogels in different synthesis.

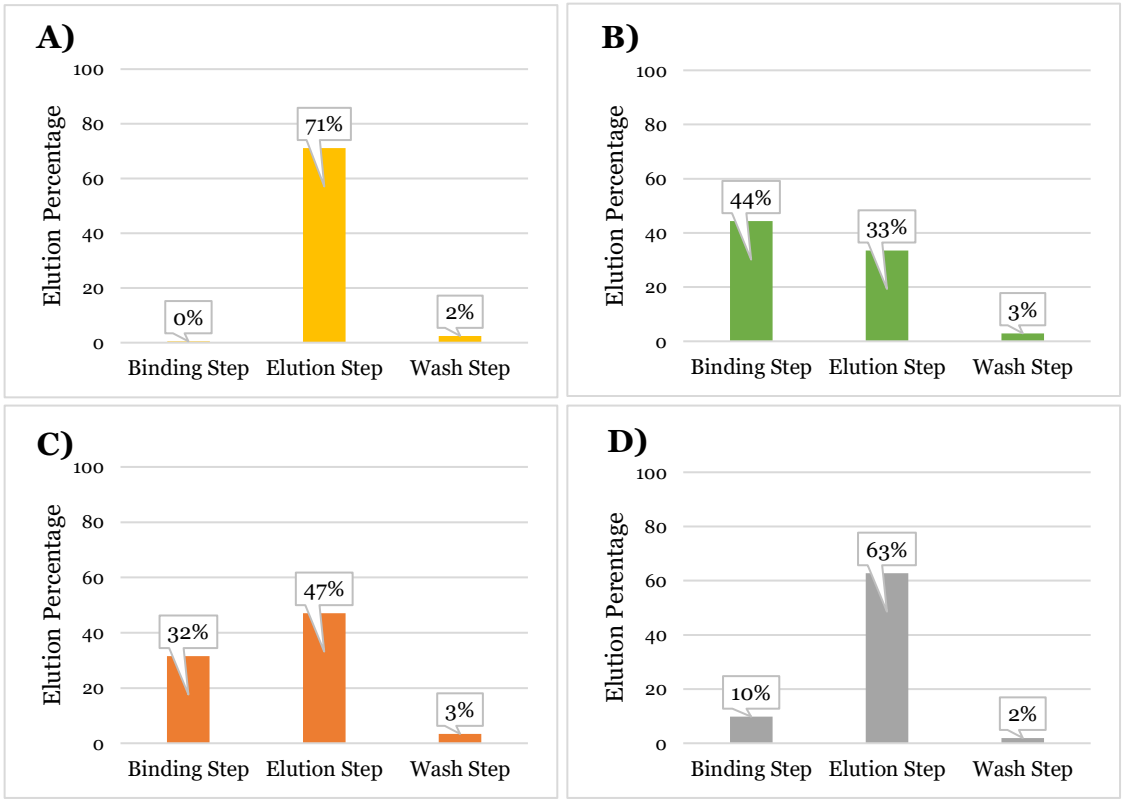

Figure 26. Reproducibility of the new synthesized cryogels regarding their binding and elution profile, using the conditions established for assay 5. A) pHEMA-ProT0, B) pHEMA-ProT25, C) pHEMA-ProT37.5 and D) pHEMA-ProT50.

The difficulty of obtaining reproducible cryogels is observed by comparing the results of T25 (Figure 25, B) and ns-T25 (Figure 26, B), showing significant differences in binding/elution of LMW RNA. Similar results are seen for the ns-T50, which outperformed the cryogel T50, that previously obtained elution percentages of 73% and

15%, for the binding and elution steps, respectively. For cryogels T0, T37.5, ns-T0 and ns-T37.5, the results were similar for both binding and elution, being consistent between the two cryogels.

4.5 Preliminary studies of the Binding/Elution of mRNA

Once completed the screening with LMW RNA as a model, ns-T0, ns-T25 and ns-T50 cryogels were chosen to proceed with the analysis of the behaviour of an mRNA sample without any type of previous treatment. The ns-T37.5 cryogel was eliminated from mRNA binding/elution studies, as it showed similar behaviour to ns-T25 (Figure 26, B and D). As ns-T50 demonstrated higher potential for binding/elution of LMW RNA (Figure 26, D) it was also included in the study of mRNA binding.

An 80 μg mRNA sample obtained by IVT was prepared for each performed experiment in 10 mM Sodium-Acetate buffer, pH = 5.0 and used in the various assays described below. The binding and elution were analysed by measuring absorbance at 260 nm and drawing a chromatographic profile for each assay. The fractions corresponding to the elution of some species were collected, concentrated, and analysed by 1% agarose gel electrophoresis enabling a better understanding of what was occurring over the course of the various experiments.

Five assays were performed for each selected cryogel. Assay 1 was done in order to verify if the conditions chosen as ideal in the screening of binding/elution of LMW RNA were also optimal in the binding and elution of the mRNA. From assay 2 to assay 5, different elution buffers with a concentration of NaCl of 250 mM, 150 mM, 100 mM and 77 mM were used, aiming the separation between the linearized pNZY28-BruMEDI3622 and the BruMEDI3622 mRNA.

4.5.1 pHEMA-ProT0 Cryogel

The ns-T0 cryogel has already shown its potential for nucleic acid purification, demonstrating the ability to bind all nucleic acids from a clarified lysate sample [135]. In addition, it was possible to purify the pDNA from the same sample [135]. Thus, it is expected that this cryogel will be able to promote the binding of mRNA and pDNA at the same time, however, regarding the separation between these two biomolecules, we do not know how the behaviour will be. Since we do not have any ligand that confers selectivity for the mRNA, it is presumable that there is no tendency for separation between this biomolecule and the linearized pDNA. However, understanding the behaviour of this cryogel for mRNA is crucial, as it will allow us to conclude whether functionalization with the ProT ligand had promising effects on mRNA purification or not.

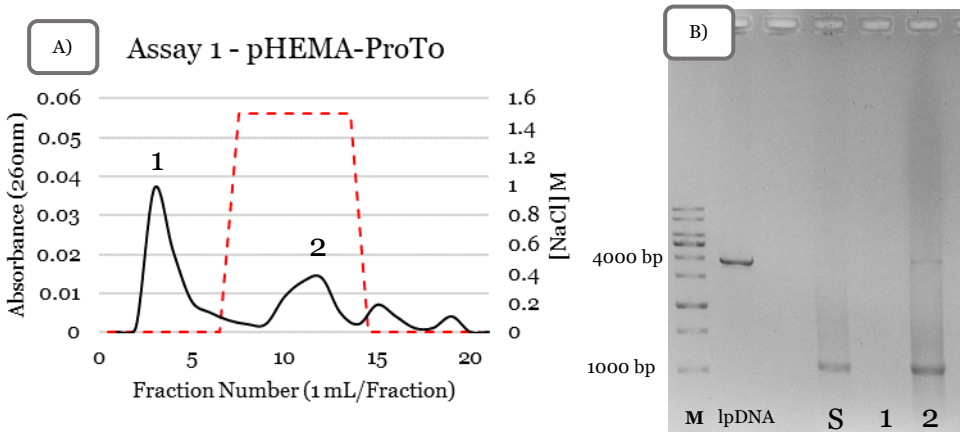

Figure 27. A) Chromatographic profile obtained with the pHEMA-ProTo cryogel support. For the binding step 10 mM sodium acetate buffer pH = 5.0, for the elution step **1.5 M NaCl** in 10 mM sodium acetate buffer pH = 5.0 (represented by the red dashed line); B) agarose electrophoresis of the collected fractions, M- Molecular marker; lpDNA – linearized pNZY28-BruMEDI3622 (3931 bp); S – Injected Sample; 1 and 2 – respective peaks of the chromatogram.

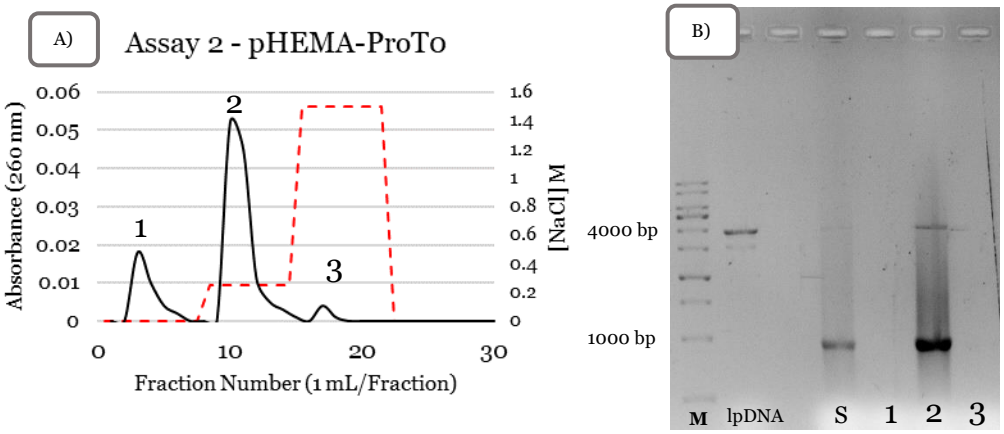

Figure 28. A) Chromatographic profile obtained with the pHEMA-ProTo cryogel support. For the binding step 10 mM sodium acetate buffer pH = 5.0, for the first elution step **250 mM NaCl** in 10 mM sodium acetate buffer pH = 5.0, for the second elution step **1.5 M NaCl** in 10 mM sodium acetate buffer pH = 5.0, (represented by the red dashed line); B) agarose electrophoresis of the collected fractions, M- Molecular marker, lpDNA – linearized pNZY28-BruMEDI3622 (3931 bp), S – Injected Sample; 1, 2 and 3 – respective peaks of the chromatogram.

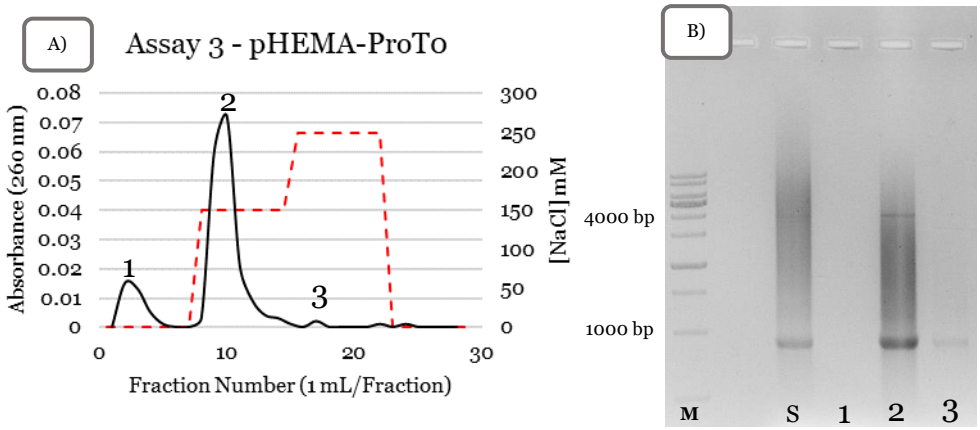

Figure 29. A) Chromatographic profile obtained with the pHEMA-ProTo cryogel support. For the binding step 10 mM sodium acetate buffer pH 5.0, for the first elution step **150 mM NaCl** in 10 mM sodium acetate buffer pH = 5.0, for the second elution step **250 mM NaCl** in 10 mM sodium acetate buffer pH = 5.0, (represented by the red dashed line); B) agarose electrophoresis of the collected fractions, M- Molecular marker, S – Injected Sample; 1, 2 and 3 - respective peaks of the chromatogram.

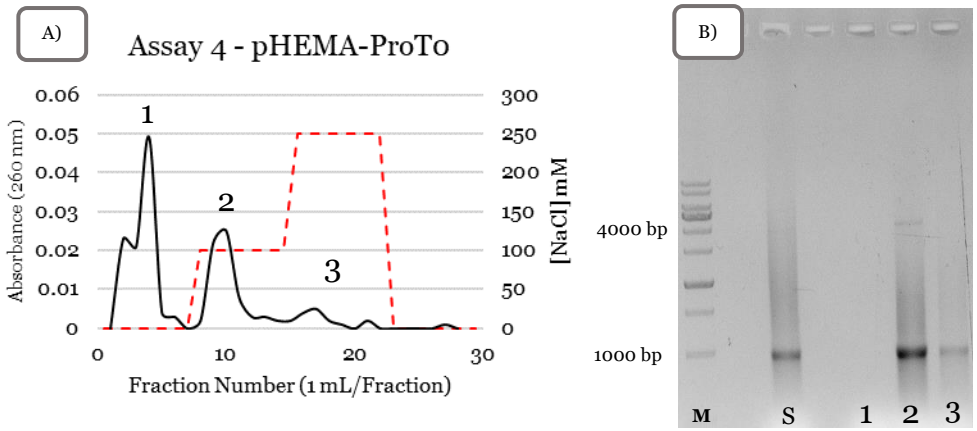

Figure 30. A) Chromatographic profile obtained with the pHEMA-ProTo cryogel support. For the binding step 10 mM sodium acetate buffer pH = 5.0, for the first elution step **100 mM NaCl** in 10 mM sodium acetate buffer pH = 5.0, for the second elution step **250 mM NaCl** in 10 mM sodium acetate buffer pH = 5.0, (represented by the red dashed line); B) agarose electrophoresis of the collected fractions, M- Molecular marker, S – Injected Sample; 1, 2 and 3 - respective peaks of the chromatogram.

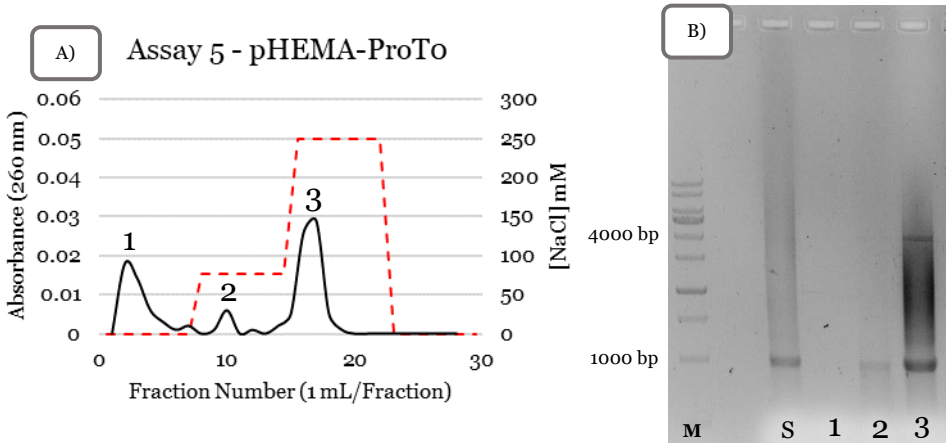

Figure 31. A) Chromatographic profile obtained with the pHEMA-ProTo cryogel support. For the binding step 10 mM sodium acetate buffer pH = 5.0, for the first elution step **77 mM NaCl** in 10 mM sodium acetate buffer pH = 5.0, for the second elution step **250 mM NaCl** in 10 mM sodium acetate buffer pH = 5.0 (represented by the red dashed line); B) agarose electrophoresis of the collected fractions, M- Molecular marker, S – Injected Sample; 1, 2 and 3 - respective peaks of the chromatogram.

From the analysis of the 5 assays performed with ns-To cryogel (Figures 27 to 31), it is possible to confirm that the binding of mRNA was successfully achieved under the chosen conditions (10 mM sodium acetate buffer pH 5.0). Although, as it was previously found for pVAX1-LacZ isoforms by *Santos et al. 2018*, the pDNA template used for IVT was also retained during the binding step [135]. Additionally, looking at the elution profiles of the performed experiments, the first peak does not correspond to the elution of mRNA or pDNA, instead, given the complexity of the IVT samples, unreacted ribonucleotides could be washed off in this initial step, which can also absorb at 260 nm. This could be confirmed through the use of an analytical method like analytical high-performance liquid chromatography (HPLC) which has recently been implemented along with the upstream processes of IVT, giving insight about the quantity of ribonucleotides present in a reaction mixture and also, quantifying the formation of the mRNA [189].

Concerning the elution results for the ns-To cryogel, there were no significant differences from the assays 2 to 5 (Figures 28 to 31), instead, mRNA and pDNA have eluted together in practically all assays. Once no ligand exists in the cryogel, the results indicate that HEMA monomers had the capacity for equally binding and eluting the mRNA and pDNA. Additionally, compared with the results of Santos *et al. 2018*, the elution of pDNA was accomplished in a much lower NaCl concentration (100 mM) (see Figure 30) instead of 600 mM being more economically advantageous. This could be due to the fact that the pDNA for IVT is linearized, so its elution behaviour could be different from the supercoiled and open circular pDNA isoforms studied in the previous work [135].

4.5.2 pHEMA-ProT25 Cryogel

The ns-T25 cryogel, created by copolymerizing HEMA and ProT monomers, was evaluated to determine whether it was possible to establish a separation method between the mRNA and the linearized pDNA, by exploring the affinity between the mRNA's poly(A) tail and ProT ligands. The EDXA data allowed us to deduce that the ligand was incorporated into the polymeric matrix. As a result, it is believed that the mRNA will be more retained than the linearized pDNA with this support. First, it was evaluated if the conditions previously established in assay 5 of LMW RNA could also function for the mRNA binding/elution. After that, several elution conditions were tested in order to separate the linearized pDNA and the mRNA, as presented below.

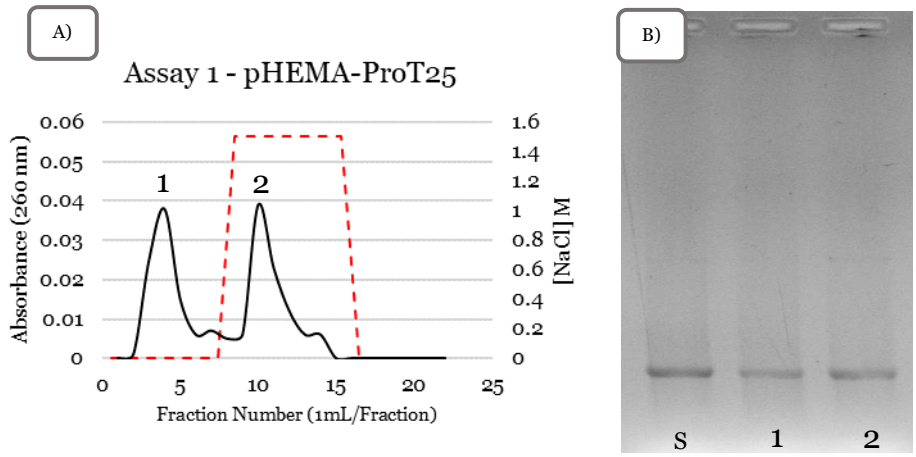

Figure 32. A) Chromatographic profile obtained with the pHEMA-ProT25 cryogel support. For the binding step 10 mM sodium acetate buffer pH = 5.0, for the elution step **1.5 M NaCl** in 10 mM sodium acetate buffer pH = 5.0 (represented by the red dashed line); B) agarose electrophoresis of the collected fractions, S – Injected Sample; 1 and 2 - respective peaks of the chromatogram.

T25 cryogel has demonstrated some differences regarding the ns-T0 cryogel. In the binding step, some elution of the target mRNA was observed, what could indicate that the functionalization of the cryogel could reduce the amount of mRNA that can bind to the matrix. A study using samples with different amounts of mRNA should be done with the purpose of verifying the validity of this hypothesis, allowing a better understanding if the maximum binding capacity is being surpassed. The initial mRNA sample preparation proved to be a challenge because it was not possible to accurately quantify the amount of mRNA that was being injected due to the existence of several impurities that can absorb at 260 nm. Therefore, the amount of mRNA that is being injected for each assay can slightly vary. This variation can result from the fact that the IVT was terminated after 4 hours without knowing if the reagents, specifically the ribonucleotides, had been completely used. As already mentioned, through the use of analytical HPLC, in which small volumes of samples are taken gradually from each IVT reaction mixture and injected onto an HPLC system, it would be possible to quantify the

remaining ribonucleotides and produced mRNA before proceeding with the purification stage [189].

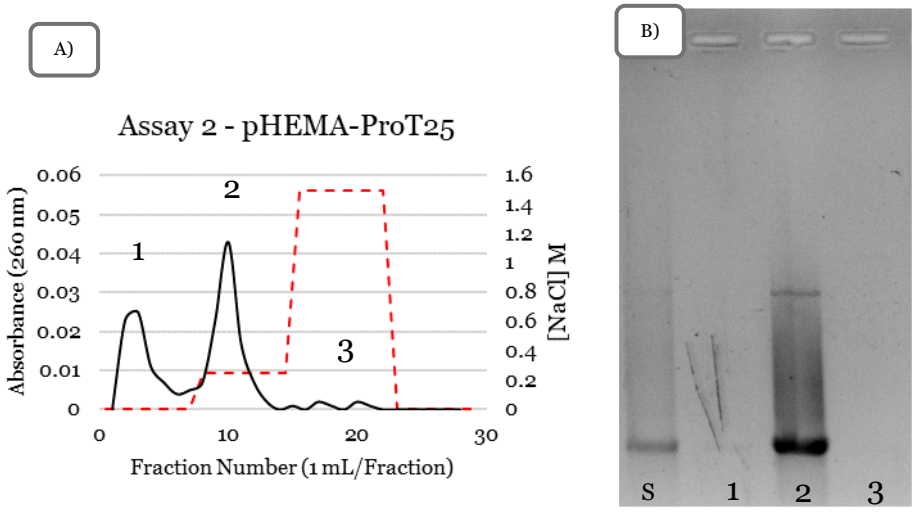

Figure 33. A) Chromatographic profile obtained with the pHEMA-ProT25 cryogel support. For the binding step 10 mM sodium acetate buffer pH = 5.0, for the first elution step **250 mM NaCl** in 10 mM sodium acetate buffer pH = 5.0, for the second elution **1.5 M NaCl** in step 10 mM sodium acetate buffer pH = 5.0 (represented by the red dashed line); B) agarose electrophoresis of the collected fractions, S – Injected Sample; 1, 2 and 3 - respective peaks of the chromatogram.

In contrast to what was observed in assay 1 (Figure 32), with these conditions (Figure 33) only a negligible losse of mRNA was detected in the binding step. Observing the absorbance of the peaks 1 and 2 from the assays 1 and 2, it is possible to conclude that mass injected in both assays was different. In assay 1, both peak 1 and 2 had same absorbance, around 0.040 abdorbance units (AU). For assay 2, peak 1 and 2 had a aproximatly 0.025 AU and 0.042 AU, respectively. Renforcing, the previously stated hypothesis that possibly the binding limit of mRNA is being reached. Nevertheless, a total elution of the bound material was accomplished with 250 mM of NaCl, showing that the strategy used in this assay was not suitable for the separation between mRNA and the linearized pDNA. Therefore, two other strategies using as first elution step 150 mM NaCl (Assay 3, Figure 34) and 100 mM NaCl (Assay 4, Figure 35), were evaluated.

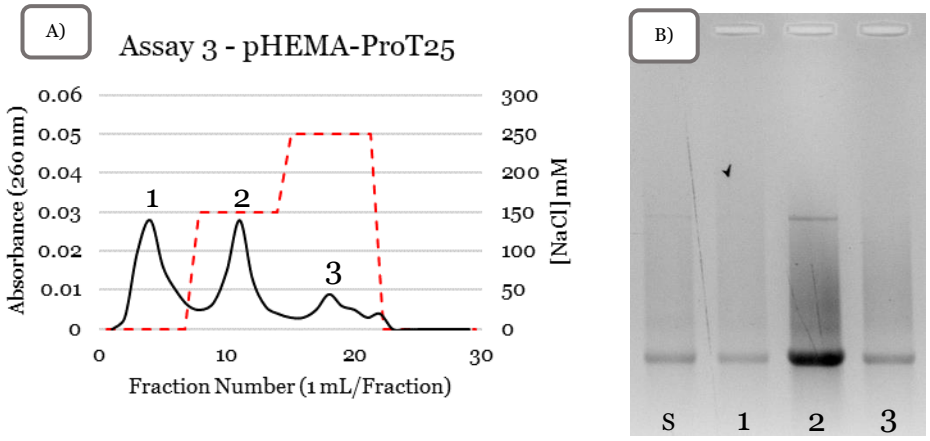

Figure 34. A) Chromatographic profile obtained with the pHEMA-ProT25 cryogel support. For the binding step 10 mM sodium acetate buffer pH = 5.0, for the first elution step **150 mM NaCl** in 10 mM sodium acetate buffer pH = 5.0, for the second elution step **250 M NaCl** in 10 mM sodium acetate buffer pH = 5.0 (represented by the red dashed line); B) agarose electrophoresis of the collected fractions, S – Injected Sample; 1, 2 and 3 - respective peaks of the chromatogram.

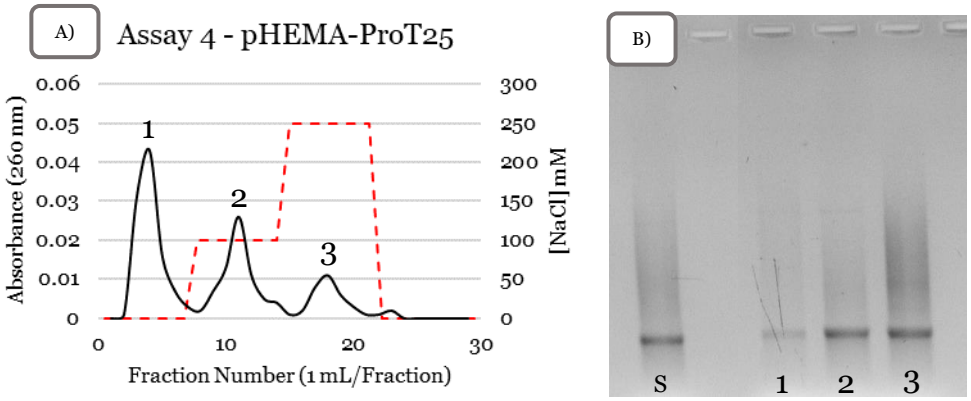

Figure 35. A) Chromatographic profile obtained with the pHEMA-ProT25 cryogel support. For the binding step 10 mM sodium acetate buffer pH = 5.0, for the first elution step **100 mM NaCl** in 10 mM sodium acetate buffer pH = 5.0, for the second elution step **250 M NaCl** in 10 mM sodium acetate buffer pH = 5.0 (represented by the red dashed line); B) agarose electrophoresis of the collected fractions, M- Molecular marker, S – Injected Sample; 1, 2 and 3 - respective peaks of the chromatogram.

From the analysis of assays 3 (Figures 34) and 4 (Figure 35), it can be observed that some distribution of mRNA started to occur, indicating that it can be possible to achieve the separation between mRNA and pDNA. The majority of mRNA eluted together with the linearized pDNA, making these two approaches inadequate for the intended objective. However, it is possible to verify that there is a separation tendency. Observing the peak in which the mRNA elutes in both assays, it can be seen that as the ionic strength is

reduced in the first elution step from 150 (Figure 34) to 100 mM (Figure 35) of NaCl, there is an increase in the amount of mRNA that remains bound, only eluting in the second step with the increase of NaCl concentration to 250 mM NaCl. Therefore, a fifth experiment was performed with a concentration of NaCl of 77 mM in the first elution step, in order to verify if it was possible to achieve the separation between the mRNA and the linearized pDNA.

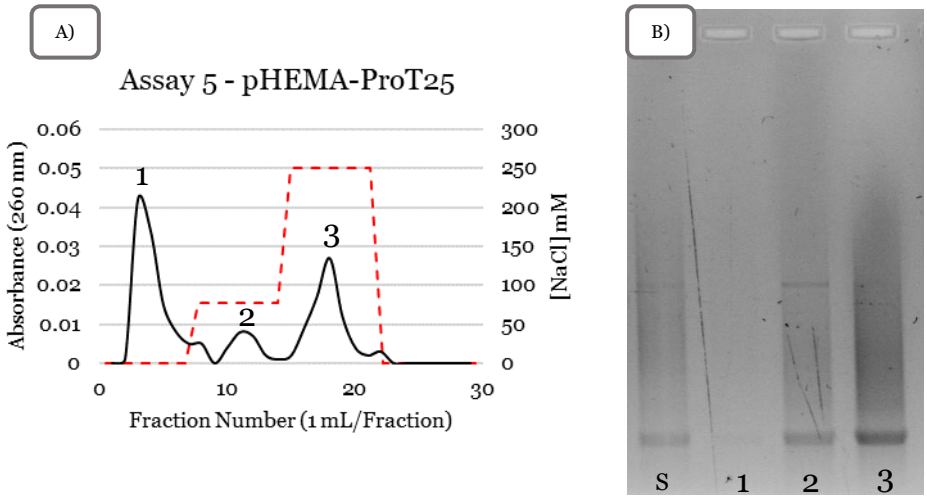

Figure 36. A) Chromatographic profile obtained with the pHEMA-ProT25 cryogel support. For the binding step 10 mM sodium acetate buffer pH = 5.0, for the first elution step **77 mM NaCl** in 10 mM sodium acetate buffer pH = 5.0, for the second elution step **250 M NaCl** in 10 mM sodium acetate buffer pH = 5.0 (represented by the red dashed line); B) agarose electrophoresis of the collected fractions, S – Injected Sample; 1, 2 and 3 - 1, 2 and 3 - respective peaks of the chromatogram.

Notably, the separation between pDNA and mRNA is more likely favoured in this support, in assay 5 (Figure 36), with the first elution step with 77 mM of NaCl. In this step, the pDNA eluted from the column along with some mRNA, but the majority of the target mRNA only eluted at the second elution step with a NaCl concentration of 250 mM. Comparing the results from this assay from those obtained in To cryogel (Figure 27), we can conclude that the functionalization had an impact on the retention of pDNA, since with T25 cryogel it eluted first, instead of eluting together with mRNA as it happens with To. This could be explained also by the structural differences between the pDNA and mRNA. mRNA possess a single stranded structure, so, the nucleotides are more exposed and prone to interact with the ligands through hydrogen bonds. Also, the presence of poly (A) tail, could have a crucial role to this higher affinity comparing with the pDNA which possess a double stranded sequence structure, and so, it is more difficult to the nucleotides to establishing hydrogen bonds with ProT, which was the expected. The differences observed between these two cryogels seem to prove that the functionalization allows a higher specificity towards mRNA. Although, optimizations to the chromatographic strategy, like an adjustment on the NaCl gradient and pH, should

be done to give some insight into how those parameters could affect the elution and contribute to the total separation of the bound pDNA and mRNA. Also, a binding step implementing some ionic strength could be used in the future, as a way to get rid of a larger number of contaminants in this initial step.

4.5.3 pHEMA-ProT50 Cryogel

From the results of the reproducibility present in Figure 24, ns-T50 cryogel was chosen to proceed to the mRNA purification studies, due to its good binding and eluting behaviour for LMW RNA samples. The characterization studies also showed promising results, namely EDXA, where a slightly bigger N% in this support told us that it can also have some ProT ligand in its structure, comparing to the control cryogel. So, following the experimental setting of ns-T25 cryogel, it was first evaluated if the ns-T50 cryogel had the same binding and elution behaviour towards the purification of mRNA, a binding step of 10 mM Sodium-Acetate pH = 5.0 was done, followed by an increase in the ionic strength with a 1.5 M NaCl in 10 mM Sodium-Acetate pH = 5.0. Subsequently, the capacity for this support to separate between mRNA and the linearized pDNA, was done by varying the salt concentration in different elution buffers.

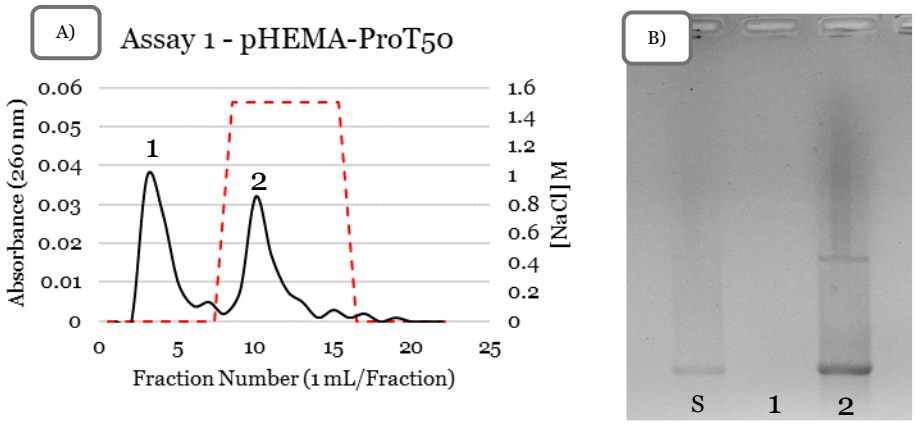

Figure 37. A) Chromatographic profile obtained with the pHEMA-ProT50 cryogel support. For the binding step 10 mM sodium acetate buffer pH = 5.0, for the elution step **1.5 M NaCl** in 10 mM sodium acetate buffer pH = 5.0 (represented by the red dashed line); B) agarose electrophoresis of the collected fractions, S – Injected Sample; 1 and 2 - respective peaks of the chromatogram.

From the analysis of the assay 1, some differences to the ns-T0 (Figure 27) and ns-T25 (Figure 32) were found. Regarding the ns-T0 cryogel, and comparing with these results obtained for the ns-T50 cryogel (Figure 37), we were able to perceive that, for the ns-T50, the elution of the bound material occurs with a higher resolution with a well-defined peak, where the mRNA and the linearized pDNA elute. As for ns-T0 (Figure 27), there is a division of the elution over 3 peaks, it should be noted that there was elution of material in the washing step. This demonstrates that the presence of the ProT ligand promoted an increase in selectivity for mRNA and pDNA, managing to elute these two biomolecules

in a single elution step. Comparing further with the results for the ns-T25 cryogel (Figure 32), we see that there was no elution of mRNA in the binding step, although the absorbances between the peaks of the chromatograms were very similar. In the future, after determining the binding capacity of the cryogels, it will be seen whether, in fact, there is a greater ability of the ns-T50 cryogel to bind a higher amount of mRNA relatively to ns-T25.

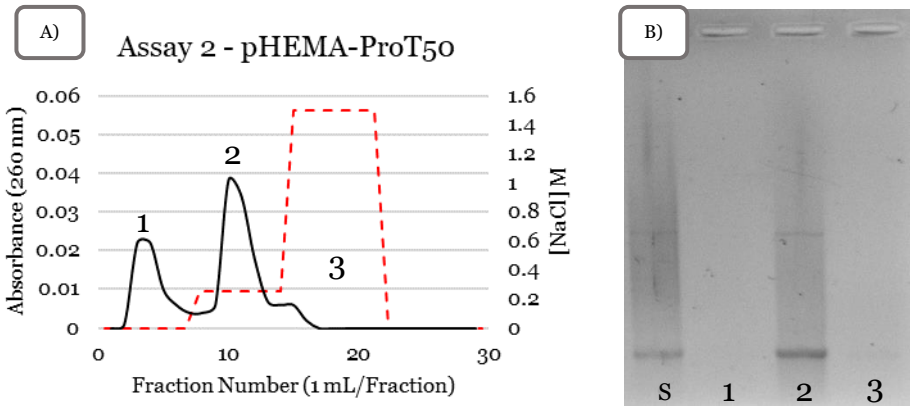

Figure 38. A) Chromatographic profile obtained with the pHEMA-ProT50 cryogel support. For the binding step 10 mM sodium acetate buffer pH = 5.0, for the first elution step **250 mM NaCl** in 10 mM sodium acetate buffer pH = 5.0, for the second elution step **1.5 M NaCl** in 10 mM sodium acetate buffer pH = 5.0 (represented by the red dashed line); B) agarose electrophoresis of the collected fractions, S – Injected Sample; 1, 2 and 3 - respective peaks of the chromatogram.

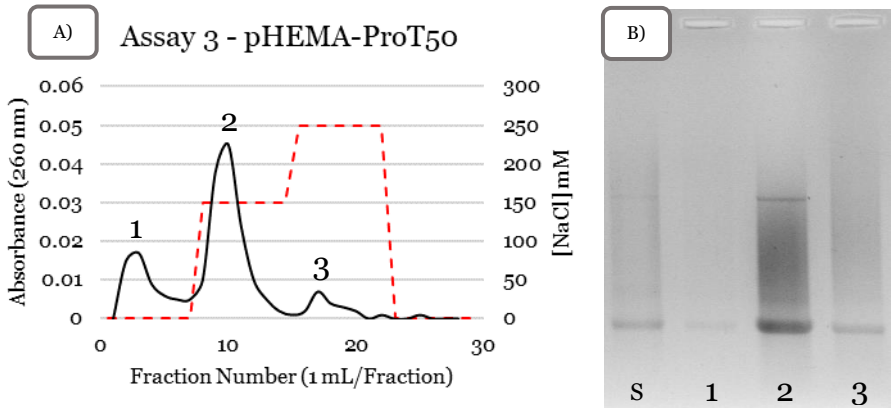

Figure 39. A) Chromatographic profile obtained with the pHEMA-ProT50 cryogel support. For the binding step 10 mM sodium acetate buffer pH = 5.0, for the first elution step **150 mM NaCl** in 10 mM sodium acetate buffer pH = 5.0, for the second elution step **250 M NaCl** in 10 mM sodium acetate buffer pH = 5.0 (represented by the red dashed line); B) agarose electrophoresis of the collected fractions, S – Injected Sample; 1, 2 and 3 - respective peaks of the chromatogram.

The analysis of the assays 2 (Figure 38) and 3 (Figure 39) revealed that there was practically total elution of the bound material from the column in the first elution step with a concentration of 250 mM of NaCl (assay 2) and 150 mM of NaCl (assay 3) was

enough to elute what was retained onto the column. With these conditions it was not possible to separate the mRNA from the linearized pDNA. However, similarly to what was found for ns-T25, a separation tendency could be observed. With a decrease in salt concentration in the first elution step, the ns-T50 cryogel had the ability to separate mRNA and linearized pDNA, as visible in the assay represented in Figure 39. Similarlly to ns-T25, this selectivity is a result from the presence of the ProT ligand in the polymeric support, allowing a stronger interaction with mRNA.

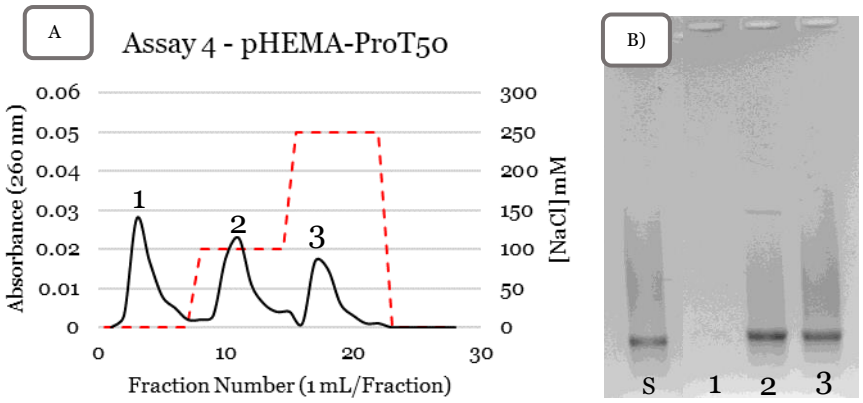

Figure 40. A) Chromatographic profile obtained with the pHEMA-ProT50 cryogel support. For the binding step 10 mM sodium acetate buffer pH = 5.0, for the first elution step **100 mM NaCl** in 10 mM sodium acetate buffer pH = 5.0, for the second elution step **250 M NaCl** in 10 mM sodium acetate buffer pH = 5.0 (represented by the red dashed line); B) agarose electrophoresis of the collected fractions, S – Injected Sample; 1, 2 and 3 - respective peaks of the chromatogram.

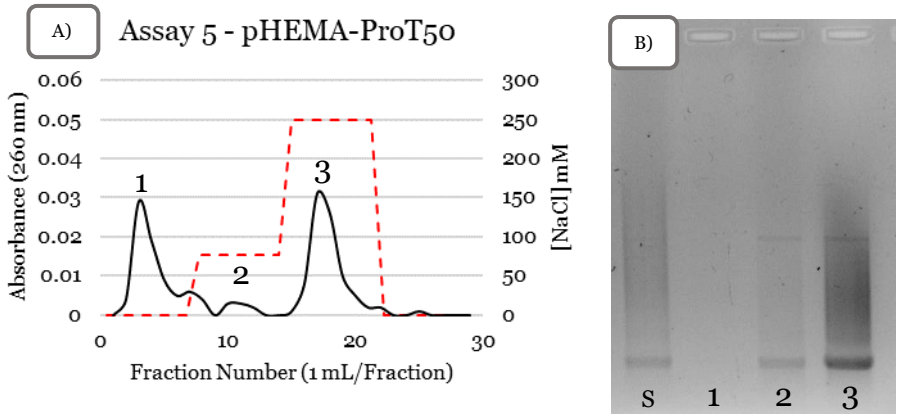

Figure 41. A) Chromatographic profile obtained with the pHEMA-ProT50 cryogel support. For the binding step 10 mM sodium acetate buffer pH = 5.0, for the first elution step **77 mM NaCl** in 10 mM sodium acetate buffer pH = 5.0, for the second elution step **250 M NaCl** in 10 mM sodium acetate buffer pH = 5.0 (represented by the red dashed line); B) agarose electrophoresis of the collected fractions, S – Injected Sample; 1, 2 and 3 - respective peaks of the chromatogram.

From the analysis of the assays performed with ns-T50 cryogel, it was observed that on the contrary to the binding results of ns-T25, mRNA was not significantly lost in the

binding step. Observing the results of assay 4 (Figure 40), the separation between the mRNA and the pDNA is visible, however, a large part of the mRNA elutes together with the pDNA when an elution step with 100 mM of NaCl is implemented, which is not desirable. These results demonstrate that, unlike the ns-T25 cryogel, which presents a greater separation capacity for pDNA using a concentration of 77 mM of NaCl in the first elution step, the ns-T50 demonstrates this capacity using a concentration of 100 mM of NaCl. The findings of EDXA showed a lower N% for ns-T50 than for ns-T25 (Table 9, sample 1), which could be related to the smaller amount of ligand present in ns-T50 cryogel regarding ns-T25. Nevertheless, studies by EA and solid state NMR have to be performed to confirm the EDXA results. We could presume that as the amount of ProT present in ns-T50 is smaller, the selectivity of this support for mRNA and the ability to separate it from pDNA is affected, demonstrating a similar behaviour to ns-T0. It is necessary to use higher salt concentrations to elute the pDNA, as it is possible to see in figure 40, when using a concentration of 77 mM of NaCl, it is not enough to elute it completely. It should also be noted that T0 has shown to have great affinity for pDNA, which is mainly favoured by the HEMA monomer.

Moreover, analysing the results from assay 5 (Figure 41) with those obtained for the same assay for the ns-T25 cryogel (Figure 36), mRNA has the same behaviour, eluting at the last step. However, the pDNA was distributed between the two elution steps with 77 mM and 250 mM of NaCl, respectively. This could also possibly be explained by the differences observed in the N% of the EDXA results for ns-T25 and ns-T50 (Table 9, Sample 1), implying a potential lower amount of the ligand in the polymeric matrix of ns-T50, resulting in a reduced selectivity for mRNA when compared to ns-T25 cryogel.

Chapter 5 - Conclusions and Future Perspectives

In the present days, the high demand for large amounts of mRNA has increased largely due to emerging molecular therapies, leading to a widespread need to improve mRNA production scale and purification processes. Nevertheless, impurities linked to the mRNA manufacturing process, namely the presence of mRNA subproducts formed during IVT, raise the possibility of immunogenic effects, and reduces translatability into the clinic. Thus, the separation of functional transcripts from process-related contaminants by affinity chromatography has shown promising results as a key capture step. In the present study, we took advantage of the structure and flow dynamics of cryogels by combining a bioinspired functional monomer with the cryogel matrix. A novel nucleotide-based functional monomer inspired in the naturally occurring thymine nitrogenous base was developed and inserted as a ligand into the polymeric structure of the cryogel, to establish a natural interaction with the RNA. The synthesized support benefits of cryogels structural and flow-dynamics properties, while allows a specific recognition through the Adenine – Thymine interactions to the target RNAs.

Herein, a thymine derivative (ProT) was successfully synthesized through an alkylation reaction using allyl bromide and isolated from other components in the reaction mixture.

Additionally, four cryogels were synthesized, where one served as a control with no ligand incorporated, and the others were functionalized, through a co-polymerization method performed with 25, 37.5 and 50 mg of allyl thymine (T25, T37.5 and T50, respectively). The synthesized cryogels were submitted to a characterization study, where the swelling capacity, the morphology and the atomic percentage of nitrogen (N%) were acquired using SEM and EDXS. The swelling capacity was not affected by the functionalization procedure with allyl thymine. Nevertheless, a more detailed study with different masses of ligand should be done in order to confirm how the amount used in the functionalization protocol affects the morphology of the cryogel and the behaviour of cryogels in the purification assays. Another parameter that could influence the morphology of the cryogel is the temperature of the acetone bath during the cryogenic treatment. Additionally, the conventional/pre-freezing cryogel synthesis should be carried out to see if the morphological characteristics between the synthesized cryogels are influenced by this process, as well as their performance in the chromatographic assays.

Furthermore, the EDXA results indicate that the functionalization of the T25 successfully occurred. However, the results for the T37.5 and T50 cryogels were not conclusive due to the large measurement error of this approach. Therefore, alternative confirmation

techniques like solid-state NMR and EA should be used in the future to corroborate the EDXA results.

The ability of the synthesized cryogels to retain LMW RNA was first tested and the optimal conditions for the binding and elution were found. From this initial screening, it was possible to verify that the major player by which the RNA binds to the cryogel matrix is HEMA. The T0 cryogel exhibited great affinity to the RNA samples, being only surpassed by T25, suggesting that the functionalization increased the affinity for the LMW RNA. In addition, the T50 cryogel demonstrated the poorest outcomes for the binding and elution of the LMW RNA, having failed to establish a retention profile in the optimal conditions. On the other hand, cryogels T0, T25, and T37.5 exhibited the ability to retain LMW RNA while simultaneously enabling its elution. However, to not compromise the retention behaviour as a result of the high use of cryogels in this initial screening, a new synthesis of cryogels was performed, in order to move on with the chromatographic investigations of the mRNA.

Concerning the chromatographic experiments with the cryogels ns-T0, ns-T25, and ns-T50 to assess their capacity to purify mRNA, it was verified that all the cryogels tested were able to bind and elute mRNA. However, for ns-T25 cryogel, the findings showed that the functionalization had a dual impact; first, it restricted the mRNA's ability to bind to the matrix during the binding step, and second, it promoted the mRNA's retention to the ns-T25 cryogel, enabling the partial separation between the pDNA and the mRNA. The finest chromatographic conditions for their separation are yet to be optimized. Concerning the ns-T50 cryogel, it also demonstrated the ability to separate between mRNA and the linearized pDNA, although a greater portion of mRNA eluted together with pDNA. In regard to the control cryogel ns-T0, it revealed no capacity for separating pDNA from mRNA at this preliminary stage.

Overall, although the synthesis of cryogels is relatively quick and simple, the present work was able to highlight the complexity of the process because it depends on a number of variables. Because of this, optimization of the conditions still needs to be done, e.g., temperature at which cryogelation occurs and the mass of the ligand that should be used. In conclusion, the functionalization of the cryogels had increased their affinity for both the LMW RNA and the mRNA, being able to partially separate the target mRNA from de linearized pDNA. However, the presence of other contaminants should be addressed in the future while the separation between mRNA and pDNA is optimized. Finally, the ProT functionalized cryogels appear to be a novel and successful approach to overcome some of the challenges related to the mRNA purification processes.

Chapter 6 - References

1. Pierce, B.A., *Genetics: a conceptual approach*. 7th ed. 2020: Macmillan.
2. Martins, R., J. Queiroz, and F. Sousa, *Ribonucleic acid purification.* Journal of Chromatography A, 2014. **1355**: p. 1-14.
3. Liang, X., H. Kuhn, and M.D. Frank-Kamenetskii, *Monitoring single-stranded DNA secondary structure formation by determining the topological state of DNA catenanes.* Biophysical journal, 2006. **90**(8): p. 2877-2889.
4. Marathe, I.A., et al., *Protein cofactors and substrate influence Mg2+-dependent structural changes in the catalytic RNA of archaeal RNase P.* Nucleic acids research, 2021. **49**(16): p. 9444-9458.
5. Lehman, N., *RNA in evolution.* Wiley Interdisciplinary Reviews: RNA, 2010. **1**(2): p. 202-213.
6. Saldi, T., et al., *Alternative RNA structures formed during transcription depend on elongation rate and modify RNA processing.* Molecular cell, 2021. **81**(8): p. 1789-1801. e5.
7. Baptista, B., et al., *mRNA, a Revolution in Biomedicine.* Pharmaceutics, 2021. **13**(12): p. 2090.
8. Baptista, B., et al., *Non-coding RNAs: Emerging from the discovery to therapeutic applications.* Biochemical Pharmacology, 2021. **189**: p. 114469.
9. Brenner, S., F. Jacob, and M. Meselson, *An unstable intermediate carrying information from genes to ribosomes for protein synthesis.* Nature, 1961. **190**(4776): p. 576-581.
10. Dimitriadis, G.J., *Translation of rabbit globin mRNA introduced by liposomes into mouse lymphocytes.* Nature, 1978. **274**(5674): p. 923-924.
11. Malone, R.W., P.L. Felgner, and I.M. Verma, *Cationic liposome-mediated RNA transfection.* Proceedings of the National Academy of Sciences, 1989. **86**(16): p. 6077-6081.
12. Wolff, J.A., et al., *Direct gene transfer into mouse muscle in vivo.* Science, 1990. **247**(4949): p. 1465-1468.
13. Pardi, N., M.J. Hogan, and D. Weissman, *Recent advances in mRNA vaccine technology*. Current opinion in immunology, 2020. **65**: p. 14-20.
14. Wang, Y., et al., *mRNA vaccine: a potential therapeutic strategy.* Molecular cancer, 2021. **20**(1): p. 1-23.
15. Naik, R. and K. Peden, *Regulatory considerations on the development of mRNA vaccines*, in *Current Topics in Microbiology and Immunology*. 2020, Springer.
16. Boczkowski, D., et al., *Dendritic cells pulsed with RNA are potent antigen-presenting cells in vitro and in vivo.* The Journal of experimental medicine, 1996. **184**(2): p. 465-472.
17. Weide, B., et al., *Results of the first phase I/II clinical vaccination trial with direct injection of mRNA.* Journal of immunotherapy, 2008. **31**(2): p. 180-188.
18. Pascolo, S., *Messenger RNA-based vaccines.* Expert opinion on biological therapy, 2004. **4**(8): p. 1285-1294.
19. Karikó, K., et al., *Suppression of RNA recognition by Toll-like receptors: the impact of nucleoside modification and the evolutionary origin of RNA.* Immunity, 2005. **23**(2): p. 165-175.
20. Roy, I., M.K. Stachowiak, and E.J. Bergey, *Nonviral gene transfection nanoparticles: function and applications in the brain.* Nanomedicine: Nanotechnology, Biology and Medicine, 2008. **4**(2): p. 89-97.
21. Granot-Matok, Y., et al., *Therapeutic mRNA delivery to leukocytes.* Journal of Controlled Release, 2019. **305**: p. 165-175.

22. Sahu, I., et al., *Recent developments in mRNA-based protein supplementation therapy to target lung diseases.* Molecular Therapy, 2019. **27**(4): p. 803-823.
23. Trepotec, Z., et al., *Delivery of mRNA therapeutics for the treatment of hepatic diseases.* Molecular Therapy, 2019. **27**(4): p. 794-802.
24. Shin, H., et al., *Recent advances in RNA therapeutics and RNA delivery systems based on nanoparticles.* Advanced Therapeutics, 2018. **1**(7): p. 1800065.
25. Deal, C.E., A. Carfi, and O.J. Plante, *Advancements in mRNA encoded antibodies for passive immunotherapy.* Vaccines, 2021. **9**(2): p. 108.
26. Probst, J., et al., *Spontaneous cellular uptake of exogenous messenger RNA in vivo is nucleic acid-specific, saturable and ion dependent.* Gene therapy, 2007. **14**(15): p. 1175-1180.
27. Kornberg, R.D., *The molecular basis of eukaryotic transcription.* Proceedings of the National Academy of Sciences, 2007. **104**(32): p. 12955-12961.
28. Jang, M.-K., J.-H. Kim, and M.H. Jung, *Histone H3K9 demethylase JMJD2B activates adipogenesis by regulating H3K9 methylation on PPARγ and C/EBPα during adipogenesis.* PLoS One, 2017. **12**(1): p. e0168185.
29. Yang, M.Q., et al., *Genome-wide detection of a TFIID localization element from an initial human disease mutation.* Nucleic Acids Research, 2011. **39**(6): p. 2175-2187.
30. Hahn, S., *Structure and mechanism of the RNA polymerase II transcription machinery.* Nature structural & molecular biology, 2004. **11**(5): p. 394-403.
31. Roos, D. and M. de Boer, *Mutations in cis that affect mRNA synthesis, processing and translation.* Biochimica et Biophysica Acta (BBA)-Molecular Basis of Disease, 2021. **1867**(9): p. 166166.
32. Jia, L., et al., *Decoding mRNA translatability and stability from the 5′ UTR.* Nature Structural & Molecular Biology, 2020. **27**(9): p. 814-821.
33. Moore, M.J. and N.J. Proudfoot, *Pre-mRNA processing reaches back totranscription and ahead to translation.* Cell, 2009. **136**(4): p. 688-700.
34. Wahl, M.C., C.L. Will, and R. Lührmann, *The spliceosome: design principles of a dynamic RNP machine.* Cell, 2009. **136**(4): p. 701-718.
35. Ghigna, C., C. Valacca, and G. Biamonti, *Alternative splicing and tumor progression.* Current genomics, 2008. **9**(8): p. 556-570.
36. Mandel, C.R., Y. Bai, and L. Tong, *Protein factors in pre-mRNA 3′-end processing.* Cellular and Molecular Life Sciences, 2008. **65**(7): p. 1099-1122.
37. Sonenberg, N. and A.G. Hinnebusch, *Regulation of translation initiation in eukaryotes: mechanisms and biological targets.* Cell, 2009. **136**(4): p. 731-745.
38. Leppek, K., R. Das, and M. Barna, *Functional 5′ UTR mRNA structures in eukaryotic translation regulation and how to find them.* Nature reviews molecular cell biology, 2018. **19**(3): p. 158-174.
39. Nakagawa, S., et al., *Diversity of preferred nucleotide sequences around the translation initiation codon in eukaryote genomes.* Nucleic acids research, 2008. **36**(3): p. 861-871.
40. Zarghampoor, F., et al., *Improved translation efficiency of therapeutic mRNA.* Gene, 2019. **707**: p. 231-238.
41. Nicholson, A.L. and A.E. Pasquinelli, *Tales of detailed poly (A) tails.* Trends in cell biology, 2019. **29**(3): p. 191-200.
42. Lorsch, J.R. and T.E. Dever, *Molecular view of 43 S complex formation and start site selection in eukaryotic translation initiation.* Journal of Biological Chemistry, 2010. **285**(28): p. 21203-21207.

43. Jia, L. and S.-B. Qian, *Therapeutic mRNA Engineering from Head to Tail.* Accounts of Chemical Research, 2021. **54**(23): p. 4272-4282.
44. Zhong, Z., et al., *mRNA therapeutics deliver a hopeful message.* Nano today, 2018. **23**: p. 16-39.
45. Züst, R., et al., *Ribose 2′-O-methylation provides a molecular signature for the distinction of self and non-self mRNA dependent on the RNA sensor Mda5.* Nature immunology, 2011. **12**(2): p. 137-143.
46. Devarkar, S.C., et al., *Structural basis for m7G recognition and 2′-O-methyl discrimination in capped RNAs by the innate immune receptor RIG-I.* Proceedings of the National Academy of Sciences, 2016. **113**(3): p. 596-601.
47. Mauer, J., et al., *Reversible methylation of m6Am in the 5′ cap controls mRNA stability.* Nature, 2017. **541**(7637): p. 371-375.
48. Wei, J., et al., *Differential m6A, m6Am, and m1A demethylation mediated by FTO in the cell nucleus and cytoplasm.* Molecular cell, 2018. **71**(6): p. 973-985. e5.
49. Galloway, A. and V.H. Cowling, *mRNA cap regulation in mammalian cell function and fate.* Biochimica et Biophysica Acta (BBA)-Gene Regulatory Mechanisms, 2019. **1862**(3): p. 270-279.
50. Daffis, S., et al., *2′-O methylation of the viral mRNA cap evades host restriction by IFIT family members.* Nature, 2010. **468**(7322): p. 452-456.
51. Montoya, J., D. Ojala, and G. Attardi, *Distinctive features of the 5′-terminal sequences of the human mitochondrial mRNAs.* Nature, 1981. **290**(5806): p. 465-470.
52. Haimov, O., H. Sinvani, and R. Dikstein, *Cap-dependent, scanning-free translation initiation mechanisms.* Biochimica et Biophysica Acta (BBA)-Gene Regulatory Mechanisms, 2015. **1849**(11): p. 1313-1318.
53. Hentze, M.W., et al., *Identification of the iron-responsive element for the translational regulation of human ferritin mRNA.* Science, 1987. **238**(4833): p. 1570-1573.
54. Meyuhas, O. and T. Kahan, *The race to decipher the top secrets of TOP mRNAs.* Biochimica et Biophysica Acta (BBA)-Gene Regulatory Mechanisms, 2015. **1849**(7): p. 801-811.
55. Avni, D., et al., *Vertebrate mRNAs with a 5′-terminal pyrimidine tract are candidates for translational repression in quiescent cells: characterization of the translational cis-regulatory element.* Molecular and cellular biology, 1994. **14**(6): p. 3822-3833.
56. Lacerda, R., J. Menezes, and L. Romão, *More than just scanning: the importance of cap-independent mRNA translation initiation for cellular stress response and cancer.* Cellular and Molecular Life Sciences, 2017. **74**(9): p. 1659-1680.
57. Qin, X. and P. Sarnow, *Preferential translation of internal ribosome entry site-containing mRNAs during the mitotic cycle in mammalian cells.* Journal of Biological Chemistry, 2004. **279**(14): p. 13721-13728.
58. Spriggs, K.A., et al., *Re-programming of translation following cell stress allows IRES-mediated translation to predominate.* Biology of the Cell, 2008. **100**(1): p. 27-38.
59. Chew, G.-L., A. Pauli, and A.F. Schier, *Conservation of uORF repressiveness and sequence features in mouse, human and zebrafish.* Nature communications, 2016. **7**(1): p. 1-10.
60. van der Horst, S., et al., *Novel pipeline identifies new upstream ORFs and non-AUG initiating main ORFs with conserved amino acid sequences in the 5′ leader of mRNAs in Arabidopsis thaliana.* RNA, 2019. **25**(3): p. 292-304.

61. Kurihara, Y., *uORF shuffling fine-tunes gene expression at a deep level of the process.* Plants, 2020. **9**(5): p. 608.
62. Renz, P.F., F. Valdivia-Francia, and A. Sendoel, *Some like it translated: small ORFs in the 5′ UTR.* Experimental cell research, 2020. **396**(1): p. 112229.
63. Fujii, K., et al., *Pervasive translational regulation of the cell signalling circuitry underlies mammalian development.* Nature communications, 2017. **8**(1): p. 1-13.
64. Vattem, K.M. and R.C. Wek, *Reinitiation involving upstream ORFs regulates ATF4 mRNA translation in mammalian cells.* Proceedings of the National Academy of Sciences, 2004. **101**(31): p. 11269-11274.
65. Lee, A.S., P.J. Kranzusch, and J.H. Cate, *eIF3 targets cell-proliferation messenger RNAs for translational activation or repression.* Nature, 2015. **522**(7554): p. 111-114.
66. Ji, Z. and B. Tian, *Reprogramming of 3′ untranslated regions of mRNAs by alternative polyadenylation in generation of pluripotent stem cells from different cell types.* PloS one, 2009. **4**(12): p. e8419.
67. Zhang, H., J.Y. Lee, and B. Tian, *Biased alternative polyadenylation in human tissues.* Genome biology, 2005. **6**(12): p. 1-13.
68. Otsuka, H., et al., *Emerging evidence of translational control by AU-rich element-binding proteins.* Frontiers in genetics, 2019. **10**: p. 332.
69. Friedman, R.C., et al., *Most mammalian mRNAs are conserved targets of microRNAs.* Genome research, 2009. **19**(1): p. 92-105.
70. Bhattacharyya, S.N., et al., *Relief of microRNA-mediated translational repression in human cells subjected to stress.* Cell, 2006. **125**(6): p. 1111-1124.
71. To, K.K. and W.C. Cho, *An overview of rational design of mRNA-based therapeutics and vaccines.* Expert Opinion on Drug Discovery, 2021. **16**(11): p. 1307-1317.
72. Fuchs, A.-L., A. Neu, and R. Sprangers, *A general method for rapid and cost-efficient large-scale production of 5′ capped RNA.* RNA, 2016. **22**(9): p. 1454-1466.
73. Vaidyanathan, S., et al., *Uridine depletion and chemical modification increase Cas9 mRNA activity and reduce immunogenicity without HPLC purification.* Molecular Therapy-Nucleic Acids, 2018. **12**: p. 530-542.
74. Pasquinelli, A., J.E. Dahlberg, and E. Lund, *Reverse 5'caps in RNAs made in vitro by phage RNA polymerases.* RNA, 1995. **1**(9): p. 957-967.
75. Jemielity, J., et al., *Novel "anti-reverse" cap analogs with superior translational properties.* RNA, 2003. **9**(9): p. 1108-1122.
76. Kuhn, A., et al., *Phosphorothioate cap analogs increase stability and translational efficiency of RNA vaccines in immature dendritic cells and induce superior immune responses in vivo.* Gene therapy, 2010. **17**(8): p. 961-971.
77. Pelletier, J. and N. Sonenberg, *Insertion mutagenesis to increase secondary structure within the 5′ noncoding region of a eukaryotic mRNA reduces translational efficiency.* Cell, 1985. **40**(3): p. 515-526.
78. Kariko, K., A. Kuo, and E. Barnathan, *Overexpression of urokinase receptor in mammalian cells following administration of the in vitro transcribed encoding mRNA.* Gene therapy, 1999. **6**(6): p. 1092-1100.
79. Van Driessche, A., et al., *Clinical-grade manufacturing of autologous mature mRNA-electroporated dendritic cells and safety testing in acute myeloid leukemia patients in a phase I dose-escalation clinical trial.* Cytotherapy, 2009. **11**(5): p. 653-668.

80. Rybakova, Y., et al., *mRNA delivery for therapeutic anti-HER2 antibody expression in vivo.* Molecular Therapy, 2019. **27**(8): p. 1415-1423.
81. Linares-Fernández, S., et al., *Tailoring mRNA vaccine to balance innate/adaptive immune response.* Trends in molecular medicine, 2020. **26**(3): p. 311-323.
82. Hia, F., et al., *Codon bias confers stability to human mRNA s.* EMBO reports, 2019. **20**(11): p. e48220.
83. Mordstein, C., et al., *Codon usage and splicing jointly influence mRNA localization.* Cell systems, 2020. **10**(4): p. 351-362. e8.
84. Tiwari, P.M., et al., *Engineered mRNA-expressed antibodies prevent respiratory syncytial virus infection.* Nature communications, 2018. **9**(1): p. 1-15.
85. Lima, S.A., et al., *Short poly (A) tails are a conserved feature of highly expressed genes.* Nature structural & molecular biology, 2017. **24**(12): p. 1057-1063.
86. Lim, J., et al., *Mixed tailing by TENT4A and TENT4B shields mRNA from rapid deadenylation.* Science, 2018. **361**(6403): p. 701-704.
87. Goubau, D., S. Deddouche, and C.R. e Sousa, *Cytosolic sensing of viruses.* Immunity, 2013. **38**(5): p. 855-869.
88. Andries, O., et al., *N1-methylpseudouridine-incorporated mRNA outperforms pseudouridine-incorporated mRNA by providing enhanced protein expression and reduced immunogenicity in mammalian cell lines and mice.* Journal of Controlled Release, 2015. **217**: p. 337-344.
89. Karikó, K., et al., *Incorporation of pseudouridine into mRNA yields superior nonimmunogenic vector with increased translational capacity and biological stability.* Molecular therapy, 2008. **16**(11): p. 1833-1840.
90. Kormann, M.S., et al., *Expression of therapeutic proteins after delivery of chemically modified mRNA in mice.* Nature biotechnology, 2011. **29**(2): p. 154-157.
91. Vallazza, B., et al., *Recombinant messenger RNA technology and its application in cancer immunotherapy, transcript replacement therapies, pluripotent stem cell induction, and beyond.* Wiley Interdisciplinary Reviews: RNA, 2015. **6**(5): p. 471-499.
92. Ho, P.Y. and A.M. Yu, *Bioengineering of noncoding RNAs for research agents and therapeutics.* Wiley Interdisciplinary Reviews: RNA, 2016. **7**(2): p. 186-197.
93. Shukla, S., C.S. Sumaria, and P. Pradeepkumar, *Exploring chemical modifications for siRNA therapeutics: a structural and functional outlook.* ChemMedChem, 2010. **5**(3): p. 328-349.
94. Chen, Q., Y. Zhang, and H. Yin, *Recent advances in chemical modifications of guide RNA, mRNA and donor template for CRISPR-mediated genome editing.* Advanced Drug Delivery Reviews, 2021. **168**: p. 246-258.
95. Rabinovich, P.M., et al., *Synthetic messenger RNA as a tool for gene therapy.* Human gene therapy, 2006. **17**(10): p. 1027-1035.
96. Henderson, J.M., et al., *Cap 1 Messenger RNA Synthesis with Co-transcriptional CleanCap® Analog by In Vitro Transcription.* Current protocols, 2021. **1**(2): p. e39.
97. Mockey, M., et al., *mRNA transfection of dendritic cells: synergistic effect of ARCA mRNA capping with Poly (A) chains in cis and in trans for a high protein expression level.* Biochemical and biophysical research communications, 2006. **340**(4): p. 1062-1068.
98. Schenborn, E.T. and R.C. Mierendorf Jr, *A novel transcription property of SP6 and T7 RNA polymerases: dependence on template structure.* Nucleic acids research, 1985. **13**(17): p. 6223-6236.

99. Weissman, D., *mRNA transcript therapy*. Expert review of vaccines, 2015. **14**(2): p. 265-281.
100. Schlake, T., et al., *Developing mRNA-vaccine technologies.* RNA biology, 2012. **9**(11): p. 1319-1330.
101. Munroe, D. and A. Jacobson, *mRNA poly (A) tail, a 3'enhancer of translational initiation.* Molecular and cellular biology, 1990. **10**(7): p. 3441-3455.
102. Walker, S.E. and J. Lorsch, *RNA purification–precipitation methods*, in *Methods in enzymology*. 2013, Elsevier. p. 337-343.
103. Chomczynski, P. and N. Sacchi, *The single-step method of RNA isolation by acid guanidinium thiocyanate–phenol–chloroform extraction: twenty-something years on.* Nature protocols, 2006. **1**(2): p. 581-585.
104. Petrov, A., et al., *RNA purification by preparative polyacrylamide gel electrophoresis.* Methods Enzymol, 2013. **530**: p. 315-330.
105. Rosa, S.S., et al., *mRNA vaccines manufacturing: Challenges and bottlenecks*. Vaccine, 2021. **39**(16): p. 2190-2200.
106. Corbett, K.S., et al., *SARS-CoV-2 mRNA vaccine design enabled by prototype pathogen preparedness.* Nature, 2020. **586**(7830): p. 567-571.
107. Cui, T., et al., *Comprehensive studies on building a scalable downstream process for mRNAs to enable mRNA therapeutics.* Biotechnology Progress, 2022: p. e3301.
108. Ouranidis, A., et al., *Pharma 4.0 continuous mRNA drug products manufacturing.* Pharmaceutics, 2021. **13**(9): p. 1371.
109. Zhang, N.-N., et al., *A thermostable mRNA vaccine against COVID-19.* Cell, 2020. **182**(5): p. 1271-1283. e16.
110. Akash, M.S.H. and K. Rehman, *Column chromatography*, in *Essentials of Pharmaceutical Analysis*. 2020, Springer. p. 167-174.
111. Kwon, S., et al., *mRNA vaccines: the most recent clinical applications of synthetic mRNA.* Archives of Pharmacal Research, 2022: p. 1-18.
112. Edelmann, F.T., A. Niedner, and D. Niessing, *Production of pure and functional RNA for in vitro reconstitution experiments.* Methods, 2014. **65**(3): p. 333-341.
113. McKenna, S.A., et al., *Purification and characterization of transcribed RNAs using gel filtration chromatography.* Nature protocols, 2007. **2**(12): p. 3270-3277.
114. Easton, L.E., Y. Shibata, and P.J. Lukavsky, *Rapid, nondenaturing RNA purification using weak anion-exchange fast performance liquid chromatography.* RNA, 2010. **16**(3): p. 647-653.
115. Koubek, J., et al., *Strong anion-exchange fast performance liquid chromatography as a versatile tool for preparation and purification of RNA produced by in vitro transcription.* RNA, 2013. **19**(10): p. 1449-1459.
116. Urayama, S.-i., et al., *A new fractionation and recovery method of viral genomes based on nucleic acid composition and structure using tandem column chromatography.* Microbes and environments, 2015. **30**(2): p. 199-203.
117. Ponchon, L. and F. Dardel, *Purification of RNA Expressed In Vivo Inserted in a tRNA Scaffold*, in *Recombinant and In Vitro RNA Synthesis*. 2013, Springer. p. 1-8.
118. Kim, I., et al., *Rapid purification of RNAs using fast performance liquid chromatography (FPLC).* RNA, 2007. **13**(2): p. 289-294.
119. Lukavsky, P.J. and J.D. Puglisi, *Large-scale preparation and purification of polyacrylamide-free RNA oligonucleotides.* RNA, 2004. **10**(5): p. 889-893.

120. Baiersdörfer, M., et al., *A facile method for the removal of dsRNA contaminant from in vitro-transcribed mRNA.* Molecular Therapy-Nucleic Acids, 2019. **15**: p. 26-35.
121. Karikó, K., et al., *Generating the optimal mRNA for therapy: HPLC purification eliminates immune activation and improves translation of nucleoside-modified, protein-encoding mRNA.* Nucleic acids research, 2011. **39**(21): p. e142-e142.
122. Baronti, L., et al., *A guide to large-scale RNA sample preparation.* Analytical and Bioanalytical Chemistry, 2018. **410**(14): p. 3239-3252.
123. Kanwal, F. and C. Lu, *A review on native and denaturing purification methods for non-coding RNA (ncRNA).* Journal of Chromatography B, 2019. **1120**: p. 71-79.
124. Flook, K., *Supporting development of mRNA-based therapies by addressing large-scale purification challenges.* Cell and gene therapy insights, 2021. **7**(5): p. 489-502.
125. Schafer-Nielsen, C. and C. Rose, *Separation of nucleic acids and chromatin proteins by hydrophobic interaction chromatography.* Biochimica et Biophysica Acta (BBA)-Gene Structure and Expression, 1982. **696**(3): p. 323-331.
126. Hage, D.S. and R. Matsuda, *Affinity chromatography: a historical perspective.* Affinity chromatography, 2015: p. 1-19.
127. Pereira, P., et al., *Affinity approaches in RNAi-based therapeutics purification.* Journal of Chromatography B, 2016. **1021**: p. 45-56.
128. Magdeldin, S., *Affinity chromatography*. InTech. 2012: BoD–Books on Demand.
129. Köse, K., et al., *PolyAdenine cryogels for fast and effective RNA purification.* Colloids and Surfaces B: Biointerfaces, 2016. **146**: p. 678-686.
130. Köse, K. and L. Uzun, *PolyGuanine methacrylate cryogels for ribonucleic acid purification.* Journal of Separation Science, 2016. **39**(10): p. 1998-2005.
131. Phillips, L.A., et al., *Poly (U)-agarose affinity chromatography: specific, sensitivity selectivity, and affinity of binding.* Preparative Biochemistry, 1980. **10**(1): p. 11-26.
132. Bancel, S., et al., *Manufacturing Methods for Production of RNA transcripts*. U.S. Patent No 10,138,507. 2018. 27(11).
133. Bakhshpour, M., et al., *Biomedical applications of polymeric cryogels.* Applied Sciences, 2019. **9**(3): p. 553.
134. Memic, A., et al., *Latest advances in cryogel technology for biomedical applications.* Advanced Therapeutics, 2019. **2**(4): p. 1800114.
135. Santos, T., et al., *Influenza DNA vaccine purification using pHEMA cryogel support.* Separation and Purification Technology, 2018. **206**: p. 192-198.
136. Shiekh, P.A., et al., *Designing cryogels through cryostructuring of polymeric matrices for biomedical applications.* European Polymer Journal, 2021. **144**: p. 110234.
137. Saylan, Y. and A. Denizli, *Supermacroporous composite cryogels in biomedical applications.* Gels, 2019. **5**(2): p. 20.
138. Lozinsky, V.I., et al., *Polymeric cryogels as promising materials of biotechnological interest.* Trends in Biotechnology, 2003. **21**(10): p. 445-451.
139. Plieva, F.M., et al., *Characterization of supermacroporous monolithic polyacrylamide based matrices designed for chromatography of bioparticles.* Journal of Chromatography B, 2004. **807**(1): p. 129-137.
140. Oelschlaeger, C., F. Bossler, and N. Willenbacher, *Synthesis, structural and micromechanical properties of 3D hyaluronic acid-based cryogel scaffolds.* Biomacromolecules, 2016. **17**(2): p. 580-589.

141. Tripathi, A. and A. Kumar, *Multi-featured macroporous agarose–alginate cryogel: Synthesis and characterization for bioengineering applications.* Macromolecular bioscience, 2011. **11**(1): p. 22-35.
142. Koshy, S.T., et al., *Injectable, porous, and cell-responsive gelatin cryogels.* Biomaterials, 2014. **35**(8): p. 2477-2487.
143. Jain, E., A.A. Karande, and A. Kumar, *Supermacroporous polymer-based cryogel bioreactor for monoclonal antibody production in continuous culture using hybridoma cells.* Biotechnology progress, 2011. **27**(1): p. 170-180.
144. Savina, I.N., et al., *A simple method for the production of large volume 3D macroporous hydrogels for advanced biotechnological, medical and environmental applications.* Scientific reports, 2016. **6**(1): p. 1-9.
145. Ertürk, G. and B. Mattiasson, *Cryogels-versatile tools in bioseparation.* Journal of Chromatography A, 2014. **1357**: p. 24-35.
146. Guven, I., et al., *Calixarene-immobilized monolithic cryogels for preparative protein chromatography.* Journal of Chromatography A, 2018. **1558**: p. 59-68.
147. Le Noir, M., et al., *Macroporous molecularly imprinted polymer/cryogel composite systems for the removal of endocrine disrupting trace contaminants.* Journal of Chromatography A, 2007. **1154**(1-2): p. 158-164.
148. Srivastava, A., A.K. Shakya, and A. Kumar, *Boronate affinity chromatography of cells and biomacromolecules using cryogel matrices.* Enzyme and microbial technology, 2012. **51**(6-7): p. 373-381.
149. Sahin, U., K. Karikó, and Ö. Türeci, *mRNA-based therapeutics—developing a new class of drugs.* Nature reviews Drug discovery, 2014. **13**(10): p. 759-780.
150. Brunetti-Pierri, N., et al., *Bioengineered factor IX molecules with increased catalytic activity improve the therapeutic index of gene therapy vectors for hemophilia B.* Human gene therapy, 2009. **20**(5): p. 479-485.
151. Ramaswamy, S., et al., *Systemic delivery of factor IX messenger RNA for protein replacement therapy.* Proceedings of the National Academy of Sciences, 2017. **114**(10): p. E1941-E1950.
152. Chabanovska, O., et al., *mRNA–A game changer in regenerative medicine, cell-based therapy and reprogramming strategies.* Advanced Drug Delivery Reviews, 2021. **179**: p. 114002.
153. Magadum, A., et al., *Pkm2 regulates cardiomyocyte cell cycle and promotes cardiac regeneration.* Circulation, 2020. **141**(15): p. 1249-1265.
154. Magadum, A., et al., *Ablation of a single N-glycosylation site in human FSTL 1 induces cardiomyocyte proliferation and cardiac regeneration.* Molecular Therapy-Nucleic Acids, 2018. **13**: p. 133-143.
155. Miao, L., Y. Zhang, and L. Huang, *mRNA vaccine for cancer immunotherapy.* Molecular Cancer, 2021. **20**(1): p. 1-23.
156. Van Nuffel, A.M., et al., *Overcoming HLA restriction in clinical trials: immune monitoring of mRNA-loaded DC therapy.* Oncoimmunology, 2012. **1**(8): p. 1392-1394.
157. Di Trani, C.A., et al., *Advances in mRNA-based drug discovery in cancer immunotherapy.* Expert opinion on drug discovery, 2022. **17**(1): p. 41-53.
158. Kunert, R. and D. Reinhart, *Advances in recombinant antibody manufacturing.* Applied microbiology and biotechnology, 2016. **100**(8): p. 3451-3461.
159. Lu, R.-M., et al., *Development of therapeutic antibodies for the treatment of diseases.* Journal of biomedical science, 2020. **27**(1): p. 1-30.

160. Vázquez-Rey, M. and D.A. Lang, *Aggregates in monoclonal antibody manufacturing processes*. Biotechnology and bioengineering, 2011. **108**(7): p. 1494-1508.
161. Xu, Z., J. Li, and J.X. Zhou, *Process development for robust removal of aggregates using cation exchange chromatography in monoclonal antibody purification with implementation of quality by design.* Preparative Biochemistry and Biotechnology, 2012. **42**(2): p. 183-202.
162. Kose, N., et al., *A lipid-encapsulated mRNA encoding a potently neutralizing human monoclonal antibody protects against chikungunya infection.* Science immunology, 2019. **4**(35): p. eaaw6647.
163. Pardi, N., et al., *Administration of nucleoside-modified mRNA encoding broadly neutralizing antibody protects humanized mice from HIV-1 challenge.* Nature communications, 2017. **8**(1): p. 1-8.
164. Sabnis, S., et al., *A novel amino lipid series for mRNA delivery: improved endosomal escape and sustained pharmacology and safety in non-human primates.* Molecular Therapy, 2018. **26**(6): p. 1509-1519.
165. Thran, M., et al., *mRNA mediates passive vaccination against infectious agents, toxins, and tumors.* EMBO molecular medicine, 2017. **9**(10): p. 1434-1447.
166. Van Hoecke, L. and K. Roose, *How mRNA therapeutics are entering the monoclonal antibody field.* Journal of Translational Medicine, 2019. **17**(1): p. 1-14.
167. Schumacher, N. and S. Rose-John, *ADAM17 orchestrates Interleukin-6, TNFα and EGF-R signaling in inflammation and cancer.* Biochimica et Biophysica Acta (BBA)-Molecular Cell Research, 2022. **1869**(1): p. 119141.
168. Scheller, J., et al., *ADAM17: a molecular switch to control inflammation and tissue regeneration.* Trends in immunology, 2011. **32**(8): p. 380-387.
169. Blobel, C.P., *ADAMs: key components in EGFR signalling and development.* Nature reviews Molecular cell biology, 2005. **6**(1): p. 32-43.
170. Yan, I., et al., *ADAM17 controls IL-6 signaling by cleavage of the murine IL-6Rα from the cell surface of leukocytes during inflammatory responses.* Journal of leukocyte biology, 2016. **99**(5): p. 749-760.
171. Calligaris, M., et al., *Strategies to target ADAM17 in disease: from its discovery to the iRhom revolution.* Molecules, 2021. **26**(4): p. 944.
172. Peng, L., et al. *Molecular basis for the mechanism of action of an anti-TACE antibody*. in *MAbs*. 2016. Taylor & Francis.
173. Rios-Doria, J., et al., *A Monoclonal Antibody to ADAM17 Inhibits Tumor Growth by Inhibiting EGFR and Non–EGFR-Mediated PathwaysADAM17 Monoclonal Antibody Inhibits Tumor Growth.* Molecular Cancer Therapeutics, 2015. **14**(7): p. 1637-1649.
174. Stadler, C.R., et al., *Elimination of large tumors in mice by mRNA-encoded bispecific antibodies.* Nature medicine, 2017. **23**(7): p. 815-817.
175. Eberle, F., et al., *Stabilization of poly (A) sequence encoding Dna sequences*. U.S. Patent No. 10,717,982. 2020. 21(7).
176. Rocha, D.H., et al., *Customizable and Regioselective One-Pot N− H Functionalization of DNA Nucleobases to Create a Library of Nucleobase Derivatives for Biomedical Applications.* European Journal of Organic Chemistry, 2021. **2021**(31): p. 4423-4433.
177. Sacarescu, L., et al., *Microwave-assisted N-allylation of uracil and thymine pyrimidine bases.* Chemistry of Heterocyclic Compounds, 2011. **47**(5): p. 602-606.

178. Thibon, J., L. Latxague, and G. Déléris, *Synthesis of silicon analogues of acyclonucleotides incorporable in oligonucleotide solid-phase synthesis.* The Journal of Organic Chemistry, 1997. **62**(14): p. 4635-4642.
179. Vlád, G. and I.T. Horváth, *Improved synthesis of 2, 2 '-bipyrimidine.* The Journal of organic chemistry, 2002. **67**(18): p. 6550-6552.
180. Cong, Y., et al., *Solubility modelling, solvent effect, preferential solvation and solution thermodynamic of thymine form AH A° in ten mono solvents and two solvent mixtures.* Journal of Molecular Liquids, 2020. **300**: p. 112257.
181. Doğan, T., et al., *Trametes versicolor laccase immobilized poly (glycidyl methacrylate) based cryogels for phenol degradation from aqueous media.* Journal of Applied Polymer Science, 2015. **132**(20).
182. Martins, A.S.P., *Desenvolvimento de criogéis funcionalizados com barbituratos para a purificação de uma vacina de DNA plasmídico contra o Influenza*. Diss. 2016.
183. Özgür, E., et al., *PHEMA cryogel for in-vitro removal of anti-dsDNA antibodies from SLE plasma.* Materials Science and Engineering: C, 2011. **31**(5): p. 915-920.
184. Uygun, M., et al., *A new metal-chelated cryogel for reversible immobilization of urease.* Applied biochemistry and biotechnology, 2013. **170**(8): p. 1815-1826.
185. Pirathiba, S. and B. Dayananda, *Extract of raphanus raphanistrum peel waste as reducing agent for the synthesis of silver and gold nanoparticles.* Digest journal of nanomaterials and biostructures, 2022. **17**(1): p. 335-345.
186. Pestov, A., et al., *A new approach to the green synthesis of imidazole-containing polymer ligands and cryogels.* European Polymer Journal, 2019. **115**: p. 356-363.
187. Pereira, P., et al., *Purification of pre-miR-29 by arginine-affinity chromatography.* Journal of Chromatography B, 2014. **951**: p. 16-23.
188. Ongkudon, C.M. and M.K. Danquah, *Process optimisation for anion exchange monolithic chromatography of 4.2 kbp plasmid vaccine (pcDNA3F).* Journal of Chromatography B, 2010. **878**(28): p. 2719-2725.
189. Kostelec, T., et al., *Production and Purification of mRNA.* BioProcess International, 2021. **19**: p. 6.

Chapter 7 - Appendices

GGACAGATCGCCTGGAGACGCCATCCACGCTGTTTTGACCTCCATAGAAGACACCGGGACCGA
TCCAGCCTCCGCGGCCGGGAACGGTGCATTGGAACGCGGATTCCCCGTGCCAAGAGTGACTCA
CCGTCCTTGACACGATGGACATCCAGATGACCCAGTCTCCATCCTCCCTGTCTGCATCTGTAGG
AGACAGAGTCACCATCACTTGCCGATCCAGTCAGAGCATTCCCAGCTATTTAAATTGGTATCAG
CAGAAACCAGGGAAAGCCCCTAAGCTCCTGATCTATGCTGCATCCCGTTTACAATCCGGGGTCC
CATCAAGGTTCAGTGGCAGTGGATCTGGGACAGATTTCACTCTCACCATCAGCAGTCTGCAACC
TGAAGATTTTGCAACTTACTACTGTCAACAGAGTTACAGTACCCCCCTCACTTTCGGCGGAGGG
ACCAAGGTGGAGATCAAAGGAGGAGGCGGCTCTGGAGGTGGCGGCAGTGGTGGAGGCGGGT
CTGGCGGTGGCGGATCTGGAGGTGGTGGGAGCGAAGTTCAATTGTTAGAGTCTGGTGGCGGT
CTTGTTCAGCCTGGTGGTTCTTTACGTCTTTCTTGCGCTGCTTCCGGATTCACTTTCTCTTCCTA
CCCTATGAATTGGGTTCGCCAAGCTCCTGGTAAAGGTTTGGAGTGGGTTTCTTATATCTCTCCC
TTCGGTGGCATGACTGATTATGCTACCTCCGTTAAAGGTCGCTTCACTATCTCTAGAGACAACT
CTAAGAATACTCTCTACTTGCAGATGAACAGCTTAAGGGCTGAGGACACGGCCGTGTATTACT
GTGCGAGAGACGCTATGAGGGGGGCAGAGGTGGACTACTGGGGCCAGGGCACCCTGGTCACC
GTCTCAAGCTGACGGGTGGCATCCCTGTGACCCCTCCCCAGTGCCTCTCCTGGCCCTGGAAGTT
GCCACTCCAGTGCCCACCAGCCTTGTCCTAATAAAATTAAGTTGCATCAAGCTAAAAAAAAAAAA
AAAAAAAAAAAAAAAAAAAAGCATATGACTAAAAAAAAAAAAAAAAAAAAAAAAAAAAAAAAA
AAAAAAAAAAAAAAAAAAAAAAAAAAAAAAAAAA

Appendix 1. Final mRNA sequence of BruMEDI3622.

ATGACCATGATTACGCCAAGCTCTAATACGACTCACTATAGGGAAAGCTT**GGACAGATCGCCTGGAGA**
CGCCATCCACGCTGTTTTGACCTCCATAGAAGACACCGGGACCGATCCAGCCTCCGCGGCCGG
GAACGGTGCATTGGAACGCGGATTCCCCGTGCCAAGAGTGACTCACCGTCCTTGACACGATGG
ACATCCAGATGACCCAGTCTCCATCCTCCCTGTCTGCATCTGTAGGAGACAGAGTCACCATCAC
TTGCCGATCCAGTCAGAGCATTCCCAGCTATTTAAATTGGTATCAGCAGAAACCAGGGAAAGC
CCCTAAGCTCCTGATCTATGCTGCATCCCGTTTACAATCCGGGGTCCCATCAAGGTTCAGTGGC
AGTGGATCTGGGACAGATTTCACTCTCACCATCAGCAGTCTGCAACCTGAAGATTTTGCAACTT
ACTACTGTCAACAGAGTTACAGTACCCCCCTCACTTTCGGCGGAGGGACCAAGGTGGAGATCA
AAGGAGGAGGCGGCTCTGGAGGTGGCGGCAGTGGTGGAGGCGGGTCTGGCGGTGGCGGATC
TGGAGGTGGTGGGAGCGAAGTTCAATTGTTAGAGTCTGGTGGCGGTCTTGTTCAGCCTGGTG
GTTCTTTACGTCTTTCTTGCGCTGCTTCCGGATTCACTTTCTCTTCCTACCCTATGAATTGGGTT
CGCCAAGCTCCTGGTAAAGGTTTGGAGTGGGTTTCTTATATCTCTCCCTTCGGTGGCATGACTG
ATTATGCTACCTCCGTTAAAGGTCGCTTCACTATCTCTAGAGACAACTCTAAGAATACTCTCTA
CTTGCAGATGAACAGCTTAAGGGCTGAGGACACGGCCGTGTATTACTGTGCGAGAGACGCTAT
GAGGGGGGCAGAGGTGGACTACTGGGGCCAGGGCACCCTGGTCACCGTCTCAAGCTGACGGG
TGGCATCCCTGTGACCCCTCCCCAGTGCCTCTCCTGGCCCTGGAAGTTGCCACTCCAGTGCCCA
CCAGCCTTGTCCTAATAAAATTAAGTTGCATCAAGCTAAAAAAAAAAAAAAAAAAAAAAAAAAA
AAAAGCATATGACTAAAAAAAAAAAAAAAAAAAAAAAAAAAAAAAAAAAAAAAAAAAAAAAAA
AAAAAAAAAAAAAAAAAAAAAAGAATTCACTGGCCGTCGTTTTACAACGTCGTGACTGGGAAAACCCT
GGCGTTACCCAACTTAATCGCCTTGCAGCACATCCCCCTTTCGCCAGCTGGCGTAATAGCGAAGAGGCCCG
CACCGATCGCCCTTCCCAACAGTTGCGCAGCCTGAATGGCGAATGGAAATTGTAAGCGTTAATATTTTGTT
AAAATTCGCGTTAAATTTTTGTTAAATCAGCTCATTTTTTAACCAATAGGCCGAAATCGGCAAAATCCCTTA
TAAATCAAAAGAATAGACCGAGATAGGGTTGAGTGTTGTTCCAGTTTGGAACAAGAGTCCACTATTAAAG
AACGTGGACTCCAACGTCAAAGGGCGAAAAACCGTCTATCAGGGCGATGGCCCACTACGTGAACCATCAC
CCTAATCAAGTTTTTTGGGGTCGAGGTGCCGTAAAGCACTAAATCGGAACCCTAAAGGGAGCCCCCGATTT
AGAGCTTGACGGGGAAAGCCGGCGAACGTGGCGAGAAAGGAAGGGAAGAAAGCGAAAGGAGCGGGCGC
TAGGGCGCTGGCAAGTGTAGCGGTCACGCTGCGCGTAACCACCACACCCGCCGCGCTTAATGCGCCGCTA
CAGGGCGCGTCAGGTGGCACTTTTCGGGGAAATGTGCGCGGAACCCCTATTTGTTTATTTTTCTAAATACA
TTCAAATATGTATCCGCTCATGAGACAATAACCCTGATAAATGCTTCAATAATATTGAAAAAGGAAGAGTA
TGAGTATTCAACATTTCCGTGTCGCCCTTATTCCCTTTTTTGCGGCATTTTGCCTTCCTGTTTTTGCTCACC
CAGAAACGCTGGTGAAAGTAAAAGATGCTGAAGATCAGTTGGGTGCACGAGTGGGTTACATCGAACTGGA
TCTCAACAGCGGTAAGATCCTTGAGAGTTTTCGCCCCGAAGAACGTTTTCCAATGATGAGCACTTTTAAAG
TTCTGCTATGTGGCGCGGTATTATCCCGTATTGACGCCGGGCAAGAGCAACTCGGTCGCCGCATACACTAT
TCTCAGAATGACTTGGTTGAGTACTCACCAGTCACAGAAAAGCATCTTACGGATGGCATGACAGTAAGAG
AATTATGCAGTGCTGCCATAACCATGAGTGATAACACTGCGGCCAACTTACTTCTGACAACGATCGGAGGA
CCGAAGGAGCTAACCGCTTTTTTGCACAACATGGGGGATCATGTAACTCGCCTTGATCGTTGGGAACCGG
AGCTGAATGAAGCCATACCAAACGACGAGCGTGACACCACGATGCCTGTAGCAATGGCAACAACGTTGCG
CAAACTATTAACTGGCGAACTACTTACTCTAGCTTCCCGGCAACAATTAATAGACTGGATGGAGGCGGATA
AAGTTGCAGGACCACTTCTGCGCTCGGCCCTTCCGGCTGGCTGGTTTATTGCTGATAAATCTGGAGCCGGT
GAGCGTGGGTCTCGCGGTATCATTGCAGCACTGGGGCCAGATGGTAAGCCCTCCCGTATCGTAGTTATCT
ACACGACGGGGAGTCAGGCAACTATGGATGAACGAAATAGACAGATCGCTGAGATAGGTGCCTCACTGAT
TAAGCATTGGTAACTGTCAGACCAAGTTTACTCATATATACTTTAGATTGATTTAAAACTTCATTTTTAATT
TAAAAGGATCTAGGTGAAGATCCTTTTTGATAATCTCATGACCAAAATCCCTTAACGTGAGTTTTCGTTCC
ACTGAGCGTCAGACCCCGTAGAAAAGATCAAAGGATCTTCTTGAGATCCTTTTTTTCTGCGCGTAATCTGC

TGCTTGCAAACAAAAAAACCACCGCTACCAGCGGTGGTTTGTTTGCCGGATCAAGAGCTACCAACTCTTTT
TCCGAAGGTAACTGGCTTCAGCAGAGCGCAGATACCAAATACTGTTCTTCTAGTGTAGCCGTAGTTAGGCC
ACCACTTCAAGAACTCTGTAGCACCGCCTACATACCTCGCTCTGCTAATCCTGTTACCAGTGGCTGCTGCC
AGTGGCGATAAGTCGTGTCTTACCGGGTTGGACTCAAGACGATAGTTACCGGATAAGGCGCAGCGGTCGG
GCTGAACGGGGGGTTCGTGCACACAGCCCAGCTTGGAGCGAACGACCTACACCGAACTGAGATACCTACA
GCGTGAGCTATGAGAAAGCGCCACGCTTCCCGAAGGGAGAAAGGCGGACAGGTATCCGGTAAGCGGCAG
GGTCGGAACAGGAGAGCGCACGAGGGAGCTTCCAGGGGGAAACGCCTGGTATCTTTATAGTCCTGTCGG
GTTTCGCCACCTCTGACTTGAGCGTCGATTTTTGTGATGCTCGTCAGGGGGGCGGAGCCTATGGAAAAAC
GCCAGCAACGCGGCCTTTTTACGGTTCCTGGCCTTTTGCTGGCCTTTTGCTCACATGTTCTTTCCTGCGTTA
TCCCCTGATTCTGTGGATAACCGTATTACCGCCTTTGAGTGAGCTGATACCGCTCGCCGCAGCCGAACGAC
CGAGCGCAGCGAGTCAGTGAGCGAGGAAGCGGAAGAGCGCCCAATACGCAAACCGCCTCTCCCCGCGCGT
TGGCCGATTCATTAATGCAGCTGGCACGACAGGTTTCCCGACTGGAAAGCGGGCAGTGAGCGCAACGCAA
TTAATGTGAGTTAGCTCACTCATTAGGCACCCCAGGCTTTACACTTTATGCTTCCGGCTCGTATGTTGTGT
GGAATTGTGAGCGGATAACAATTTCACACAGGAAACAGCT

Appendix 2. Final construct of pNZY-28 BruMEDI3622 sequence.

SÍNTESE DE CRIOGEIS FUNCIONALIZADOS COM TIMINA PARA A PURIFICAÇÃO DE mRNA

Bruno Rodrigues[1,2*], Micaela Riscado[1,2] Renato E. Boto[1,2], Fani Sousa[1,3], Cândida Tomaz[1,2]

[1] CICS-UBI – Centro de Investigação em Ciência da Saúde, Universidade da Beira Interior, 6200-506 Covilhã, Portugal; [2] Departamento de química, Faculdade de Ciências, Universidade da Beira Interior, 6201-001 Covilhã, Portugal; [3] Departamento de Ciências Médicas, Faculdade de Ciências da Saúde, Universidade da Beira Interior, 6200-506 Covilhã, Portugal; (*) Email: b.rodrigues99@gmail.com

Resumo

O elevado interesse no RNA mensageiro (mRNA) devido ao seu grande potencial no tratamento do cancro, e também à sua aplicação na vacinação contra o SARS-CoV-2, levou à necessidade de otimizar os processos de produção e purificação desta biomolécula. Assim, os criogeis surgem como uma nova alternativa aos suportes cromatográficos particulados convencionais para a purificação de moléculas com elevado peso molecular, como o mRNA, possuindo uma estrutura supermacroporosa que permite uma difusão facilitada, altas taxas de fluxo e alta capacidade. Atualmente, a estratégia de eleição para a purificação do mRNA é a cromatografia de afinidade, utilizando nucleótidos como ligandos, cuja especificidade do emparelhamento das bases adenina e timina promove interações altamente seletivas e específicas. Deste modo, o objetivo do trabalho é desenvolver criogeis funcionalizados com timina para purificar o mRNA. Para isso, o ligando 1-(2-propenil) Timina (ProT) foi sintetizado e caracterizado por RMN, sendo posteriormente preparados criogeis à base de 2-hidroxietilmetacrilato (HEMA), por copolimerização dos monómeros HEMA e ProT, com diferentes rácios e submetidos a um tratamento criogénico. Os criogeis foram caracterizados por FTIR, SEM, Análise Elementar, e testes de capacidade de reidratação. Os ensaios de purificação foram realizados em diferentes condições, variando a força iónica e o tipo de sal (NaCl ou $(NH_4)_2SO_4$) no eluente e tirando partido da afinidade entre os ligandos ProT e a poli (A) presente no mRNA. Os resultados demonstram que os criogeis funcionalizados com timina parecem ser uma abordagem inovadora para superar os desafios na purificação do RNA.

Palavras-chave: Criogeis, mRNA, Cromatografia de Afinidade, Timina.

CICS-UBI
Centro de Investigação em Ciências da Saúde
Health Sciences Research Centre

FACULDADE CIÊNCIAS DA SAÚDE

Síntese de criogeis funcionalizados com timina para a purificação de mRNA

Bruno Rodrigues[1,2], Micaela Riscado[1,2], Renato E. Boto[1,2], Fani Sousa[1,3], Cândida Tomaz[1,2]

[1]CICS-UBI - Centro de Investigação de Ciências da Saúde, Universidade de Beira Interior, 6200-506 Covilhã, Portugal;
[2]Departamento de Química, Faculdade de Ciências, Universidade de Beira Interior, 6201-001 Covilhã, Portugal;
[3]Departamento de Ciências Médicas, Faculdade de Ciências da Saúde, Universidade de Beira Interior, 6200-506 Covilhã, Portugal.

Introdução e Objetivo

- O elevado interesse no RNA mensageiro (mRNA) devido ao seu grande potencial no tratamento do cancro, e também à sua aplicação na vacinação contra o SARS-CoV-2, levou à necessidade de otimizar os processos de produção e purificação desta biomolécula [1].
- Os criogeis têm demonstrado resultados promissores na purificação de moléculas com elevado peso molecular como o DNA plasmídico (pDNA), devido à sua estrutura supermacroporosa que permite uma difusão facilitada, altas taxas de fluxo e alta capacidade, surgindo assim como uma estratégia inovadora para a purificação do mRNA [2].
- **Deste modo, o presente trabalho visa a funcionalização de criogeis com timina para purificar mRNA produzido por transcrição *in vitro* (IVT). Adicionalmente, para determinação inicial das melhores condições de purificação foi utilizada uma amostra de RNA de baixo peso molecular (RNA BPM) como modelo.**

Materiais e Métodos

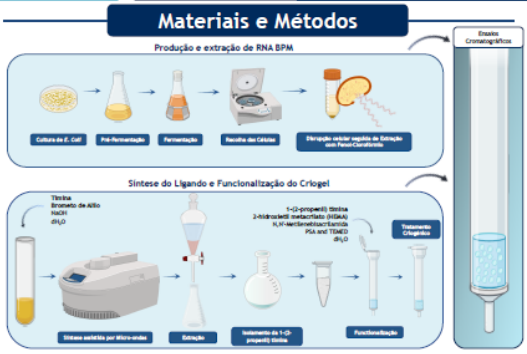

Resultados

Síntese do ligando 1-(2-propenil) timina

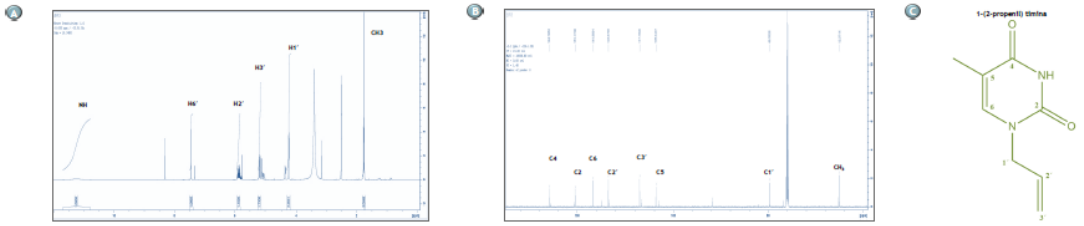

Figura 1. Confirmação da síntese do ligando 1-(2-propenil) timina por RMN. A) Espectro ^{1}H RMN da 1-(2-propenil) timina em DMSO-d_6. B) Espectro ^{13}C RMN da 1-(2-propenil) timina em DMSO-d_6. C) Estrutura química da 1-(2-propenil) timina.

Avaliação da ligação e eluição do RNA BPM

Tabela 1. Comportamento geral dos criogeis em condições hidrofóbicas e iónicas, os resultados foram analisados tendo por base a percentagem de eluição de RNA BPM. Legenda: + + (75 % - 100 %); + (50% - 75%); - (25 % - 50 %); - - (0 %-25 %).

	Interações Hidrofóbicas		Interações Iónicas	
	Ligação	Eluição	Ligação	Eluição
pHEMA-ProT0	+	-	- -	+
pHEMA-ProT25	+	-	- -	+ +
pHEMA-ProT35.5	+	-	-	-
pHEMA-ProT50	+	- -	+ +	- -

Figura 2. Resultados da avaliação da ligação e eluição do RNA BPM (Interações Iónicas). A) pHEMA-ProT0; B) pHEMA-ProT25; Ligação: Acetato de Sódio 10 mM, pH = 5.0; Eluição: Acetato de Sódio 10 mM, 250 mM/1.5M NaCl, pH = 5.0; Lavagem: Água DEPC.

Tabela 2. Análise quantitativa dos resultados dos gráficos da Figura 2 A) e B).

	RNA Injetado (µg)	Ligação (µg)	Eluição 1 (µg)	Eluição 2 (µg)	Lavagem (µg)
pHEMA-ProT0	77.6	12	31.2	18.4	3.6
pHEMA-ProT25	80.4	5.2	44	14.4	0

Conclusões

- No presente trabalho demonstrou-se que a síntese do ligando 1-(2-propenil) timina foi realizada com sucesso, apesar da presença de pequenas quantidades de contaminantes devido à semelhança estrutural com o ligando o que torna difícil a sua purificação.
- Os criogeis de poli(Timina) exibiram diferentes comportamentos relativamente à ligação e eluição do RNA BPM. Os mais promissores foram o pHEMA-ProT0 e pHEMA-ProT25, utilizando condições iónicas.
- Futuramente, pretende-se avaliar o comportamento dos criogeis pHEMA-ProT0 e pHEMA-ProT25 na purificação do mRNA e efetuar uma caracterização mais detalhada dos suportes cromatográficos sintetizados.

[1] Rosa, S. S., Prazeres, D. M. F., Azevedo, A. M. & Marques, M. P. C. mRNA vaccines manufacturing: Challenges and bottlenecks. Vaccine 39, 2190-2200 (2021).
[2] Santos, T. et al. Influenza DNA-vector purification using pHEMA cryogel support. Sep. Purif. Technol. 204, 192-198 (2018).

Os autores agradecem aos projetos CICS-UBI UIDB/00709/2020 e UIDP/00709/2020, financiados por FCT/MCTES. Projeto PTDC/BII-BBF/29496/2017 financiado por FEDER, através do COMPETE2020-POCI, e por fundos nacionais através do projeto FCT/MCTES COMBINE concedido pelo Binov 2021 (SERRA Ordem dos Farmacêuticos). M. Riscado agradece à FCT pela bolsa de doutoramento 2021.07658.BD.

FCT Fundação para a Ciência e a Tecnologia
COMPETE 2020
PORTUGAL 2020

Appendix 3. Certificate of the best poster award at the VIII cycle of conferences of the Faculty of Sciences of the University of Beira Interior.

POLYTHYMINE CRYOGELS AS A NOVEL APPROACH TO mRNA PURIFICATION FOR *IN VIVO* DELIVERY OF ADAM17 ANTIBODIES

Bruno Rodrigues[1,2*], Micaela Riscado[1,2] Renato E. Boto[1,2], Fani Sousa[1,3], Cândida Tomaz[1,2]
[1] CICS-UBI – Health Sciences Research Centre, Universidade de Beira Interior, 6200-506 Covilhã, Portugal
[2] Department of Chemistry, Faculty of Sciences, Universidade de Beira Interior, 6201-001 Covilhã, Portugal
[3] Department of Medical Sciences, Faculty of Health Sciences, Universidade de Beira Interior, 6200-506 Covilhã, Portugal
(*) *Email:* b.rodrigues99@gmail.com

ABSTRACT

The demand for large amounts of messenger RNA (mRNA) has increased largely due to emerging molecular therapies, leading to a widespread need to improve mRNA production scale and purification processes. Cryogels appear as a new alternative to conventional particulate chromatographic supports for purification of large molecules like mRNA, due to the supermacroporous structure that allows unhindered diffusion, high flow rates and high capacity (1). Currently, the strategy for RNA purification by affinity chromatography relies on nucleotides as ligands based on the base pairing specificity of adenine with thymine to achieve highly selective and specific interactions. Herein, we aimed to develop cryogels functionalized with thymine to purify *In Vitro* Transcribed mRNA encoding a single chain variable fragment (scFV) antibody anti-ADAM17. For this, a thymine derivative was synthesized (1-(2-propenyl) thymine (ProT)) and characterized by NMR. Then, 2-hydroxyethyl methacrylate (HEMA)-based cryogels were prepared with copolymerization of the monomers HEMA and ProT with different ratios in an aqueous solution by a cryogelation process. The cryogels were characterized by FTIR, SEM, DSC and swelling tests. The purification experiments were performed using different conditions, by varying the ionic strength and the type of salt (NaCl or $(NH_4)_2SO_4$) in the eluent and taking advantage of the affinity between the thymine ligands and the poly(A) present in mRNA. The results demonstrate that thymine-cryogels seem to be a novel approach to overcome the challenges in RNA purification.

(1) Santos, T. et al. Influenza DNA vaccine purification using pHEMA cryogel support. Sep. Purif. Technol. 206, 192–198 (2018).

Acknowledgments: CICS-UBI projects UIDB/00709/2020 and UIDP/00709/2020, financed by FCT/MCTES. Project PTDC/BII-BBF/29496/2017 funded by FEDER, through COMPETE2020-POCI, and by national funds through FCT/MCTES" COMBINE project granted by BInov 2021 (SRSRA of Pharmacists Order).

Keywords: Affinity Chromatography, Cryogels, mRNA, Thymine derivatives.

Preference for communication: Poster

CICS-UBI
Centro de Investigação em Ciências da Saúde
Health Sciences Research Centre

FACULDADE CIÊNCIAS DA SAÚDE

POLYTHYMINE CRYOGELS AS A NOVEL APPROACH TO mRNA PURIFICATION FOR *IN VIVO* DELIVERY OF ADAM17 ANTIBODIES

Bruno Rodrigues[1,2], Micaela Riscado[1,2], Renato E. Boto[1,2], Fani Sousa[1,3], Cândida Tomaz[1,2]

[1]CICS-UBI - Health Sciences Research Centre, Universidade de Beira Interior, 6200-506 Covilhã, Portugal;
[2]Department of Chemistry, Faculty of Sciences, Universidade de Beira Interior, 6201-001 Covilhã, Portugal;
[3]Department of Medical Sciences, Faculty of Health Sciences, Universidade de Beira Interior, 6200-506 Covilhã, Portugal.

Introduction and Objective

- Recently, the applicability of messenger RNA (mRNA) has been exploited in a variety of fields, namely in antibody-based therapeutics, allowing the *in situ* production of antibodies in a cost- and labour-effective manner (1).
- The high demand for pure and stable mRNA has increased largely due to the emerging of molecular therapies, leading to a widespread need to improve mRNA production scale and purification processes (2).
- Cryogels are a novel approach for the purification of large molecules like mRNA, characterized by a supermacroporous structure, high flow rates and binding capacity, make it an interesting strategy to test in mRNA purification (3).
- Therefore, the present work aims to functionalize cryogels with thymine to purify *in vitro* transcribed (IVT) mRNA that encodes for the antibody anti-ADAM17. As initial screening for the purification conditions a low molecular weight RNA (LMW RNA) sample was used.

Materials and Methods

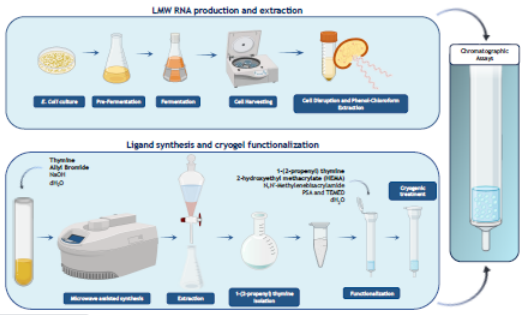

Results

Ligand Synthesis 1-(2-propenyl) thymine

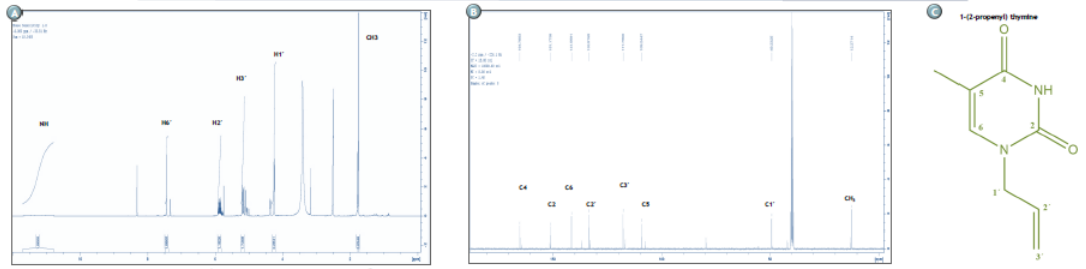

Figure 1. Confirmation of 1-(2-propenyl) thymine synthesis by NMR. A) ^{1}H NMR spectrum of 1-(2-propenyl) thymine in DMSO. B) ^{13}C NMR spectrum of 1-(2-propenyl) thymine in DMSO. C) Chemical structure of 1-(2-propenyl) thymine.

Screening of the RNA binding and elution

	Hydrophobic Interactions		Ionic Interactions	
	Binding Step	Elution Step	Binding Step	Elution Step
pHEMA-ProT0	+	+ +	+	- -
pHEMA-ProT25	-	+ +	+	-
pHEMA-ProT35.5	+	+	+	-
pHEMA-ProT50	-	+ +	+	- -

Table 1. General behaviour of the cryogels in ionic conditions, the results were analysed based on the elution percentage of RNA. Table caption : ++ (75% - 100%); + (50% - 75%); - (25% - 50%); -- (0%-25%).

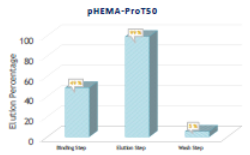

Graphic 2. Better result in the hydrophobic interactions screening conditions. Equilibrium: Tris-HCl 10 mM, Ammonium Sulphate 1.5 M, pH = 8.01; Elution: Tris-HCl 10 mM, pH = 8.01.

Graphic 1. Better result in the ionic interactions screening conditions. Equilibrium: Sodium Acetate 200 mM, pH = 5.52; Elution: Tris-HCl 10 mM, pH = 8.03.

Concluding Remarks

- The present work showed that the synthesis of the ligand (1-(2-propenyl) Thymine) occurred successfully. Small amounts of contaminants still a problem due to the similar structure to our ligand.
- Poly (Thymine) cryogels exhibited different behaviour toward the binding and elution properties of RNAs, being the most promising seems to be pHEMA-ProT25 and pHEMA-ProT50, used in hydrophobic conditions.
- Looking forward, we pretend to evaluate the behaviour of the pHEMA-ProT25 and pHEMA-ProT50 cryogels in the mRNA purification and perform a more detailed characterization of the synthesized chromatographic supports.

1. Deal, C. E., Carfi, A. & Plante, O. J. Advancements in mRNA Encoded Antibodies for Passive Immunotherapy. Vaccines 9, 108 (2021).
2. Rosa, S. S., Prazeres, D. M. F., Azevedo, A. M. & Marques, M. P. C. mRNA vaccines manufacturing: Challenges and bottlenecks. Vaccine 39, 2190–2200 (2021).
3. Santos, T. et al. Influenza DNA vaccine purification using pHEMA cryogel support. Sep. Purif. Technol. 204, 192–198 (2018).

The authors acknowledge to CICS-UBI projects UIDB/00709/2020 and UIDP/00709/2020, financed by FCT/MCTES. Project PTDC/BII-BBF/29496/2017 funded by FEDER, through COMPETE2020-POCI, and by national funds through FCT/MCTES' COMBINE project granted by Bincv 2021 (SRSRA of Pharmacists Order). M. Riscado acknowledge FCT for the PhD fellowship 2021.07658.BD

FCT Fundação para a Ciência e a Tecnologia
COMPETE 2020
PORTUGAL 2020

Appendix 4. Certificate of the presented poster at the XVII International Symposium of CICS-UBI.